

**CHARACTERIZATION OF A NOVEL
SIGNALING MOTIF IN THE CD3 ϵ SUBUNIT OF THE T CELL RECEPTOR**

APPROVED BY THE SUPERVISORY COMMITTEE

Nicolai S.C. van Oers, Ph.D.

Zhijian J. Chen, Ph.D.

Richard H. Scheuermann, Ph.D.

Melanie H. Cobb, Ph.D.

James Forman, D.M.D., Ph.D.

DEDICATION

To my husband, Jon, and my parents for their unfailing love and support.

Acknowledgements

I would like to begin by thanking my mentor, Dr. Nicolai van Oers. You have been an outstanding educator in biomedical research. You have taught me to think both critically and independently. Your enthusiasm for science, as well as your dedication to your career, students, and family, has been truly inspirational. To the other members of the van Oers lab, thank you so much for your help throughout this process. I would especially like to acknowledge Dr. Lisa Pitcher for her assistance in working with kinases, Dr. Jennifer Young for help with siRNA and western blotting, and Amy Becker for expertise in flow cytometry.

To the members of my dissertation committee, Dr. James Forman, Dr. Richard Scheuermann, Dr. Zhijian Chen, and Dr. Melanie Cobb, I would like to offer my sincerest thanks. I truly appreciate your willingness to take time out of your busy schedules to assist me in completing my dissertation research. Your efforts in keeping me on goal and heading toward relevant, meaningful answers have been invaluable.

I would also like to thank other staff members at UTSW, in particular Karen Kazemzadeh, Karen Ellison, Bettye Puryear, Renee Gugino, Cathy Smith, Mariana Ibarra, and Angie Mobley, who have contributed on a daily basis with their friendship and technical assistance.

To my parents, Bill and Lisa DeFord and Carl and Martha Baugh, I hardly know where to begin. Your love and encouragement have been an inspiration to me throughout my life. You have taught me to value hard work and to approach life's problems with integrity and discipline. These lessons have been invaluable throughout my educational

career. Even when I doubted what direction I should choose, I never doubted that you were proud of me.

In addition to my parents, I would like to thank all the other members of my family for their support. I would particularly like to acknowledge my brother, Matt, sister-in-law, Micaela, and my nephews, Jackson and Hudson. Having your family near during my graduate career has been a blessing. To my new family (Mike and Donna Watts; Wes, Erin, and Will Stecker; and Matt, Katie, Alathia, and Abigayle Watts), I would like to offer my gratitude for welcoming me into your family so warmly.

To Baranda, my former-roommate and close friend, I'm so thankful for the day we met on the elevator. Had it not been for your friendship, my first year of graduate school may have turned out much different. Thank you for hanging in there with me.

Megan, although I wish you had lived closer during my graduate education, your friendship has been precious, in spite of the distance. I hope you know how much I appreciate the sacrifice you've made for our country, as well as how much your friendship means to me.

Finally, to my husband: If I had gained nothing else during my graduate career, the privilege of meeting and marrying you would have been well worth my efforts. You have been my reason to smile on more days than I can remember. Your loving nature, generosity, and gentleness have been an extraordinary example to me throughout this process. You have taught me how to take life in stride and enjoy the simple things. I can't thank you enough for loving me so well.

CHARACTERIZATION OF A NOVEL
SIGNALING MOTIF IN THE CD3 ϵ SUBUNIT OF THE T CELL RECEPTOR

By

Laura Michelle Watts

DISSERTATION

Presented to the Faculty of the Graduate School of Biomedical Sciences

The University of Texas Southwestern Medical Center at Dallas

In Partial Fulfillment of the Requirements

For the Degree of

DOCTOR OF PHILOSOPHY

The University of Texas Southwestern Medical Center at Dallas

Dallas, Texas

March, 2008

Copyright

by

LAURA MICHELLE WATTS, 2008

All Rights Reserved

**CHARACTERIZATION OF A NOVEL
SIGNALING MOTIF IN THE CD3 ϵ SUBUNIT OF THE T CELL RECEPTOR**

Laura Michelle Watts, Ph.D.

The University of Texas Southwestern Medical Center at Dallas, 2008

Supervising Professor: Nicolai S.C. van Oers, Ph.D.

The T cell receptor (TCR) complex consists of the ligand-binding α/β heterodimer as well as four associated signaling chains (CD3 γ , δ , ϵ , and ζ). Each of the CD3 subunits contains one or more copies of a signaling motif termed an immunoreceptor tyrosine-based activation motif (ITAM). Phosphorylation of tyrosine residues within the ITAMs is critical for TCR-mediated signaling events. We identified an additional signaling motif in the cytoplasmic tail of CD3 ϵ that we termed the basic-rich stretch (BRS). Biochemical analyses revealed that this motif uniquely interacted with the serine/threonine kinase, G protein-coupled receptor kinase 2 (GRK2).

Interactions between the BRS and GRK2 contribute to the ability of the TCR to cross talk with G protein-coupled receptors, such as CXCR4. The BRS was also capable of mediating interactions with certain charged phospholipids. To address the role of the BRS in T cell functions, several murine CD3 ϵ transgenic lines bearing distinct mutations of the BRS were generated. Analyses of these mice on a CD3 ϵ null background revealed that modifications of the BRS suppressed T cell development. Taken together, these findings demonstrate that the BRS of CD3 ϵ plays an important role in TCR signaling and T cell development by regulating unique protein-protein and protein-lipid interactions.

TABLE OF CONTENTS

Acknowledgements	iii
Abstract	vi
Table of Contents	ix
List of Publications	xiv
List of Figures	xv
List of Abbreviations	xx
CHAPTER I: INTRODUCTION	1
<i>Overview of TCR-mediated Signaling</i>	1
<i>The Ectodomain of CD3 ϵ: Structure and Regulation of CD3 Pairing</i>	4
<i>Transmembrane Region of CD3 ϵ</i>	6
<i>The Cytoplasmic Tail of CD3 ϵ Contains Three Distinct Subregions:</i>	
<i>The Basic-rich Stretch</i>	7
<i>The Proline-rich Sequence</i>	8
<i>The Immunoreceptor Tyrosine-based Activation Motif</i>	10
<i>T Cell Receptor/G Protein-Coupled Receptor Crosstalk</i>	12
<i>G Protein-coupled Receptor Desensitization</i>	15
<i>G Protein-Couple Receptor Kinases</i>	15
<i>Summary</i>	17
CHAPTER II: MATERIALS AND METHODS	
<i>Mice</i>	24

<i>Southern Blot Analysis</i>	25
<i>Antibodies</i>	26
<i>Recombinant Proteins</i>	27
<i>Cell Lines and Plasmids</i>	27
<i>Fusion Protein Preparation</i>	27
<i>Affinity Column Preparation</i>	29
<i>Isolation of CD3 ϵ From Surface Versus Intracellular Pools</i>	30
<i>Immunoprecipitations, Western Blots, and In Vitro Kinase Reactions</i>	30
<i>Phosphoamino Acid Analysis</i>	31
<i>SDF-1 α Stimulations</i>	32
<i>Chromatography Purifications</i>	33
<i>Transfections and siRNA Knockdown</i>	34
<i>Phospholipid Binding</i>	35
<i>FACS Analysis</i>	36
<i>Stimulations</i>	36

**CHAPTER III: IDENTIFICATION AND CHARACTERIZATION OF A NOVEL
INTERACTION BETWEEN THE MEMBRANE-PROXIMAL BASIC-RICH
STRETCH OF CD3 ϵ AND THE SERINE/THREONINE KINASE GRK2**

Introduction	40
Results	43
<i>CD3 ϵ Associates with a Kinase Activity</i>	43

<i>Interactions between CD3 ϵ and Its Associated Kinase Activity</i>	
<i>Occur Independently of ZAP-70</i>	45
<i>Interactions between CD3 ϵ and Its Associated Kinase Activity</i>	
<i>Primarily Occur within Intracellular Compartments</i>	46
<i>CD3 ϵ Constitutively Associates with a Serine/Threonine Kinase</i>	
<i>Distinct from the PKC, PI3K and MAPK Families</i>	48
<i>The Membrane-Proximal Basic-Rich Stretch of CD3 ϵ Mediates</i>	
<i>the Kinase Interaction</i>	49
<i>Western Blot Analysis of Candidate Ser/Thr Kinases</i>	51
<i>Identification of GRK2 as a BRS-associated Kinase</i>	52
<i>CD3 ϵ Can Interact with Endogenous GRK2</i>	55
<i>Interactions between CD3 ϵ and GRK2 Occur Predominantly</i>	
<i>within Subcellular Compartments in a pH-sensitive Fashion</i>	56
<i>The Effect of GRK2 siRNA Treatment on the BRS/CD3 ϵ-associated</i>	
<i>Kinase Activity</i>	57
<i>SDF-1α Treatment of Primary Thymocytes Significantly Reduces the</i>	
<i>CD3 ϵ-associated Kinase Activity</i>	58
Discussion	61
CHAPTER IV: CHARACTERIZATION OF THE MEMBRANE-PROXIMAL	
BASIC-RICH STRETCH OF CD3 ϵ IN T CELL FUNCTIONS	
Introduction	88

Results	91
<i>The BRS of CD3 ϵ Allows for Interactions with Select Phospholipids</i>	91
<i>Modifications within the BRS of CD3 ϵ Do Not Interfere with CD3 ϵ</i>	
<i>Protein Expression or TCR Assembly in Transfected Cells</i>	92
<i>Distinct Modifications within the BRS Interfere with Nck Binding and</i>	
<i>ITAM Phosphorylation</i>	93
<i>Expression of a Transgene Encoding Mutations in the BRS Restores</i>	
<i>CD3 ϵ Protein Expression in CD3 ϵ-Deficient Mice</i>	94
<i>Select modifications of the BRS Block T Cell Development in</i>	
<i>Transgenic Mice</i>	96
<i>TCR β Gene Rearrangement and Invariant Chain Pairing Occur</i>	
<i>Normally in the BRS-Displace Mice</i>	97
<i>The Induction of Phosphoproteins and CD69 Expression is Normal</i>	
<i>in the BRS-Substitute and -Truncate Transgenic Mice</i>	99
Discussion	101
CHAPTER V: DISCUSSION	
Overview	123
<i>Potential Role for BRS/GRK2 Interactions</i>	124
<i>Interactions Between the BRS and Phospholipids May Provide a</i>	
<i>Mechanism for Conformational Changes in CD3 ϵ</i>	128
<i>Elucidating a Role for the BRS in T cell Development</i>	131
Overall Conclusions	132

BIBLIOGRAPHY	138
VITAE	151

PUBLICATIONS

1. Pitcher, L.A., Mathis, M.A., Young, J.A., **DeFord, L.M.**, van Oers, N.S. The CD3 $\gamma\epsilon/\delta\epsilon$ signaling module provides normal T cell functions in the absence of the TCR ζ immunoreceptor tyrosine-based activation motifs. *European Journal of Immunology*. 2005. 35(12):3643-54.
2. Becker, A.M. **DeFord-Watts, L.M.**, Wuelfing, C., van Oers, N.S. The constitutive tyrosine phosphorylation of CD3 ζ results from TCR-MHC Interactions that are independent of thymic selection. *Journal of Immunology*. 2007. 178:4120-4128.
3. **DeFord-Watts, L.M.**, Young, J.A., Pitcher, L.A., van Oers, N.S. The membrane-proximal portion of CD3 ϵ associates with the serine/threonine kinase GRK2. *Journal of Biological Chemistry*. 2007. 282(22):16126-34.
4. **DeFord-Watts, L.M.**, Murphy, T.C., Albanesi, J.P., Love, P.E., van Oers, N.S. T cell receptor functions are regulated by a basic-rich stretch in the cytoplasmic domain of CD3 ϵ . In preparation.

LIST OF FIGURES

Figure 1: <i>Diagram of the T cell receptor signaling complex.</i>	19
Figure 2: <i>TCR-mediated signaling events.</i>	20
Figure 3: <i>The cytoplasmic tail of CD3 ϵ shares a high degree of homology among numerous species.</i>	21
Figure 4: <i>Three subregions within the cytoplasmic tail of CD3 ϵ mediate distinct protein interactions.</i>	22
Figure 5: <i>Signaling pathways induced by chemokine receptor ligation.</i>	23
Figure 6: <i>Southern blot analysis of the CD3 ϵ BRS-transgenic founders.</i>	38
Figure 7: <i>The cytoplasmic tail of CD3 ϵ uniquely associates with a kinase activity.</i>	65
Figure 8: <i>Full-length CD3 ϵ associates with a kinase in a CD3 ζ ITAM-independent manner.</i>	66
Figure 9: <i>The CD3 ϵ-associated kinase is distinct and independent of ZAP-70.</i>	67
Figure 10: <i>The CD3 ϵ-associated kinase activity is predominantly intracellular.</i>	68
Figure 11: <i>Interactions between CD3 ϵ and a kinase activity are constitutive in ex vivo thymocytes.</i>	69
Figure 12: <i>CD3 ϵ associates with a serine/threonine kinase.</i>	70
Figure 13: <i>The basic-rich stretch of CD3 ϵ mediates the kinase association.</i>	71
Figure 14: <i>The full-length basic-rich stretch is required to precipitate the optimal amount of the CD3 ϵ-associated kinase activity.</i>	72
Figure 15: <i>The positively charged residues within the BRS mediate a kinase association and/or activity.</i>	73

Figure 16: <i>The BRS of CD3 ϵ associates with a Ser/Thr kinase other than ERK1/2 and HPK1.</i>	74
Figure 17: <i>PKA does not constitutively associate with CD3 ϵ in peripheral T cells.</i>	75
Figure 18: <i>Isolation of the CD3 ϵ-associated kinase activity by anion-exchange chromatography.</i>	76
Figure 19: <i>Purification of the CD3 ϵ-associated kinase activity using affinity chromatography.</i>	77
Figure 20: <i>Silver stain of proteins isolated by sequential chromatography purifications of murine thymocyte lysates.</i>	79
Figure 21: <i>GRK2 elutes in the Q-Sepharose and affinity purified fractions that also contain the BRS-associated kinase activity.</i>	81
Figure 22: <i>HnRNPA1 can co-precipitate with GST-BRS.</i>	82
Figure 23: <i>GRK2 is capable of interacting with CD3 ϵ.</i>	83
Figure 24: <i>Intracellular pools of CD3 ϵ interact with GRK2.</i>	84
Figure 25: <i>Interactions between the BRS and GRK2 are optimal at a low pH.</i>	85
Figure 26: <i>Reduced expression of GRK2 decreases the BRS-associated kinase activity.</i>	86
Figure 27: <i>SDF-1α treatment of primary thymocytes significantly decreases the amount of CD3 ϵ-associated kinase activity.</i>	87
Figure 28: <i>The BRS of CD3 ϵ mediates phospholipid binding.</i>	105
Figure 29: <i>The BRS of CD3 ϵ can bind phospholipid in the context of a bilayer.</i>	106
Figure 30: <i>Schematic representation of the CD3 ϵ BRS transgenic constructs.</i>	107

Figure 31: <i>CD3 ϵ protein expression and pairing with CD3 γ or δ are not disrupted by mutations within the BRS.</i>	108
Figure 32: <i>Displacing the BRS interferes with Nck binding in transfected cells.</i>	109
Figure 33: <i>CD3 ϵ BRS-Substitute and -Truncate are more readily detected as phosphoproteins in transfected cells.</i>	110
Figure 34: <i>Protein expression and thymic cellularity in the BRS transgenic mice.</i>	111
Figure 35: <i>Select mutations within the BRS alter thymic development.</i>	112
Figure 36: <i>The BRS of CD3 ϵ contributes to the progression of thymocytes through the DN stages of development.</i>	113
Figure 37: <i>Select mutations within the BRS alter the production of mature T cell in the lymph node.</i>	114
Figure 38: <i>Certain modifications of the BRS interfere with the production of mature T cell in the spleen.</i>	115
Figure 39: <i>The percentage of mature T and B cells in the lymph node varies depending on the mutation made within the BRS.</i>	116
Figure 40: <i>Select mutations of the BRS alter the percentage of mature T and B cells found in the spleen.</i>	117
Figure 41: <i>CD3 ϵ BRS-Displace transgenic mice exhibit normal TCR β gene rearrangements and CD3 γ/ϵ or δ/ϵ pairing.</i>	118
Figure 42: <i>Anti-CD3 ϵ mAb Injections into BRS-Displace transgenic mice does not induce thymocytes proliferation or differentiation.</i>	119
Figure 43: <i>Early phosphoprotein induction is normal in the BRS-Truncate transgenic mice.</i>	120

Figure 44: <i>CD69 upregulation on CD4⁺ lymphocytes is comparable in the BRS-Wild Type, -Truncate and -Substitute transgenic mice.</i>	121
Figure 45: <i>CD69 upregulation on CD8⁺ lymphocytes is comparable in the BRS-Wild Type, -Truncate, and -Substitute transgenic mice.</i>	122
Figure 46: <i>Functional model for BRS/GRK2 interactions within intracellular compartments.</i>	134
Figure 47: <i>Model I for the regulation of TCR signaling by the BRS of CD3 ϵ.</i>	135
Figure 48: <i>Model II for the regulation of TCR signaling by the BRS of CD3 ϵ.</i>	136
Figure 49: <i>α-helical wheel model for the BRS of CD3 ϵ.</i>	137

LIST OF TABLES

Table I: <i>Quantitation of protein expression in several of the CD3 ϵ BRS transgenic mice.</i>	39
Table II: <i>Purification of the CD3 ϵ associated Ser/Thr kinase from murine thymocytes.</i>	78
Table III: <i>Representative table of proteins identified by mass spectrometry analysis of affinity-purified fractions.</i>	80

LIST OF ABBREVIATIONS

α – anti

Ab – Antibody

APC – Antigen Presenting Cell

ATP – Adenosine triphosphate

BRS – Basic-rich stretch

BSA – Bovine serum albumin

CBB – Coomassie brilliant blue

CD – Cluster of differentiation

CXCR4 – Chemokine (C-X-C motif) receptor 4

DAG – Diacylglycerol

DN – Double negative

DP – Double positive

EGFR – Epidermal growth factor receptor

Eps8L1 – Epidermal growth factor receptor pathway substrate 8-related protein 1

ERK – Extracellular signal-regulated kinase

GDP – Guanosine diphosphate

GPCR – G protein-coupled receptor

GRK2 – G protein-coupled receptor kinase 2

GST – Glutathione *S*-transferase

GTP – Guanosine triphosphate

HEK 293T cell – Human embryonic kidney 293

HnRNP – Heterogeneous nuclear ribonucleoprotein

HPK1 – Hematopoietic progenitor kinase 1

HRP – Horse radish peroxidase

IB - Immunoblot

IC – Intracellular

IgH – Immunoglobulin heavy chain

IgL – Immunoglobulin light chain

IP – Immunoprecipitation

IP₃ – Inositol 1,4,5-trisphosphate

ITAM – Immunoreceptor tyrosine-based activation motif

i.v.k. – *in vitro* kinase

kb – Kilobase

kD – Kilodalton

LAT – Linker for activation of T cells

M – Molar

mAb – Monoclonal antibody

mAU – UV absorbance

MAPK – Mitogen-activated protein kinase

MBP – Myelin basic protein

MHC – Major histocompatibility complex

NF-κB – Nuclear factor kappa B

NMR – Nuclear magnetic resonance

P116 – Jurkat T cell line deficient in ZAP-70 expression

PA – Phosphatidic acid

PD – Pull down

PH – Pleckstrin homology

PI – Phosphoinositides

PI(3)P – Phosphatidylinositol-3-phosphate (PI(3)P)

PI(3,4)P₂ – Phosphatidylinositol-3,4-bisphosphate

PI(3,4,5)P₃ – Phosphoinositide-3,4,5-trisphosphate

PI(4)P – Phosphatidylinositol-4-monophosphate

PI(4,5)P₂ – Phosphatidylinositol-4,5-biphosphate

PI(5)P – Phosphatidylinositol-5-phosphate

PKA – cAMP-dependent protein kinase A

PKC – Protein kinase C

PLC-β – Phospholipase C-β

PLC-γ – Phospholipase C-γ

PRS – Proline-Rich Sequence

PTK – Protein tyrosine kinase

PVDF – Polyvinylidene fluoride

rGRK2 – Recombinant G protein-coupled receptor kinase 2

RGS – Regulator of G Protein Signaling

RH – RGS homology

RLU – Relative light unit

SDF-1 α – Stromal cell-derived factor-1 α

Ser/Thr – Serine/Threonine

SH2 domain – Src homology 2 domain

SH3 domain – Src homology 3 domain

siRNA – Short interfering RNA

SLP-76 – SH2 domain-containing leukocyte protein of 76 kDa

SP – Single positive

TCR – T cell receptor

Tf – Transfect

V β – Variable β

WCL – Whole cell lysate

ZAP-70 – ζ -associated protein of 70 kDa

CHAPTER I

INTRODUCTION

Overview of TCR-mediated Signaling

T lymphocytes are critical members of the white blood cell (WBC) population due to their ability to both directly kill infected cells and influence the activity of other cells of the immune system. The ability of T cells to ward off infection requires their recognition of the antigenic portions of an invading pathogen. Unlike other WBCs, T cells do not recognize free, soluble antigen. Rather, T cells require that pathogen derived proteins be degraded by antigen presenting cells (APC). APCs then load the pathogenic peptide fragments into the major histocompatibility complex (MHC) and express them on their cell surface. When a T cell encounters an APC expressing self-MHC loaded with foreign peptide, it will respond by way of cytokine production, proliferation, or direct killing of the target cell.

T cells recognize peptide-MHC complexes through their surface-expressed T cell receptor (TCR) (Fig. 1). The TCR is comprised of six type I membrane-spanning proteins (1). The ligand-binding subunits of the TCR generally consist of a disulfide-linked α/β heterodimer. However, a smaller, less-defined subset of T cells express a ligand-binding γ/δ heterodimer (2). In the endoplasmic reticulum (ER) of the cell, the α/β heterodimer associates with the signaling components of the TCR, which are known as the CD3 invariant chains (CD3 γ , δ , ϵ , and ζ). Proper assembly in the ER results in the surface expression of a TCR that contains an α/β heterodimer, a disulfide-linked ζ - ζ

homodimer, a CD3 γ/ϵ heterodimer, and a CD3 δ/ϵ heterodimer (1, 3-5) (Fig. 1).

Although the α/β heterodimer provides the TCR with the ability to engage peptide-MHC, intracellular signals are not propagated through these chains since they possess relatively short cytoplasmic domains. Rather, signaling is regulated by the CD3 polypeptides, which contain short extracellular portions and much longer cytoplasmic tails. Each CD3 chain has one or more copies of a conserved signaling motif, termed an immunoreceptor tyrosine-based activation motif (ITAM). This motif contains two critically-spaced tyrosine residues ($Yxx(L/I)_{x_{6-8}}Yxx(L/I)$) that are phosphorylated by Src family protein tyrosine kinases (PTKs) following extracellular engagement of the α/β heterodimer (6-8). A single TCR contains 10 ITAMs, with 6 ITAMs residing in cytoplasmic tails of the CD3 ζ homodimer, and a single ITAM residing in each of the other chains (Fig. 1). As bi-phosphorylated proteins, the CD3 ITAMs are complexed by signaling molecules that possess tandem Src-homology (SH2) domains. Examples include the PTKs, ζ -associated protein of 70kD (ZAP-70) and Syk (9, 10) (Fig. 2). Upon binding the ITAMs, ZAP-70 is catalytically activated by auto- and Src-dependent tyrosine phosphorylations.

Catalytically-active ZAP-70 phosphorylates many downstream signaling molecules, including linker for activation of T cells (LAT) and SH2 domain-containing leukocyte protein of 76 kDa (SLP-76) (11, 12). The phosphorylation of these adaptor proteins enhances the recruitment and activation of additional effector molecules, including phospholipase C- γ (PLC- γ), Itk, and vav. Once bound to phospho-LAT, PLC- γ is catalytically activated, enabling this enzyme to hydrolyze phosphatidylinositol 4,5-bisphosphate (PI(4,5)P₂ or PIP₂) into the second messengers diacylglycerol (DAG) and inositol 1,4,5-trisphosphate (IP₃) (13, 14). Interactions between IP₃ and the inositol 1,4,5-

triphosphate receptor mediate the release of calcium from intracellular stores (15). Membrane-associated DAG contributes to the activation of the Ras pathway through interactions with the RasGRP, as well as the activation of kinases belonging to the protein kinase C (PKC) family (16-18). These early events lead to the sequential phosphorylation of the Mitogen-activated protein (MAP) kinases and the degradation of the I κ B components. Ultimately, these adaptor-protein regulated signals converge on a variety of transcription factors (NF- κ B, NF-AT, AP-1, etc.) which then enter the nucleus. The magnitude and duration of transcription factor activation and nuclear localization controls a wide-range of T cell process, including development, differentiation, proliferation, effector function, and/or apoptosis (Reviewed in (6)).

Biochemical analysis of the contributions made from each of the CD3 chains have lead to the hypothesis that the invariant chains function as two autonomous signaling modules, with the CD3 ζ/ζ homodimer comprising one module and the CD3 γ/ϵ - δ/ϵ heterodimers another (8). Studies have shown that the more ITAMs that are available for signaling, the stronger the signal that is generated (19, 20). Based on these findings, the CD3 ζ homodimer has been hypothesized to serve as the predominant signaling module of the TCR since it contains 6 of the 10 ITAMs. However, analysis of mice lacking the tyrosine residues of the CD3 ζ ITAMs demonstrated that certain T cell functions, including TCR-mediated signal transduction and proliferation, were intact without contributions from the CD3 ζ ITAMs (20, 21). These observations have led to the model that in terms of their ITAMs, the CD3 chains serve somewhat redundant functions (8).

Among the CD3 γ , δ , and ϵ chains, more emphasis has been placed on understanding the role of CD3 ϵ . This is due to several factors, including the appearance

of CD3 ϵ twice in the TCR signaling complex (present in both the CD3 γ/ϵ and δ/ϵ heterodimers), as well as recent data suggesting that a conformational change within the cytoplasmic tail of CD3 ϵ may be one of the earliest detectable events to occur in T cell activation (1, 22). In our own investigations of CD3 ϵ , we have identified a cluster of positively charged residues located in the membrane-proximal portion of its cytoplasmic tail. We have demonstrated that this basic-rich stretch (BRS) can serve as a novel signaling motif for the TCR by mediating both protein and phospholipid interactions. In terms of protein interactions, we have found that the BRS can complex the Ser/Thr kinase, GRK2. Due to the role of this kinase in T cells, we hypothesize its interaction with the BRS may facilitate TCR crosstalk with G protein-coupled receptors (GPCR). Given these findings, the following overview will focus on the structure and function of CD3 ϵ , as well as the ability of the TCR to communicate with GPCRs.

The Ectodomain of CD3 ϵ : Structure and Regulation of CD3 Pairing

Murine CD3 ϵ is encoded by a gene consisting of 8 exons located on chromosome 9 (chromosome 11 in humans) (23). This gene produces a non-glycosylated protein approximately 25kD in size. Protein sequence analysis revealed that CD3 ϵ , like CD3 γ and δ , consists of an extracellular Ig domain, a conserved RxCxxCxE motif juxtaposed to the plasma membrane, a single transmembrane helix, and a long cytoplasmic tail (24-26). The extracellular portion of murine CD3 ϵ contains 87 amino acids that are arranged as two anti-parallel β -sheets (27, 28). Residues within these β -sheets interact with specific amino acids located in the ectodomains of CD3 γ and CD3 δ

(27, 28). For example, the cysteine residues located in the conserved RxCxxCxE motif of each of the CD3 subunits is necessary for CD3 γ and δ pairing. Mutagenesis of these cysteines significantly reduces the ability of CD3 ϵ to pair with CD3 γ and δ , suggesting that intramolecular disulfide bonds formed between these sequences may stabilize the dimerization of the CD3 γ/ϵ and δ/ϵ chains (24, 25, 29). Two additional cysteine residues located outside the RxCxxCxE motif further contribute to the structural stability of CD3 ϵ by forming intrachain disulfide links within the Ig domain (30). A stretch of acidic amino acids in the extracellular domain of CD3 ϵ are also hypothesized to mediate electrostatic interactions with the other invariant chains, particularly CD3 γ (27).

Pairing between CD3 ϵ and the other invariant chains is required for the proper folding of its ectodomain. [³⁵S]methionine/cysteine labeling of CD3 ϵ transiently expressed in CHO cells demonstrated that in its monomeric form CD3 ϵ is relatively stable (31). However, attempts to immunoprecipitate the ectodomain of CD3 ϵ in the absence of other invariant chains were unsuccessful when structurally dependent antibodies were used (32). These assays, in conjunction with nuclear magnetic resonance (NMR) spectroscopy of recombinant CD3 ϵ , indicated that the proper folding of the Ig-like domain of CD3 ϵ requires heterodimerization with an additional TCR subunit, such as CD3 γ or δ (32).

In addition to binding CD3 γ and δ , the ectodomain of CD3 ϵ has also been predicted to interact with both TCR α and β . Following the crystallization of the N15 α/β -TCR, several groups noted that there was a pocket formed between the TCR C β FG loop and certain loops within TCR C α capable of accommodating interactions with a

single invariant chain (33, 34). Based on size constraints, charge restrictions, and the requirement that the invariant chain residing in this cavity be non-glycosylated, CD3 ϵ was considered the most likely candidate. Subsequent competition assays using antibodies directed against TCR β and CD3 ϵ supported the notion that a single CD3 ϵ subunit within the TCR complex lay in close proximity to TCR β (33).

Transmembrane Region of CD3 ϵ

Each component of the TCR complex contains a specific charged amino acid(s) within the transmembrane region of the protein that is required for receptor assembly. The TCR α and β subunits each contain basic amino acids, with TCR α encoding a lysine and an arginine residue, and TCR β possessing a single lysine. Conversely, each CD3 chain contains a negatively charged aspartic or glutamic acid (26). Using sequential non-denaturing immunoprecipitations in association with amino acid mutagenesis, Call et al demonstrated that electrostatic interactions between the basic and acidic residues located in the transmembrane helices of the TCR subunits were critical for complete TCR assembly (26). The substitution of alanines for the aspartic acids in the transmembrane domain of CD3 ϵ reduced the ability of the CD3 δ/ϵ heterodimer to associate with TCR α . Similarly, mutating the aspartic acid located in CD3 δ or the lysine residue in TCR α also interfered with the assembly of the TCR $\alpha/\text{CD3 } \delta/\epsilon$ complex, although to a lesser degree. These results support a model where interactions between charged residues located in the transmembrane region of each of the invariant chains result in two distinct TCR complexes (TCR $\alpha/\text{CD3 } \delta/\text{CD3 } \epsilon$ and TCR $\beta/\text{CD3 } \gamma/\text{CD3 } \epsilon$) (26, 35). When these

two clusters associate with the CD3 ζ/ζ homodimer, the fully assembled TCR complex is released from the ER and shuttles to the plasma membrane (36).

The Cytoplasmic Tail of CD3 ϵ Contains Three Distinct Subregions: The Basic-rich Stretch

The cytoplasmic tail of CD3 ϵ is 55 amino acids in length and exhibits considerable sequence homology when different species are compared (Fig. 3). Two-dimensional $^1\text{H-NMR}$ analysis indicated that the majority of the cytoplasmic tail of CD3 ϵ is arranged as random-coil (37). Studies utilizing smaller peptide fragments of just the membrane-distal portion suggested that residues 161 – 174 can adopt an α -helical structure (37, 38). In spite of minimal structural information, the cytoplasmic tail of CD3 ϵ has been divided into three regions based on amino acid sequence comparisons with other signaling domains and distinct protein interaction studies (Fig. 4). We have termed the membrane-proximal portion of CD3 ϵ the basic-rich stretch (BRS) due to the presence of a number of lysine and arginine residues (39). Previous protein-binding studies have shown that the BRS can associate with CD3 ϵ -Associated Signal Transducer (CAST) and topoisomerase II β (40, 41). Although interactions between the BRS and CAST appeared to take place at a low stoichiometry, overexpression of a dominant-negative version of CAST suppressed the activation of NFAT (assessed by NFAT-luciferase reporter assays) as well as the production of IL-2, indicating that this interaction may be important for T cell proliferation. The ability of CD3 ϵ to bind the nuclear protein topoisomerase II β was also hypothesized to enhance IL-2 production

(41). In Chapter III, we present evidence that the BRS is capable of binding to a third signaling molecule, termed G protein-coupled receptor kinase 2 (GRK2).

An interesting feature of the BRS is its homology to polybasic clusters found in certain signaling and transport proteins, including growth associated protein 43 (GAP43) and 37 small GTPases (42). The unstructured clusters of positively charged residues within these proteins serve as a targeting-motif by mediating interactions with phospholipids expressed on specific intracellular or plasma membranes (43). Some transmembrane receptors have also been hypothesized to utilize polybasic clusters to regulate their activity. For example, interactions between a polybasic cluster located in the cytoplasmic tail of the epidermal growth factor receptor (EGFR) and PI(4,5)P₂ (expressed on the inner leaflet of the plasma membrane) inhibits the enzymatic activity of the kinase domain until ligand-binding occurs (44). The homology between the BRS and other phospholipid-binding proteins has important implications for the role of CD3 ϵ in TCR-mediated signaling. This topic is addressed in greater detail in Chapter IV.

The Proline-rich Sequence

The central portion of the cytoplasmic tail of CD3 ϵ contains a series of proline-residues and has consequently been termed the proline-rich sequence (PRS) (45). This polyproline motif can interact with several SH3-domain containing proteins, including Nck and epidermal growth factor receptor pathway substrate 8-related protein 1 (Eps8L1) (Fig. 4) (45, 46). Upon ligand engagement, the cytoplasmic tail of CD3 ϵ is thought to undergo a conformational change, allowing Nck to bind the PRS via the first of its three

SH3 domains (SH3.1) (45). The CD3 ϵ /Nck interaction is independent of Src-kinase activation and does not occur when the ITAM of CD3 ϵ is phosphorylated (45, 46). The idea that TCR cross-linking results in a conformational change within the cytoplasmic tail of CD3 ϵ was further supported by studies demonstrating that TCR engagement by either peptide/MHC or monoclonal antibodies promotes the exposure of a previously inaccessible epitope in the cytoplasmic tail of CD3 ϵ to the monoclonal antibody, AP1/1 (47). Consequently, interactions between CD3 ϵ and Nck have become a hallmark of “engaged” TCRs.

Nck has primarily been characterized as a regulator of actin cytoskeleton remodeling (45, 48, 49). To determine whether CD3 ϵ /Nck interactions were functionally significant, Vignali et al mutated the proline residues of the PRS to alanines, eliminating Nck binding (50). Retroviral vectors encoding the mutant CD3 ϵ chains were then used to transduce the bone marrow of CD3 ϵ -deficient mice. Analysis of RAG^{-/-} mice that had received bone marrow transfers from these retrovirally transduced animals revealed that when interactions between the PRS and Nck were eliminated, T cell development and activation still occurred normally (50). In spite of this, the conformational change that occurs within the cytoplasmic tail of CD3 ϵ is necessary for T cell functions. This is based on reports demonstrating that when the TCR is engaged in a manner that fails to induce the conformational change, TCR signaling does not occur (22). Rather, a conformation change and the clustering of two TCRs is required for T cell activation (i.e. ERK1/2, LAT, and PLC γ phosphorylation and calcium flux) (22). To date, the mechanism allowing for conformational readjustments within CD3 ϵ is still unclear. One hypothesis is that TCR ligation induces a structural modifications in the

constant domain of TCR α that regulate a contact site on the extracellular domain of CD3 ϵ (51, 52). This could alter the positioning of CD3 ϵ in such a way that the conformation of its cytoplasmic tail is modified. To date, this model has only been supported by one crystallographic study (51).

The functional consequence of Eps8L1 interactions with CD3 ϵ has yet to be determined. However, given that the Eps8 family of proteins is known to be involved in the Ras signaling, Eps8L1/CD3 ϵ binding may serve to contribute to cytoskeletal rearrangements following T cell activation (53).

The Immunoreceptor Tyrosine-based Activation Motif

TCR engagement results in the phosphorylation of tyrosine residues located in the CD3 ITAMs (54, 55). Numerous reports have demonstrated that the CD3 ϵ subunit can support TCR-mediated signaling events through its ITAM. Several of these studies utilized chimeric molecules, consisting of the extracellular/transmembrane domains of heterologous receptors, such as IL-2 (Tac) or CD8, fused to the cytoplasmic tail of CD3 ϵ . Cross-linking of these chimeric receptors resulted in T cell activation in Jurkat T cells (56). Further analysis of chimeric receptors revealed that the two tyrosine residues located in the ITAM of CD3 ϵ could be differentially phosphorylated (57). In a bi-phosphorylated state, the ITAM of CD3 ϵ interacts with ZAP-70. Of note, the affinity of this association is less than that of ZAP-70 for the bi-phosphorylated ITAMs located in CD3 γ , δ , or ζ (55, 58). Phosphorylation of only the membrane-distal tyrosine allows for the association of single SH2 domain-containing proteins, such as Lck and p85 (10).

To address whether the ITAM of CD3 ϵ was necessary for T cell development or activation, Sommers et al generated CD3 ϵ transgenic mice in which the membrane-distal tyrosine residues of its ITAMs were substituted with a phenylalanine (19). This mutation effectively eliminated the ability of CD3 ϵ to be phosphorylated following TCR engagement. Analyses of these mice lead to the conclusion that a functional CD3 ϵ ITAM is not critical for normal T cell development when maintained on a wild type background. However, when the ITAM-defective mice were backcrossed with HY transgenic mice (a low avidity TCR transgenic line) a defect in peripheral T cell survival was observed, indicating that the CD3 ϵ ITAM might be important under certain physiological conditions.

The cytoplasmic tail of CD3 ϵ also contains an ER retention signaling embedded within its ITAM. When expressed as a monomer, the CD3 ϵ polypeptide is retained within the ER (59). However, deleting residues 171-180 of its cytoplasmic tail allows for the surface expression of CD3 ϵ in non-T cells, such as COS cells (59). Further analysis using point mutations within the α -helix of CD3 ϵ 's ITAM demonstrated that six sequential amino acids (DLYSGL), particularly Tyr177, Leu180, and Arg183, were critical for the retention capability (38). Ultimately, this retention signal is believed to serve as a "quality control" mechanism for TCR complexes being assembled in the ER.

T Cell Receptor/G Protein-Coupled Receptor Crosstalk

Emerging evidence suggests a functional and physical couple of the TCR and chemokine receptors (60-64). Chemokine receptors belong to a family of transmembrane receptors known as G protein-coupled receptors (GPCR). GPCR are characterized by a seven-pass transmembrane configuration and make up one of the largest families of integral membrane proteins (65). GPCR ligands consist of an assortment of molecules, including hormones, odorants, neuropeptides, and chemokines. As a result, GPCR signaling regulates numerous physiological processes, ranging from the sensation of light and odor and to cellular migration (66). As their name suggests, GPCR carry out their signaling capabilities through interactions with a family of proteins known as G proteins. In an unbound state, the cytoplasmic domain of a GPCR is closely associated to an inactive heterotrimer consisting of the $G\alpha$, $G\beta$, and $G\gamma$ subunits (67). G protein complexes are typically classified by their associated $G\alpha$ subunit, which are divided into four distinct subgroups ($G\alpha_s$, $G\alpha_q$, $G\alpha_i$, and $G\alpha_{12-13}$) (Reviewed in (68)). Activation of $G\alpha_s$ generally results in the stimulation of adenylyl cyclases, while $G\alpha_i$ activation serves to both inhibit adenylyl cyclases and stimulate certain Src tyrosine kinases (Fig. 5). Chemokine receptors are most often associated with the $G\alpha_i$ subunit, and as a result are also sensitive to treatment by pertussis toxin. $G\alpha_q$ is coupled to the activation of phospholipase C- β (PLC- β), while G proteins categorized in the $G\alpha_{12-13}$ subfamily regulate Rho guanine-nucleotide exchange factors. Ligand engagement of the GPCR induces a conformation change within the receptor's cytoplasmic tail, promoting the exchange of guanosine diphosphate (GDP) for guanosine triphosphate (GTP) on the $G\alpha$

subunit (69). The GTP bound $G\alpha$ subunit and the $G\beta\gamma$ heterodimer then dissociate from each other, with each modulating the activity of distinct effector proteins within the cell (70). In terms of chemokine signaling, this can result in cellular migration, the activation of integrins, cytokine production, or even apoptosis (Fig. 5).

It has been known for some time that TCR-mediated signals can bolster, support, or in some cases override, those delivered from GPCRs and vice versa. Examples of this cross regulation include the ability of TCR signals to suppress the movement of a migrating T cell toward certain chemokine gradients (64). In other cases, signals transmitted from chemokine receptors can override those delivered through the TCR. As a consequence, a T cell may migrate out of the vicinity of APCs expressing peptide-MHC complexes for which its TCR is specific (60). It is also possible to enhance T cell migration toward certain chemokines, including MIP-1 α and - β , by stimulating through the TCR (71). Finally, stimulating T cells with certain chemokines has been shown to transactivate the TCR. For example, SDF-1 α treatment of Jurkat T cells results in the phosphorylation of the CD3 ζ ITAMs (62). This chemokine-mediated activation of the TCR was shown to be critical for the endocytosis of the chemokine receptor, CXCR4. Ultimately, the outcome of TCR/chemokine crosstalk depends on a number of factors, ranging from the differentiation/activation state of T cell to the nature of the engaging chemokine.

As for the mechanisms allowing for TCR/GPCR crosstalk, it is becoming increasingly clear that signaling molecules common to both the TCR and GPCR signaling pathways allow for reciprocal regulation between these receptors. As previously mentioned, TCR engagement induces the activation of numerous effector/adaptor

proteins, including Src and Syk PTK family members, the adaptor proteins LAT and SLP-76, and several MAP kinases. Although GPCRs generally initiate signaling events through G proteins, their signaling pathways often converge on many of these same signaling molecules. For example, treatment of human T cells with chemokines, such as RANTES and SDF-1 α , can activate ZAP-70 (62, 72). Of relevance, ligation of CXCR4 allows this chemokine receptor to physically associate with the TCR, resulting in a prolonged activation of the extracellular signal-regulated kinases (ERK1/2) (61).

The TCR can also control the activity of proteins typically associated with GPCR signaling. For instance, TCR-mediated activation of the Src kinase, Fyn, results in the phosphorylation of Pyk2, a PTK involved in GPCR activation of MAP kinase pathways (73, 74). Furthermore, engagement of the TCR can induce a physical association between $G\alpha_{q/11}$ and the CD3 ϵ chain, allowing for TCR-mediated regulation of PLC- β (Fig. 4) (75).

Under certain circumstances, crosstalk between the TCR and GPCRs appear to bolster one another. An example of this includes the finding that treating peripheral T cells with histamine (a GPCR ligand) enhances their proliferative response after TCR engagement (76). In other cases, GPCRs and the TCR function in an antagonistic fashion (60). Work by Peacock et al found that if a mature T cell was stimulated through the TCR, the surface expression of CXCR4 was reduced. As a result, T cells had a diminished ability to migrate toward a SDF-1 α gradient (63). Conversely, if the cells were pre-treated with SDF-1 α , subsequent TCR engagement resulted in less efficient phosphorylation of LAT and SLP-76. Taken together, these studies effectively demonstrate that the TCR and GPCRs can cross regulate one another.

G Protein-coupled Receptor Desensitization

Even if the cognate ligand for a GPCR remains present, a cell can rapidly lose its ability to respond through a process known as desensitization. One of the primary mechanisms for GPCR desensitization is through the activity of a family of Ser/Thr kinases known as G protein-coupled receptor kinases (GRK) (Reviewed in (77)). Within seconds to minutes of GPCR engagement, GRKs are recruited to the cytoplasmic surface of the receptor complex, where they phosphorylate specific Ser/Thr residues within the intracellular loops and COOH-terminal tail of the receptor (Fig. 5) (78, 79). This results in the association of arrestins, a family of proteins that sterically hinders G protein/GPCR interactions (80). Arrestin binding also initiates clathrin-mediated endocytosis of the GPCR (81, 82). It is interesting to note that certain GPCRs, including CXCR4, maintain G protein-independent signaling events in intracellular compartments after endocytosis (Fig. 5) (61, 83, 84). This is because GPCR-bound arrestins serve as scaffolds for certain signaling molecules, such as Src kinases, which are able to feed into MAPK signaling pathways (Reviewed in (85)). Ultimately, internalized GPCRs are either dephosphorylated, allowing them to recycle back to the surface of the cell, or shuttled to lysosomal compartments, where they are degraded.

G Protein-Couple Receptor Kinases

Seven GRKs (GRK 1–7) have been identified in humans. These kinases are divided into three subfamilies based on structural and functional similarities. GRK1,

originally termed rhodopsin kinase, and GRK7 are almost exclusively expressed in the retina and together make up the first subfamily. The second family consist of GRK2 (β -adrenergic receptor kinase-1) and GRK3 (β -adrenergic receptor kinase-2), which are ubiquitously expressed. Finally, the last subfamily consists of GRK4 (IT-11), which is primary expressed in the testis, and GRK5 and GRK6, which are both widely expressed (Reviewed in (86)).

Of the GRK family members, GRK2 has been the most extensively characterized (87). Structurally, GRK2 contains an N-terminal Regulator of G Protein Signaling (RGS) homology (RH) domain that is capable of specifically binding $G\alpha_q$ proteins, thereby inhibiting their GTPase activity (88, 89). The catalytic domain of GRK2 lies within the central portion of the protein (residues 188-467) and structurally resembles the kinase domain of other AGC kinase family members, such as cAMP-dependent protein kinase A (PKA) (90). Finally, the C-terminal portion contains a pleckstrin homology (PH) domain that allows it to interact with $G\beta\gamma$ and phosphatidylinositol (91, 92). Through these interactions, the PH domain regulates the recruitment of GRK2 to the plasma membrane (93). GRK2 is highly expressed in the immune system and serves to phosphorylate and desensitize numerous GPCRs, including the chemokine receptor CXCR4 (94). GRK2 knockout mice are embryonic lethal because of developmental defects in cardiac tissues (95). In contrast, GRK2^{+/-} mice are viable but exhibit a susceptibility to certain inflammatory diseases, such as experimental autoimmune encephalomyelitis (96). This is because reduced levels of GRK2 increase the magnitude and/or duration of GPCR signals in response to pro-inflammatory stimuli, thereby enabling activated lymphocytes to persist at sites of inflammation.

GRK2 can interact with a number of molecules important for TCR signaling. Examples of these include PKA, ERK 1/2, and c-Src (Reviewed in (97)). Furthermore, the activity and expression levels of GRK2 are regulated by T cell activation during both normal and inflammatory responses (98, 99).

Although the role of GRK2 has been well established in GPCR signaling, this kinase has never been implicated to participate in TCR-mediated signaling. Using a variety of biochemical assays, we found that the membrane-proximal portion of CD3 ϵ could constitutively bind to GRK2. This interaction predominated in intracellular compartments. To our knowledge, this is the first demonstration of direct interactions between a molecule known to negatively regulate GPCRs and the TCR/CD3 complex in primary cells.

Summary

The CD3 ϵ subunit is an essential component of the TCR complex (19, 56, 100). In the absence of CD3 ϵ , TCR assembly and cell surface expression does not take place. The cytoplasmic tail of CD3 ϵ , contains three distinct subregions (BRS, PRS, and ITAM), that facilitate TCR signaling. Independent mutagenesis of the PRS and ITAM has little consequence on T cell development and/or activation (19, 50). However, the role of the membrane-proximal portion of CD3 ϵ (a region we have termed the BRS) has not been assessed. Herein, we provide evidence that the BRS of CD3 ϵ is a novel signaling motif, capable of mediating both protein and phospholipid interactions. Using a variety of biochemical techniques, we identified GRK2 as a Ser/Thr kinase that

constitutively associated with the BRS. Interactions between the BRS and this kinase likely contribute to TCR crosstalk with G protein-coupled receptors. We also determined that the BRS of CD3 ϵ selectively binds to charged phospholipids. These interactions may provide a mechanistic basis for how the conformational change that takes place within the cytoplasmic tail of CD3 ϵ actually occurs. Finally, we have demonstrated that select modifications of the BRS can dramatically attenuate T cell development. These results demonstrate that the membrane-proximal portion of CD3 ϵ contains a critical signaling motif which affects a variety of T cell functions.

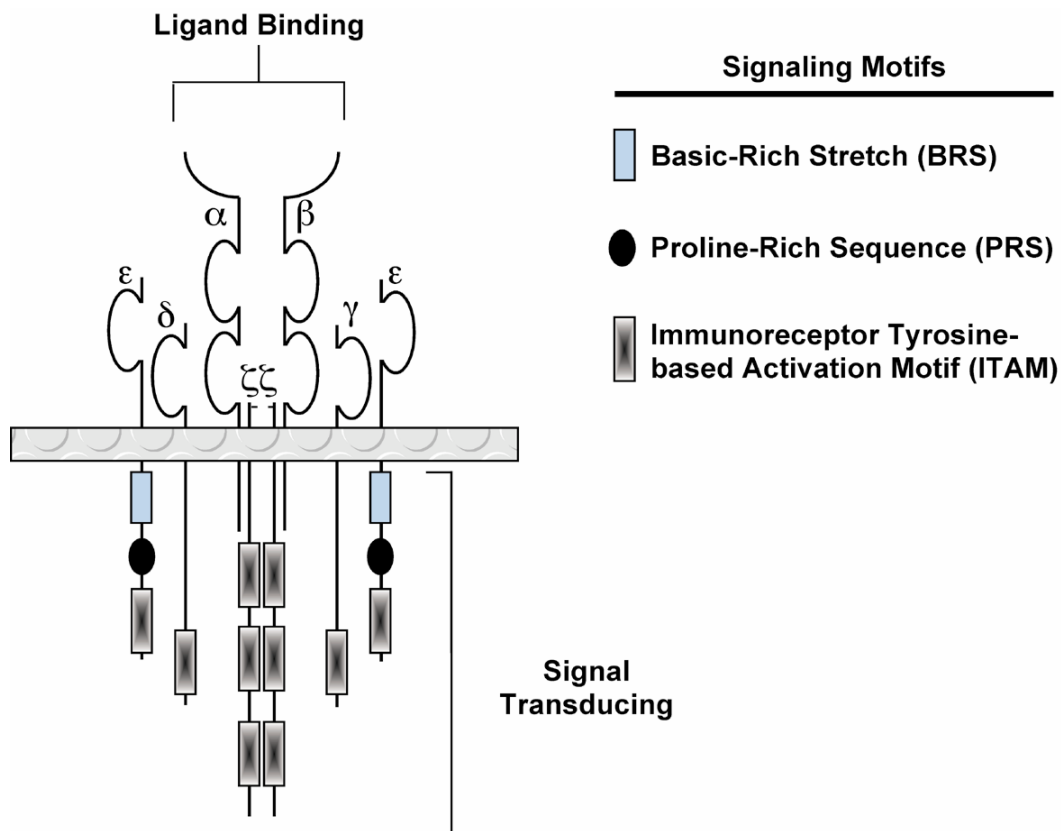


Figure 1. Diagram of the T cell receptor signaling complex. The T cell receptor is a multi-subunit complex of proteins. The α/β subunits are responsible for extracellular interactions with peptide/MHC molecules expressed on target cells. The CD3 γ , δ , ϵ , and ζ subunits are arranged as γ/ϵ and δ/ϵ heterodimers, and a ζ/ζ homodimer. These invariant chains all contain a signaling motif known as an Immunoreceptor tyrosine-based signaling motif (ITAM). The CD3 ϵ chain also contains two additional signaling sequences, termed the basic-rich stretch (BRS) and the proline-rich sequence (PRS).

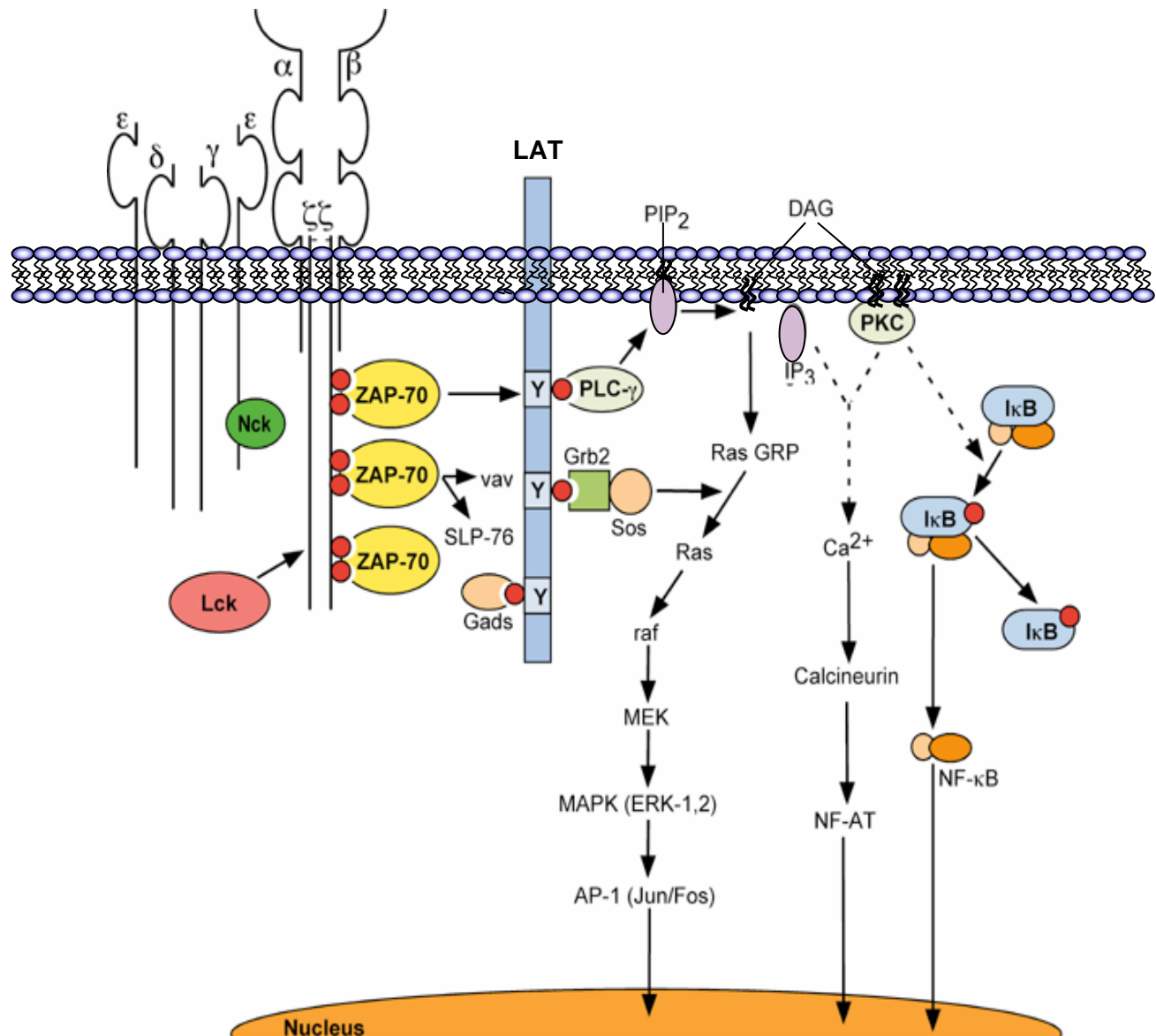


Figure 2. TCR-mediated signaling events. Antigen recognition by the α/β subunits results in Lck localization to the TCR. Lck phosphorylates tyrosine residues in the CD3 ITAMs, allowing for ZAP-70 association and catalytic activation. ZAP-70 phosphorylates LAT, which then binds Grb-2, thereby providing a docking site for Sos. Sos converts Ras-GDP to Ras-GTP, leading to the initiation of the MAPK cascade, and the activation of AP-1. PLC- γ activation results in the hydrolyzation of PIP₂ to IP₃ and DAG. PKC (activated by DAG) and increased Ca²⁺ are capable of regulating the activation of NF- κ B and NF-AT.

Species	Amino Acid Sequence
Human	KNRKAKAKPVTRGAGAGGRQRGQNKERPPPVNPDPYPIRKGQRDLYSGLNQRRRI
Mouse	KNRKAKAKPVTRGTGAGSRPRGQNKERPPPVNPDPYPIRKGQRDLYSGLNQRAV
Macaque	KNRKAKAKPVTRGAGAGGRQRGQNKERPPPVNPDPYPIRKGQQDLYSGLNQRRRI
Marmoset	KNRKAKAKPVTRGVGAGGRQRGQNKERPPPVNPDPYPIRKGQRDLYSGLNQIRGI
Cow	KSRKAKASPMTRGAGAGGRPRGQNKGRPPPVNPDPYPIRKGQRDLYAGLNQRGV
Pig	KSRKAKAMPVTRGAGAGGRPRGQNRERPPPVNPDPYPIRKGQRDLYSGLNQIR
Sheep	KSRKAKATPMTRGAGAGGRPRGQNRERPPPVNPDPYPIRKGQRDLYSGLNQIRGV
Rabbit	KNRKAKCKPVTRGAGAGGRPRGQNKERPPPVNPDPYPIRKGQRDLYSGLNQIRGI
Dog	KTRKANAKPVMRGTGAGSRPRGQNKERPPPVNPDPYPIRKGQQDLYSGLNQIRGI
Cat	KNKKASSVTMMRGPAGGRPRGQNKERPPPVNPDPYPIRKGQQDLYSGLNQIRGI
Chicken	KNKKGQSR- - - - AAAGSRPRAQKMRPPPVNPDPYPIRKGQRDVYAGLEHRGE
Sterlet	QNRKKGAKPVTRGAGAGGRQRGQNKERPPPVNPDPYPIRKGQRDLYSGLNQRRRI

Figure 3. The cytoplasmic tail of CD3 ϵ shares a high degree of homology among numerous species. The amino acid sequence of the cytoplasmic tail of the indicated species is listed.

Protein Name	Region of Interaction	Function
CAST	BRS	NFAT activation/IL-2 production (40)
Topoisomerase	BRS	Unresolved function (41)
GRK2	BRS	Possible role in TCR/GPCR crosstalk (39)
Nck	PRS	Unresolved function (45)
Nucleolin	PRS	Possible role in T cell activation (101)
Eps8L1	PRS	Unresolved function (46)
ZAP-70 (Syk)	(PO ₄) ₂ -ITAM	Signal propagation/T cell activation (9)
P85 (PI3K)	(PO ₄) ₁ -ITAM	Possible role in signal propagation/T cell activation (102)
PKA (catalytic and RI α)	Unknown (Indirect)	Inhibits T cell proliferation and cytokine production (103)
Mink	Unknown (Indirect)	Thymocyte development (104)
G $\alpha_{q/11}$	Unknown	PLC- β activation (75)

CD3 ϵ : KNRKAKAKPVTRGAGAGGRQRGQNKERPPPVPNPDYEPIRKGQRDLYSGLNQRRRI

BRS: KNRKAKAKPVTRGAGAGGRQRGQNK

PRS: ERPPPVPNPDYE

ITAM: NPDYEPIRKGQRDLYSGLNQRRRI

Figure 4: Three subregions within the cytoplasmic tail of CD3 ϵ mediate distinct protein interactions. Biochemical analysis of the CD3 ϵ subunit has identified a number of proteins capable of differentially associating with the BRS, PRS, or PO₄-ITAM. The functional consequence of these protein interactions can result in distinct outcomes. In some cases, the result of the protein interaction has yet to be determined.

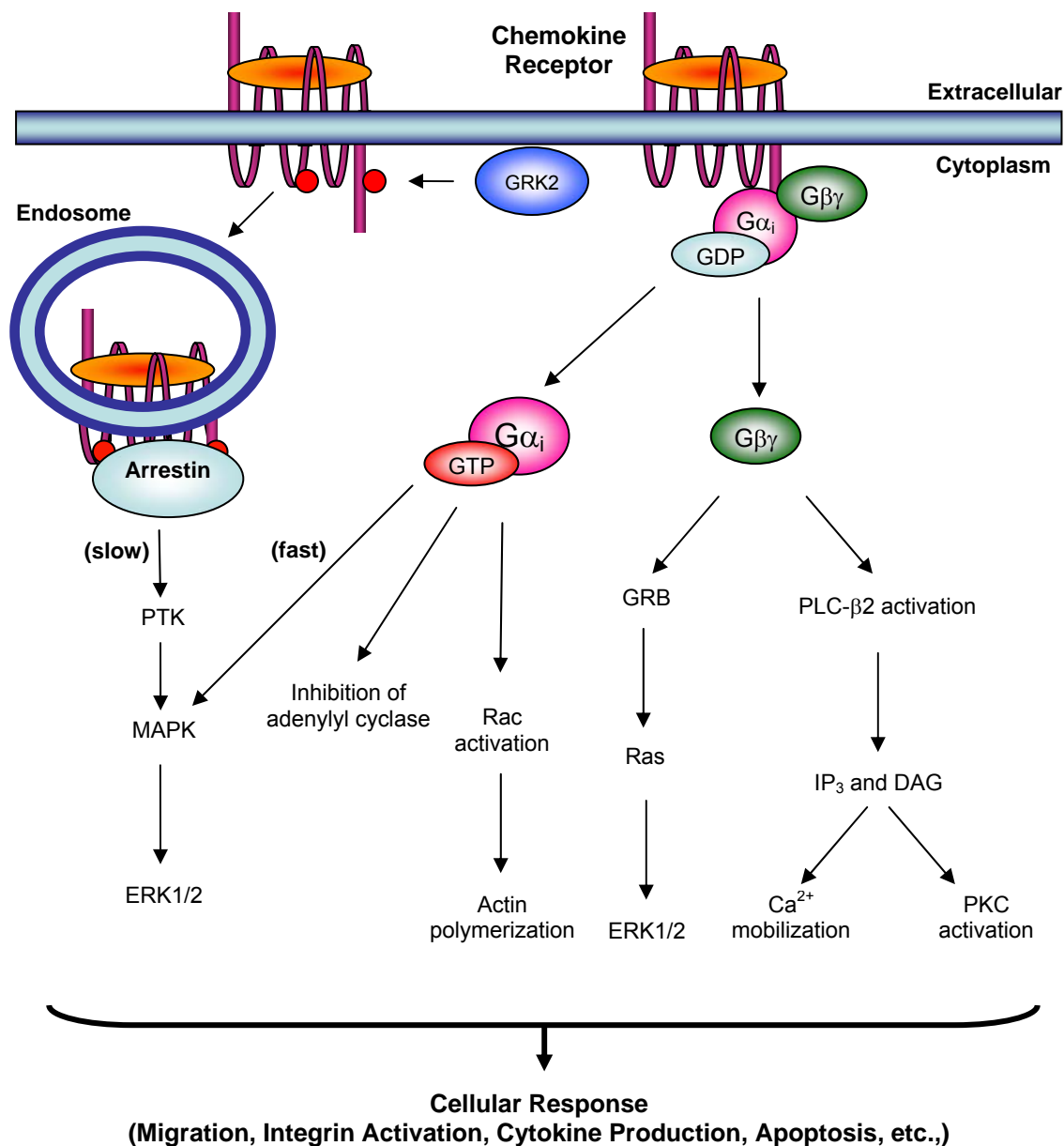


Figure 5. Signaling pathways induced by chemokine receptor ligation.

Agonist stimulation of chemokine receptors results in the exchange of GTP for GDP on the G α_i subunits. GTP•G α_i dissociates from G $\beta\gamma$ and goes on to activate effector proteins that are responsible for mediating changes to the cytoskeletal apparatus and/or transcription factors. The G $\beta\gamma$ subunits activate PLC family members, which hydrolyze PIP $_2$ into IP $_3$ and DAG. This results in a flux in intracellular calcium as well as the activation of PKC. GRK2 phosphorylation of the ligand-associated GPCR results in its endocytosis. Internalized GPCRs can also contribute to MAPK activation in a G protein-independent manner. Ultimately, these signaling events allow for a variety of cellular responses.

CHAPTER II

MATERIALS AND METHODS

Mice

Mice were housed in the Specific Pathogen Free Facility on the North campus at UT Southwestern Medical Center. All mouse procedures were undertaken with IACUC approved protocols.

The CD3 ϵ transgenic mice containing specific modifications to the BRS were generated by the Transgenic Core Facility at the University of Texas Southwestern Medical Center of Dallas. All injections were performed on a C57BL/6 background using the VA-CD2 transgenic cassette as described (105, 106). Transgenic founders were identified by PCR and confirmed by Southern blotting (Fig. 6). Transgenic founders were backcrossed onto a CD3 ϵ knockout background using CD3 ϵ deficient mice provided by Dr. Paul Love (National Institute of Child Health and Human Development, National Institutes of Health, Bethesda, Maryland). Genotyping of the BRS transgenic mice was carried out using the following primer sets:

For CD3 ϵ -/- typing: 5' TCT CCA TCT CAG GAA CCA GTG; 3' TAG TCT GGG TTG GGA ACA GG (Wild Type product size = 1.9 kb; Knockout and Heterozygote product size = 700 kb). 5' CCC CAC CCC TGT GTC CTG CAG; 3' GCC CTG CAG AGG ACA GAG GGG (Wild Type and Heterozygote product size = 680 bp; Knockout = no product). 5' GCA GGA AAG ACT CTG GTG CTG G; 3'

GCA CTC CAG GCG TTG GAG G (Wild Type and Heterozygote product size = 519 bp; Knockout = no product).

For detection of the VA-CD2 transgene: 5' GCT TTT TAT AGG TGC AGT CTC C; 3' GAG TTT TCT GCT GCC CCA TGG. All PCR reactions were performed using 1.5 mM MgCl₂, 0.5 μM of primers, 0.2 mM dNTPs, and 0.5U Taq DNA Polymerase (Roche). PCR conditions were as follows: Step 1 - 94°C (3 minutes); Step 2 - 94°C (30 seconds); Step 3 - 63°C (1 minute); Step 4 - 72°C (2.5 minutes); Step 5 - Recycle to Step 2 thirty-five times; Step 6 - 72°C (10 minutes). PCR products were analyzed by electrophoresis on 1% Agarose-TAE (40 mM Tris-acetate; 1 mM EDTA) gels.

Southern Blot Analysis

DNA isolated from tail snips was purified by phenol:chloroform extraction procedures. For Southern blotting 10 μg was digested with BamHI (Promega, Madison, WI). Digested samples were resolved by agarose gel electrophoresis and transferred onto positively charged nylon membranes (Bio-Rad, Hercules, CA), followed by hybridization with a 3' VACD2-specific ³²P-labelled probe. After washing, the membranes were exposed to x-ray film for 4 – 6 days at -80°C.

Antibodies

Anti-CD3 ϵ (145-2C11 and OKT3) and anti-Tac hybridomas were purchased from American Type Culture Collection (ATCC) (Manassas, VA). Monoclonal antibodies (mAbs) were purified from culture supernatants using standard affinity chromatography procedures. The anti-CD28 (37.51) hybridoma was kindly provided by Dr. J. Allison (University of California, Berkeley, CA). Anti-CD3 ζ (6B10.2) and anti-ZAP-70 (IE7.2) were used as described (107). Anti-GRK2/3, anti-Myc (9E10), and anti-phosphotyrosine (4G10) were purchased from Upstate Cell Signaling Solutions (Lake Placid, NY). Anti-HPK1 was purchased from Cell Signaling Technology, Inc. (Danvers, MA). Anti-GST and anti-PKA_c were obtained from BD Biosciences (Franklin Lakes, NJ). Goat anti-mouse and goat anti-rabbit secondary antibodies conjugated to horse radish peroxidase (HRP) were purchased from Bio-Rad Laboratories. Donkey anti-goat-HRP was from Santa Cruz, while the goat anti-mouse-HRP utilized for anti-phosphotyrosine immunoblotting was obtained from Zymed Laboratories (San Francisco, CA). Monoclonal antibodies utilized for flow cytometric analysis, including biotin-, fluorescein-, phycoerythrin-, cychrome-, peridinin chlorophyll protein-cyanin 5.5 tandem-, phycoerythrin-cyanine 7-, and allophycocyanin-conjugated anti-CD3 ϵ , -CD4, -CD8, -CD25, -CD44, -B220, -Thy1.2 and -NK1.1, were purchased from BD Pharmingen (San Diego, CA).

Recombinant Proteins

Recombinant murine SDF-1 α was purchased from R&D Systems (Minneapolis, MN), while recombinant bovine GRK2 was a kind gift from Dr. John Tesmer (University of Michigan, Ann Arbor, MI).

Cell Lines and Plasmids

Jurkat T cells, P116 (ZAP-70^{-/-}) Jurkat T Cells, and HEK293 T cells were obtained from ATCC. S49 Wild Type (subclone 24.3.2) and S49 kinase^{-/-} (subclone 24.6.1) Balb/c lymphoma cells were obtained from the UCSF Tissue Culture Facility (San Francisco, CA). pGEX-2TK was from Amersham Bioscience Corp (Piscataway, NJ) while pcDNATM 3.1/myc-HIS was from Invitrogen (Carlsbad, CA).

Fusion Protein Preparation

The GST-CD3 ϵ constructs were derived by PCR based strategies and/or site-directed mutagenesis procedures (Stratagene, La Jolla, CA). Primer sets used are as follows: *GST- ϵ* : 5' GTT GGA TCC AAG AAT AGG AAG GCC AAG G; 3' ATG AAT TCT CAG ACT GCT CTC TGA TTC AGG. *GST-BRS-1*: 5' GTT GGA TCC AAG AAT AGG AAG GCC AAG G; 3' ATG AAT TCT CAC CCT CTG GGC CTG CTA CC. *GST-BRS-2*: 5' GTT GGA TCC GCC AAG GCC AAG CCT GTG AAC; 3' ATG AAT TCT CAC CCT CTG GGC CTG CTA CC. *GST-BRS-3 (h)*: 5' AGG GAT

CCG CCA AGC CTG TGA C; 3' ATG AAT TCC CCT TTG CCT GCC. *GST-BRS-4*: 5' GTT GGA TCC AAG AAT AGG AAG GCC AAG G; 3' ATG AAT TCT CAC CTG CCG CCA GCA CCC GCT CC. *GST-BRS-5*: 5' GTT GGA TCC AAG AAT AGG AAG GCC AAG G; 3' ATG AAT TCT CAG CCA GCA CCC GCT CCT CG. *GST-BRS-NtoA*: 5' GTT GGA TCC AAG GCT AGG AAG GCC AAG G; 3' ATG AAT TCT CAC CCT CTG GGC CTG CTA CC. *GST-BRS-KxxK to A/G*: 5' GTT GGA TCC GCG AAT AGA GGG GCC AAG GCC; 3' ATG AAT TCT CAC CCT CTG GGC CTG CTA CC. *GST-BRS-RxxK to V/I*: 5' GTT GGA TCC AAG AAT GTG AAG GCC ATC GCC AAG C; 3' ATG AAT TCT CAC CCT CTG GGC CTG CTA CC. *GST-BRS-KxR to A/V*: 5' GTT GGA TCC GCG AAT GTG AAG GCC AAG G; 3' ATG AAT TCT CAC CCT CTG GGC CTG CTA CC. *GST-PRS (h)*: 5' GAT CCG AGA GGC CAC CAC CTG TTC CCA ACC CAG ACT ATG AGT GAG G; 3' AAT TCC TCA CTC ATA GTC TGG GTT GGG AAC AGG TGG TGG CCT CTC G. *GST-ITAM (h)*: 5' GTG GAT CCA ACC CAG ACT ATG AG; 3' ATG AAT TCC TCA GAT GAT GCG TCT.

E. coli BL21 (DE3) pLys S were transformed with the indicated pGEX-2TK expression vector encoding the appropriate CD3 construct. An overnight culture was grown at 37°C (Media = LB; Antibiotic = Ampicillin). This starter culture was used to inoculate a larger culture, which was grown at 37°C until OD=0.3 ($\lambda = 595$). Protein expression was induced by the addition of 0.3 mM IPTG. Four hrs later, the cells were pelleted and resuspended in lysis buffer (50 mM Tris-Cl (pH 7.6), 0.1% Triton X-100, 150 mM NaCl, 5 mM EDTA, 5 mM 2-mercaptoethanol, 1 mM NaF, and protease inhibitors). The lysate was sonicated with three 30 second bursts, interspersed by 1

minute intervals (Duty cycle = 40%; Output Control = 4). The lysates were then cleared by centrifugation, and the supernatant was added to Glutathione Sepharose™ beads for 1.5 hrs at 4°C (Amersham Bioscience Corp). The beads were pelleted, washed 3 times in PBST (1X PBS (without Ca²⁺/Mg²⁺), 1% Triton X-100, 2 mM EDTA, 5 mM DTT, 5 mM benzamidine, 1 mM NaF, and 5% glycerol), and stored at 4°C.

Murine GRK2 was cloned from RNA isolated from thymocytes. Full-length GRK2 was subcloned into the mammalian expression vector pcDNA™ 3.1/myc-HIS. GRK2 sequences were verified by dsDNA sequencing (DNA Sequencing Core Facility, UTSW).

Affinity Column Preparation

GST-BRS bound to Glutathione Sepharose was washed in 0.2 M sodium borate (pH 9.0). The GST-BRS was then covalently coupled to the bead matrix by the addition of 20 mM dimethylpimelimidate (Pierce, Rockford, IL). Following a 1 hr incubation at room temperature, the reaction was quenched by the addition of 0.2 M Tris (pH8.0), washed in PBS, and stored at 4°C in the presence of 0.1% sodium azide. The efficiency of covalent coupling between GST-BRS and Glutathione Sepharose was determined by gel electrophoresis and Coomassie blue staining.

Isolation of CD3 ϵ From Surface Versus Intracellular Pools

Primary murine thymocytes were resuspended at 1.0×10^8 cells/ml in 1X Dulbecco's Phosphate-Buffered Saline (DPBS) containing calcium and magnesium (Mediatech Inc., Herndon, VA). Primary lymphocytes were resuspended at 1.0×10^7 /ml. Anti-CD3 ϵ (145-2C11) or anti-CD28 (37.51) was added to the single cell suspensions at 10 μ g/ml. The cells were incubated at 4°C for 30 minutes, followed by 2 washes in ice-cold DPBS. The cells were then lysed in a 1% Triton X-100 lysis buffer and immunoprecipitations were performed by adding 20 μ ls of Protein A Sepharose 4 Fast Flow (1:1 slurry) (Amersham Bioscience Corp). The lysates were incubated for 1.5 hrs at 4°C, followed by centrifugation. The supernatants were removed and incubated with 4 μ g of anti-CD3 ϵ (145-2C11) or anti-CD28 (37.51) for an additional 1.5 hrs at 4°C.

Immunoprecipitations, Western Blots, and In Vitro Kinase Reactions

Thymocytes were lysed at 2.0×10^8 cells/ml in a 1% Triton X-100 containing lysis buffer, pH 7.6 (20 mM Tris-HCl, 30 mM NaCl, 2 mM EDTA, 1 mM NaF, and protease inhibitors). Immunoprecipitations or GST pull-downs were undertaken with Protein A/G Seize® Coated Plates (Pierce, Rockford, IL) or Glutathione Coated HS Plates (Sigma-Aldrich, Inc., St. Louis, MO) according to the manufacturer's instructions. Kinase reactions were carried out for 30 min at 30°C in a reaction mix containing 50 μ l kinase buffer (50 mM Tris-HCl (pH 7.6), 2 mM MnCl₂, 2 mM MgCl₂, 1 mM benzamidine, 1 mM sodium fluoride, 0.05% Triton X-100, and 1 mM

phenylmethylsulfonyl fluoride), 0.3 μM ATP and 1 μl of radiophosphate (10 $\mu\text{Ci}/\mu\text{l}$ of [γ - ^{32}P]ATP; Amersham Bioscience Corp). In certain assays, 2.5 μg of myelin basic protein (MBP) was added as an exogenous substrate.

Kinase reactions were stopped by adding 20 μl of pre-warmed 4X SDS-sample buffer (0.16 M Tris (pH 6.8), 4% SDS, 0.2 M DTT, 20% glycerol, 0.02% bromphenol blue). Proteins were resolved by SDS-PAGE and transferred onto a PVDF membrane (Millipore Corporation). Radiolabeled proteins were visualized using a Storm 820 phosphoimager (Amersham Bioscience Corp). Data was analyzed/quantified using ImageQuant software and represented as relative light units (RLU) for graphing.

For inhibitory studies, the kinase inhibitors were added to CD3 ϵ immunoprecipitates 10 minutes prior to the addition of the kinase reaction mix. Kinase reactions were then carried out for 30 minutes at 30°C in the presence of the indicated kinase inhibitor and MBP. The inhibitors were used at the following concentrations: SB203580 (10 μM), PD098059 (50 μM), Piceatannol (25 $\mu\text{g}/\text{ml}$), Wortmannin (100 μM), Bisindolylmaleimide (5 μM), Ly294002 (10 μM).

For western blot analysis, proteins were resolved by SDS-PAGE, transferred onto PVDF, and visualized using the Pierce ECL western blotting substrate.

Phosphoamino Acid Analysis

Phosphoamino acid content was determined as detailed (108). Briefly, following *in vitro* kinase reactions, the region of PVDF membrane corresponding to the area where ^{32}P -labeled proteins were detected by autoradiography was cut and rehydrated with

methanol, followed by ddH₂O washing. The extracted bands were then incubated with 200 μ l of 6 N Sequanal Grade Constant Boiling Hydrochloric Acid (Pierce) at 110°C for 2–4 hrs. The supernatant was transferred to a clean 1.5 ml eppendorf tube and dried overnight using a speedvac. Pellets were resuspended in 8 μ l of a pH 1.9 buffer (2.5% formic acid; 7.8% acetic acid) containing PO₄-Y, PO₄-S, and PO₄-T standards. Samples were spotted onto a Kodak TLC plate, allowing samples to air dry between the application of each spot (this step was important to keep sample as concentrated as possible). The TLC plate was overlaid with electrophoresis buffer (0.5% pyridine; 5% acetic acid) and resolved using a flatbed electrophoresis apparatus (600 volts at 4°C for 2 hours). The TLC plate was dried in a 37°C incubator for ~10 minutes, sprayed with 0.3% ninhydrin (prepared in acetone), and allowed to air dry. Phosphoamino acids were visualized by autoradiography.

SDF-1 α Stimulations

Recombinant SDF-1 α treatment was performed as described (61, 109). Briefly, single cell suspensions of primary murine thymocytes were prepared. Cells were resuspended at 1.5×10^8 cells/ml in 1X Dulbecco's Phosphate-Buffered Saline (DPBS) containing calcium and magnesium (Mediatech Inc., Herndon, VA). Cells were then placed at 37°C and incubated for 30 minutes with or without the addition of recombinant murine SDF-1 α (5.0×10^{-8} M final concentration). The cells were then washed 2 times in cold DPBS and lysed in 1% Triton X-100 containing lysis buffer for 30 minutes on ice.

The lysates were cleared by centrifugation, and immunoprecipitations and *in vitro* kinase reactions were performed as previously described in this chapter.

Chromatography Purifications

Buffer A: 50 mM Tris-HCl (pH 7.6), 2 mM 2-mercaptoethanol. Buffer B: Buffer A plus 1 M NaCl. Cellular preparations were generated from 6.5×10^9 murine thymocytes. Cells were washed 3 times in phosphate-buffer saline. Pelleted cells were then resuspended in Buffer A, supplemented with protease and phosphatase inhibitors, using a buffer volume 10 times the pellet size. The cells were dounce homogenized with 30 strokes and incubated on ice for an additional 15 minutes. Supernatants were obtained following a high-speed spin (28,000 RPM for 1 h at 4°C), filtered through a 0.22 μ m syringe filter (Millipore, MillexTM), and applied to a 2.5 x 30-cm anion-exchange column linked to an FPLCTM system (Q-Sepharose, Amersham Bioscience). Proteins retained on the column were eluted with a linear salt gradient (Buffer B) at a flow rate of 2.5 ml/min. Eighty 10 ml fractions were collected. An aliquot from each fraction was analyzed for the GST-BRS-associated kinase activity as previously described. Samples with the greatest kinase activity were pooled and diluted 1:2 in Buffer A. This was applied to a GST-BRS-affinity column. Proteins retained on the affinity matrices were eluted with a linear salt gradient (Buffer B) at a flow rate of 0.5 ml/min. Forty-five 2 ml fractions were collected. Fractions were assayed for kinase activity by GST-BRS pull-downs and kinase reactions as described.

Acetone precipitations were performed by adding 15 μ l of 20% SDS, 6 μ l of DTT (1 M), 2 μ l glycogen (20 mg/ml) and 1 ml of acetone (-80°C) per 300 μ l of sample. Samples were centrifuged for 10 min at 13,000-15,000 x g. The pellet was air-dried, resuspended in SDS-sample buffer, and resolved by SDS-PAGE. The gel was then silver stained using a GelCode® SilverSNAP® Stain Kit II (Pierce) according to the manufacture's instructions. Silver stained bands were submitted to the Protein Chemistry Technology Center at the University of Texas Southwestern Medical Center for trypsin digestion and mass spectrometry analysis.

Transfections and siRNA Knockdown

HEK 293 T cells were transfected using a standard CaPO₄ method as described (110). Briefly, HEK293 cells were grown at 37°C in DMEM (supplemented with 10% FBS, 1% L-glutamine, and 1% penicillin/streptomycin) in a 6 well-plate (3 ml/well). Once the cells reached 80% confluence, 12.5 μ l of 30 μ M chloroquine was added to each well and incubated at 37°C for 15 min. During the incubation, 5 μ g of the appropriate DNA plasmid was added to 428 μ l of sterile water and 62 μ l of 2 M CaCl₂. This was then added drop-wise to 500 μ l of HeBS (0.28 M NaCl, 0.05 M HEPES, 1.15 mM Na₂HPO₄, pH 7.6). This was added directly to the cells and allowed to incubate for 8 hrs at 37°C. The cells were then washed and fresh media was added. Following a 48 hr incubation, the cells were harvested and analyzed by western blotting.

RNA interference was carried out using a GRK2 (h) siRNA (Santa Cruz Biotechnology, Inc., Santa Cruz, CA) as described (111). Briefly, 5 x 10⁶ Jurkat T cells

were suspended in 500 μ l of RPMI (supplemented with 10 mM dextrose, 1% L-glutamine, and 20% fetal bovine serum). The cells were transferred to a 0.4 cm cuvette (Bio-Rad) and electroporated at 300 v/975 μ F in the presence of 10 μ l of 20 μ M siRNA. Following the electroporation, the cells were resuspended in 10 ml of RPMI (supplemented with 10% FBS) and incubated at 37°C for 24 hours. The following day, the electroporation was repeated, and the cells were allowed to recover an additional 24 hours. On the third day, the cells were split into two 10 ml cultures and allowed to expand 24 hours. On the fourth day, the cells were harvested and analyzed by *in vitro* kinase reactions and western blotting.

Phospholipid Binding

PIP Strips (Echelon Biosciences Incorporated, Salt Lake City, UT) were blocked for 1 hr at room temperature in 3% fatty acid-free BSA prepared in TBST (25 mM Tris, 125 mM NaCl, 0.1% Tween-20; pH 8.0). The membranes were then incubated overnight at 4°C with purified GST-tagged proteins at 5 μ g/ml in 1% fatty acid-free BSA/TBST. The membranes were washed and immunoblotted with anti-GST according to standard procedures. GST-fusion protein binding was assessed by the use of the Pierce ECL western blotting substrate.

For the generation of liposomes, lipid mixtures containing 100% phosphatidylcholine (PC) or a combination of 80% PC plus 20% of either phosphatidylinositol (PI), phosphatidylinositol 4-monophosphate (PI(4)P), or phosphatidylserine (PS) were resuspended in a HEPES buffer (50 mM HEPES (pH 7.0),

100 mM NaCl, 1 mM EDTA) containing 0.5 M sucrose and sonicated for 2-5 minutes in a water bath sonicator. The resulting liposomes were then pelleted, washed, and resuspended in HEPES buffer (without sucrose). Three μM of GST alone or GST-BRS was then incubated with 100 μg of liposomes containing the desired lipid content for 15 minutes at 4°C. The liposomes were pelleted by centrifugation (13,000 RPM at 4°C), washed three times in HEPES buffer (without sucrose), resuspended in 20 μl of SDS-sample buffer, and resolved by 12.5% SDS-PAGE. The ability of the GST-fusion proteins to bind the liposomes was assessed as previously described by anti-GST immunoblotting.

FACS Analysis

Flow cytometry was performed using FACScan and FACSCalibur cytometers. Analysis of cytometric data was performed using CellQuest Pro or Flo Jo software.

Stimulations

The lymph nodes of mice were isolated and single cell suspensions were prepared. The cells were resuspended in PBS (with $\text{Ca}^{2+}/\text{Mg}^{2+}$) at 1.0×10^8 cells/ml treated with anti-CD3 ϵ (10 $\mu\text{g}/\text{ml}$) and anti-CD28 (3 $\mu\text{g}/\text{ml}$) for 10 minutes at 37°C. The cells were then washed 2 times in cold PBS, resuspended in 1% Triton X-100 lysis buffer at 2.0×10^8 cells/ml, and incubated on ice for 30 minutes. 15-20 μl of whole cell lysate was added to 5 μl of 4X SDS-sample buffer and resolved by electrophoresis.

For CD69 FACS profiles, the cells were harvested sterily and resuspended at 1.0×10^5 cells/ml in RPMI containing 10% fetal bovine serum. The cells were then incubated in a $37^\circ\text{C}/\text{CO}_2$ incubator for 12-16 hours with or without CD3 ϵ ($10\mu\text{g}/\text{ml}$) and CD28 ($3\mu\text{g}/\text{ml}$). Then cells were washed in PBS and stained using anti-CD69 mAbs.

For pervanadate treatments, a stock of pervanadate (10 mM sodium orthovanadate; 1.0 M H_2O_2) was prepared in PBS (with $\text{Ca}^{2+}/\text{Mg}^{2+}$) just before use (112). This was added to single cell suspensions (1.0×10^8 cells/ml in PBS) for a final concentration of 100 μM sodium orthovanadate; 10 mM H_2O_2 . The cells were then incubated at 37°C for 10 minutes, pelleted, and lysed according to normal procedures.

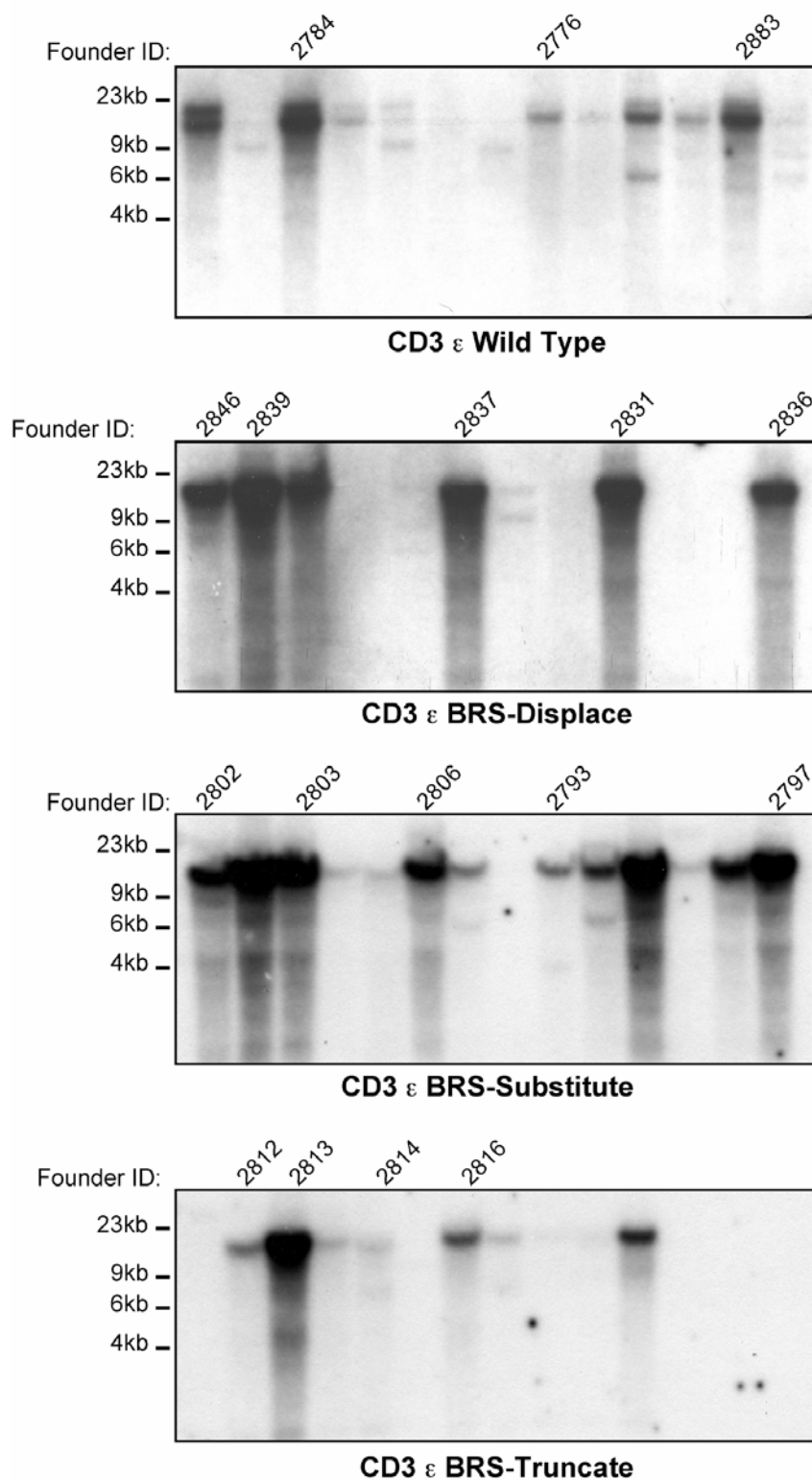


Figure 6. Southern blot analysis of the CD3 ϵ BRS-transgenic founders. Tail DNA from numerous transgenic founders was subjected to Southern blot analysis. Mice from the various CD3 ϵ transgenic lines that were chosen to be backcrossed onto a CD3 ϵ null background are indicated by their founder identification number.

Table I. Quantitation of protein expression in several of the CD3 ϵ BRS transgenic mice. The listed CD3 ϵ transgenic founders were backcrossed onto a CD3 $\epsilon^{-/-}$ background. The relative amount of CD3 ϵ protein expression was determined by western blot analysis of thymocyte whole cell lysates.

CD3 ϵ Transgenics	Founder	Designation	Relative CD3 ϵ Expression
Wild Type C57BL/6		B6	Normal (1X)
CD3 ϵ BRS-Wild Type	2883	CD3 ϵ WT.30	Intermediate (1.5 \rightarrow 2X)
CD3 ϵ BRS-Substitute	2802	KRtoA.6	Intermediate (1.5 \rightarrow 2X)
	2806	KRtoA.16	Intermediate (1.5 \rightarrow 2X)
CD3 ϵ BRS-Truncate	2812	KNRdel.6	Normal (1X)
	2813	KNRdel.8	Intermediate (1.5 \rightarrow 2X)
	2814	KNRdel.17	Low (< 0.5X)
	2816	KNRdel.23	Intermediate (1.5 \rightarrow 2X)
CD3 ϵ BRS-Displace	2837	BRSdis.20	Intermediate (2 \rightarrow 2.5X)
	2831	BRSdis.25	Intermediate (1.5 \rightarrow 2X)

CHAPTER III

IDENTIFICATION AND CHARACTERIZATION OF A NOVEL INTERACTION BETWEEN THE MEMBRANE-PROXIMAL BASIC-RICH STRETCH OF CD3 ϵ AND THE SERINE/THREONINE KINASE GRK2

Introduction

The activation of protein kinases is one of the primary mechanisms whereby the TCR propagates intracellular signals (113). Protein kinases are a type of enzyme that function by removing the γ -phosphate from adenosine triphosphate (ATP) and covalently attaching it to the hydroxyl group of a tyrosine, serine, threonine or histidine residue located within a substrate protein. To date, over 500 protein kinases have been identified in eukaryotic organisms and represent approximately 1.7% of all genes in the human genome (114). Protein kinases are divided into three groups based on the amino acid which they phosphorylate. In eukaryotic organisms, the majority of known kinases phosphorylate both serine and threonine residues (Ser/Thr kinases). Protein tyrosine kinases (PTK) preferentially phosphorylate tyrosine residues, while a third variety of kinases, known as dual-specificity kinases, can phosphorylate serine, threonine, and tyrosine residues.

Although Ser/Thr kinases constitute the bulk of kinases in eukaryotic cells, the majority of kinases identified in the earliest stages of TCR signaling are PTKs (113). As previously described, TCR ligation results in the phosphorylation of the CD3 ITAMs by PTKs belonging to the Src family (115). The phosphorylated ITAMs then serve as docking sites for additional PTKs, including ZAP-70 and PI3K. Ultimately, these early

PTK cascades will elicit the activity of numerous Ser/Thr kinases. Examples include PKA, ERK 1/2, p21-activated kinase (PAK), and PKC family members, particularly PKC θ (103, 116-118).

It is interesting to note that kinases activated through TCR engagement have also been demonstrated to influence the activity of other cell surface receptors, including chemokine receptors. For example, following engagement of CXCR4, a physical association between this chemokine receptor and the TCR occurs, allowing CXCR4 to use signaling molecules associated with the TCR, particularly ZAP-70, to propagate its own signals (61). TCR-mediated activation of PKC family members also causes the negative regulation of CXCR4 (63).

Mutations or dysregulation of the kinases involved in TCR signaling can often have dramatic consequences (119). For example, patients deficient in ZAP-70 are severely immunocompromised due to an inability of their T cells to initiate signaling cascades through the TCR (Reviewed in (120)). Additionally, mice possessing mutations within the SH2 domain of ZAP-70 exhibit chronic autoimmune symptoms due to alterations in the threshold of signaling during T cell development (121). The finding that protein kinases can play a direct role in the development of disease emphasizes the importance of defining which kinases are involved in TCR-mediated signaling cascades. Herein, we describe the biochemical identification of a constitutive interaction between the CD3 ϵ subunit of the TCR and the Ser/Thr kinase, GRK2. Although certain Ser/Thr kinases, including PKA, have been demonstrated to inducibly associate with CD3 ϵ following TCR engagement, to our knowledge, this is the first evidence that one of the signaling subunits of the TCR can constitutively interact with a Ser/Thr kinase.

Furthermore, given the nature of GRK2 functions within T cells, it is likely that this interaction allows the TCR to crosstalk with GPCRs, such as CXCR4.

Results

CD3 ϵ Associates with a Kinase Activity

The cytoplasmic domains of the CD3 subunits contain a number of signaling motifs, including the PRS and ITAMs. These motifs are known to mediate protein-protein interactions with as many as ten distinct effector/adaptor proteins (Fig. 4) (Reviewed in (8)). Given the fact that protein kinases play such a prominent role in TCR-mediated signaling events, we were interested in determining whether the cytoplasmic tails of the CD3 chains could associate with protein kinases other than ZAP-70 (a PTK known to interact with the bi-phosphorylated ITAMs). In order to address this, GST-fusion proteins containing the cytoplasmic regions of CD3 γ , δ , ϵ , or ζ were generated and used as affinity ligands to pull down associating proteins from unstimulated thymocyte lysates. After washing, the pull-downs were subjected to *in vitro* kinase reactions in the presence of [γ - 32 P]ATP. Associating proteins were resolved by SDS-PAGE, and phosphoproteins were visualized by autoradiography. Using this method, GST- ϵ was found to associate with kinase activity, as indicated by the presence and intensity of a number of 32 P-labeled proteins of varying molecular weights (Fig. 7; Lane 3). Only a modest amount of kinase activity was detected following GST- γ , - δ , or - ζ pull-downs (Lanes 1, 2 and 4).

Because GST-fusion proteins could non-specifically absorb to kinases present in cell extracts, we next sought to determine whether full-length CD3 ϵ could associate with a kinase when directly isolated from primary cells. Full-length CD3 ϵ was

immunoprecipitated from WCLs derived from unstimulated thymocytes. The immunoprecipitates were then washed and analyzed by *in vitro* kinase reactions. As seen, when CD3 ϵ was directly precipitated a significant amount of kinase activity could be detected (Fig. 8A; *Lane 1*). A small amount of activity was also observed with CD3 ζ immunoprecipitates. This activity was most likely due to the fact that antibodies directed against CD3 ζ can precipitate the entire TCR complex, including the CD3 ϵ chain and its associating proteins. As expected, immunoprecipitation of ZAP-70 also resulted in the visualization of a kinase activity. However, the banding pattern of the ^{32}P -labeled proteins detected in both the CD3 ϵ and CD3 ζ precipitates were distinct from those observed following ZAP-70 immunoprecipitations (*Lane 3*). These results indicated that the kinase activity associating with CD3 ϵ was not due to interactions with ZAP-70. Finally, no substantial activity was detected in either the CD28 immunoprecipitations or in the NMS controls (*Lanes 4 and 5*).

In thymocytes and peripheral T cells, CD3 ζ is constitutively phosphorylated on two of its three ITAMs as a result of ongoing TCR interactions with self-peptide/MHC complexes (106, 122). Following agonist-peptide/MHC cross-linking, the remaining ITAM of the CD3 ζ chains is rapidly phosphorylated, followed by the association of ZAP-70. Because phosphorylation of the CD3 ζ ITAMs is among the earliest events that can be detected following TCR engagement, the CD3 ζ chains have been considered the predominant signaling module of the TCR complex. Consequently, we wanted to address whether interactions between CD3 ϵ and its associating kinase activity required the expression of a CD3 ζ chain with functional ITAMs. This was accomplished using a series of CD3 ζ transgenic mice, termed the YF1-6 CD3 ζ transgenic line. These mice

contain select tyrosine-to-phenylalanine substitutions for the tyrosine residues located in the CD3 ζ ITAMs (Fig. 8B) (21, 122). These amino acid substitutions effectively eliminate the ability of the CD3 ζ subunits to be phosphorylated both *in vivo*, as well as following strong agonist cross-linking *in vitro*. To address whether the CD3 ζ ITAMs were capable of contributing to the CD3 ϵ -associated kinase activity, CD3 ϵ was directly immunoprecipitated from YF1-6 thymocyte lysates. The immunoprecipitates were then analyzed by *in vitro* kinase reactions. Even in the absence of phospho-CD3 ζ , phosphoimaging revealed that CD3 ϵ associated with a kinase activity several orders of magnitude more than the control CD28 and NMS immunoprecipitations (Fig. 8B; *Lanes 1, 4, and 5*). Furthermore, the ^{32}P -labeled bands in the CD3 ϵ samples were distinct from that observed with ZAP-70 immunoprecipitates. Taken together, these results indicated that CD3 ϵ was the only invariant chain capable of constitutively coupling to a kinase activity. Additionally, the kinase activity associating with CD3 ϵ was independent of the phosphorylation state of the CD3 ζ ITAMs.

Interactions between CD3 ϵ and Its Associated Kinase Activity Occur Independently of ZAP-70

To assess whether ZAP-70 might contribute to the CD3 ϵ -associated kinase activity, CD3 ϵ immunoprecipitates were western blotted using mAbs against ZAP-70 (Fig. 9A). While ZAP-70 was detected in ZAP-70 immunoprecipitations (*Lane 1*), neither CD3 ϵ immunoprecipitates nor GST- ϵ pull-downs contained any detectable ZAP-70 (*Lanes 2 and 5*).

Due to the much greater sensitivity of *in vitro* kinase assays when compared to western blotting, it was still possible that ZAP-70 affected the CD3 ϵ -associated kinase activity. To examine whether ZAP-70 was involved, a Jurkat T cell line deficient in ZAP-70 expression was utilized (123). Western blot analysis confirmed the absence of ZAP-70 in the P116 Jurkat T cells (Fig. 9B; *upper panel*). ZAP-70 and CD3 ϵ immunoprecipitations/kinase reactions were then performed using WCLs derived from either wild type Jurkat or the P116 Jurkat T cells. (58). MBP was added to verify that the kinase(s) associating with each immunoprecipitation would have an equivalent amount of substrate protein available to phosphorylate (Fig. 9B; *lower panel*). As a result, variations in the amount of kinase activity detected should reflect differences in the amount of kinase present in each immunoprecipitate, rather than the level of substrate. As seen, the kinase activity associated with ZAP-70 immunoprecipitates was reduced to background levels in the ZAP-70 deficient cells (*Lane 1 vs. 4*). In contrast, an equivalent level of CD3 ϵ -associated kinase activity was detected in both the wild type and P116 Jurkat T cells (*Lanes 2 and 5*). These results demonstrated that the CD3 ϵ -associated kinase was not ZAP-70. It also indicated that the catalytic activity of the CD3 ϵ -associated kinase was not regulated by ZAP-70.

Interactions between CD3 ϵ and Its Associated Kinase Activity Primarily Occur within Intracellular Compartments

Certain PTKs, such as Lck and ZAP-70, are known to interact with CD3 ϵ at the cell surface, thereby contributing to early TCR-mediated signal propagation (57).

Conversely, nucleolin and topoisomerase II β , have been hypothesized to bind CD3 ϵ within intracellular compartments, such as the nucleus (101). Given the fact that CD3 ϵ can differentially interact with proteins depending on its intracellular location, we sought to determine whether interactions between CD3 ϵ and the unidentified kinase were occurring at the cell surface or within subcellular compartments. For these studies, we utilized the 5C.C7 TCR transgenic mice. This was due to the fact that the presence of a transgene within these animals allows for a substantial increase in the level of TCR expression as compared to C57BL/6 mice (Fig. 10A). Experimentally, thymocytes were harvested from 5C.C7 mice, and T cells were stained at 4°C using mAbs directed against the extracellular portion of either CD3 ϵ or CD28. The stained cells were thoroughly washed to remove unbound antibody and lysed. Protein A Sepharose was then used to precipitate the Ab/protein complexes. Residual proteins that remained in the supernatant were precipitated with the addition of more anti-CD3 ϵ or anti-CD28. All samples were then subjected to *in vitro* kinase reactions in the presence of MBP. CD3 ϵ isolated from intracellular compartments associated with 82 \pm 16.5% more kinase activity than that observed in surface immunoprecipitations (p value \leq 0.05) (Fig. 10B). Almost no kinase activity was detected in CD28 immunoprecipitations prepared from cell surface or intracellular pools. The presence of over 80% more kinase activity associating with CD3 ϵ isolated from subcellular compartments strongly suggested that the CD3 ϵ /kinase interactions primarily occurred within intracellular compartments.

CD3 ϵ Constitutively Associates with a Serine/Threonine Kinase Distinct from the PKC, PI3K and MAPK Families

Because interactions between CD3 ϵ and its associating kinase were present when cells were taken *ex vivo*, we next sought to address the affects of TCR cross-linking. Thymocytes were stimulated with α -CD3 ϵ for varying time points, lysed, and CD3 ϵ immunoprecipitations/kinase reactions were performed. The CD3 ϵ -associated kinase activity increased by 16-21% after both 10 and 30 minutes of stimulation (Fig. 11; *Lanes 1-3*). Pre-culturing the cells for 4 hrs at 37°C reduced the CD3 ϵ -associated kinase activity (Fig. 11; *Lane 4*). When the cultured cells were stimulated, the kinase activity increased by 62% (Fig. 11; *Lane 6*).

As previously mentioned, Ser/Thr kinases, PTKs, and dual-specificity kinases play a pivotal role in TCR signaling. To elucidate the type of kinase(s) associating with CD3 ϵ , the phosphoamino acid content of several of the prominent ^{32}P -labeled bands obtained from CD3 ϵ immunoprecipitations was determined, including that of an exogenously added substrate, MBP (Fig. 12A). In the bands obtained from the CD3 ϵ immunoprecipitations/kinase reactions, a 1:1 ratio of ^{32}P -serine and ^{32}P -threonine was detected (Fig. 12B; *Lanes a, b, and d*). ^{32}P -tyrosine was only observed when immunoprecipitates from known PTKs, such as ZAP-70, were analyzed (*Lane c*). These results confirmed the presence of a Ser/Thr kinase.

To characterize the family to which the CD3 ϵ -associated kinase belonged, kinase reactions were performed in the presence of various kinase inhibitors, including inhibitors of PI3K, PKC, and MAPK families. Piceatannol, a resveratrol analog that blocks the

activity of certain Ser/Thr kinases and Syk family members, was the only inhibitor from this panel that consistently decreased the level of the CD3 ϵ -associated kinase activity (Fig. 12C; *Lanes 5 and 6*) (124, 125). Kinase reactions in the presence of wortmannin inhibited the CD3 ϵ -associated kinase activity to a small degree. However, this outcome was not consistent. Results using this panel of inhibitors strongly suggested that the CD3 ϵ -associated Ser/Thr kinase was distinct from the PKC, PI3K, and MAPK families.

The Membrane-Proximal Basic-Rich Stretch of CD3 ϵ Mediates the Kinase Interaction

Next, we wanted to identify the region(s) within the cytoplasmic tail of CD3 ϵ responsible for the Ser/Thr kinase association. Several sequence motifs within the cytoplasmic tail of CD3 ϵ are known to mediate protein interactions. These include the previously mentioned PRS and ITAM, as well as a region that we termed the basic-rich stretch (BRS) due to its high lysine and arginine content (Fig. 13; BRS, PRS, and ITAM) (40, 41, 45). GST-fusion proteins consisting of the BRS, PRS, or ITAM were used in pull-down/kinase assays. GST-BRS was the only fusion protein that associated with the kinase activity (Fig. 13).

The GST-tagged BRS construct contained the first 25 amino acids located within the membrane-proximal portion of CD3 ϵ (Fig. 14; GST-BRS-1). To define the amino acid sequence required for the kinase interaction, an additional series of GST-fusion proteins that contained truncations from the NH₂-terminal (GST-BRS-2 & -3) or COOH-terminal (GST-BRS-4 & -5) of the BRS were generated (Fig. 14). Elimination of the first 4 or 6 residues of the BRS at the NH₂-terminal significantly decreased the levels of

associating kinase activity by an average of $55\pm 12.5\%$ and $88\pm 8.1\%$, respectively (Fig. 14; GST-BRS-2 & -3; p value ≤ 0.001). GST-fusion proteins that were truncated at the COOH-terminus of the BRS also exhibited a significant reduction in the levels of detectable kinase activity. In five independent assays, GST-BRS-4, which only lacked three residues from its COOH-terminus, showed an average decrease in associating kinase activity of $43\pm 11.8\%$ ($p \leq 0.05$), while GST-BRS-5, which lacked five residues, exhibited an average decrease of $54\pm 10.0\%$ (p value ≤ 0.001). These experiments suggested that the number of positively charged amino acids present in the BRS enhanced the kinase association. To address this, we engineered four additional GST-fusion proteins that contained amino acid substitutions for several of the lysine and arginine residues within the NH₂-terminal of the BRS (Fig. 15A). The mutation of an uncharged residue (N) within close proximity to several lysines and arginines was also performed (GST-BRS-NtoA). This construct was developed to ensure that a reduction in kinase activity associating with fusion proteins containing lysine/arginine substitutions could be correlated with charge eliminations rather than a modification of any residue within this region. These GST-fusion proteins were then used in pull-down and *in vitro* kinase reactions as previously described. However, for these experiments the total level of kinase activity precipitating with each fusion protein was assessed by quantifying the amount of kinase activity present in the lane rather than that of an exogenously added substrate. This was done to ensure that we were detecting the total amount of phosphorylation associating with each GST-fusion protein from both autophosphorylation of the kinase as well as trans-phosphorylation of precipitated proteins. As previously shown, eliminating the first four amino acids of the BRS reduced

the association of a kinase activity significantly (Fig. 15; *Lane 3*). Kinase reactions using the charge-substituted constructs (GST-BRS–KxxK to A/G, –RxxK to V/I, and –KxR to A/V) demonstrated that when any two of the positively charged residues within the NH₂-terminus of the BRS were substituted, the associating kinase activity was reduced by an average 55.6±14.8%, 75.3±8.3%, and 64.5±16.5%, respectively ($p \leq 0.001$) (*Lanes 5, 6, and 7*). In 4 independent assays, mutagenesis of the uncharged N residue resulted in no significant variation in the level of kinase activity associating with this GST-fusion protein ($p = 0.65$). Taken together, these results indicated that interactions between the Ser/Thr kinase and the BRS of CD3 ϵ were charge-mediated. However, these assays could not exclude that a structural component may have participated in the kinase binding.

Western Blot Analysis of Candidate Ser/Thr Kinases

To identify the kinase interacting with the BRS, western blot analyses of CD3 ϵ immunoprecipitates were initially performed using mAbs directed against several Ser/Thr kinases known to be involved in TCR-mediated signaling events. These included ERK 1/2, hematopoietic progenitor kinase 1 (HPK1), PAK, PKG, PKC θ , Nck interacting kinase (NIK), MEK kinase 1 (MEKK1), and p38. None of these Ser/Thr kinases were found to interact with CD3 ϵ that was isolated from unstimulated T cells (Fig. 16A; and data not shown). HPK1 was detected in the CD3 ϵ immunoprecipitates when the T cells were first stimulated using a mAb directed against CD3 ϵ (Fig. 16B; *Lane 7*). To assess whether HPK1 could directly interact with the BRS of CD3 ϵ , GST pull-downs and

western blotting were performed. HPK1 was not identified in GST-BRS pull-downs from either unstimulated or stimulated T cells (Fig. 16C; and data not shown).

In the mid-1990's, Skalhegg et al reported that the RI α and catalytic subunits of cAMP-dependent protein kinase A (PKA) inducibly associates with CD3 ϵ in peripheral blood T cells following TCR activation (103). Since the catalytic activity of PKA is sensitive to piceatannol, we assessed whether the CD3 ϵ -associated kinase activity was due to PKA (124). The catalytic subunit of PKA (PKA_c) was found to co-precipitate with CD3 ϵ in 6 out of 23 CD3 ϵ immunoprecipitations/western blotting assays (Fig. 17A). Due to these inconsistencies, we compared two murine lymphoma S49 cell lines, one of which was deficient in PKA expression, for the presence of the CD3 ϵ -associated kinase activity. The S49 kinase^{-/-} cell line contains a mutation in an unknown gene that results in the rapid degradation of PKA_c (126). Western blot analysis of these cells indicated that the S49 kinase^{-/-} cells expressed ~73% less PKA_c than the S49 wild type cells (Fig. 17B; *upper panel*). CD3 ϵ immunoprecipitations/kinase reactions revealed that similar levels of the CD3 ϵ -associated kinase activity were obtained from both the S49 wild type and kinase^{-/-} cell lines (Fig. 17C). These results indicate that in peripheral T cells, the kinase in question was not the catalytic subunit of PKA.

Identification of GRK2 as a BRS-associated Kinase

To identify the kinase, a protein purification approach was used. A large-scale preparation of murine thymocyte homogenates was prepared and applied to a Q-SepharoseTM anion-exchange column. Proteins retained on the column were eluted with

a linear salt gradient, and a total of 80 fractions were collected (Fig. 18). An aliquot from each fraction, including the flow through, was incubated with GST-BRS, followed by *in vitro* kinase reactions in the presence of MBP (Fig. 18B). PO_4 -MBP was then measured to determine which fractions contained the highest concentration of the BRS-associated kinase. Fractions 27 through 32 contained two closely spaced peaks of kinase activity (Fig. 18A; *dotted line*). These fractions were pooled and applied to a GST-BRS affinity column that had been generated by covalently coupling GST-BRS to a Glutathione Sepharose matrix. Proteins retained on the affinity column were eluted with a linear salt gradient, and fractions containing the BRS-associated kinase activity were identified as before (Fig. 19). Three fractions (19-21), eluting between 0.11-0.16 M NaCl, were determined to contain over 90% of the kinase activity that was present in the whole cell homogenate start material. Importantly, this purification approach was found to result in up to a 137-fold enrichment of the BRS-associated kinase activity (Table II). In order to visualize their protein content, fractions 19-21 were subsequently pooled, precipitated with acetone, resolved by SDS-PAGE, and silver stained. As seen, several protein bands were detected (Fig. 20). Six bands (labeled a-f) were extracted, trypsin digested, and analyzed by mass spectrometry and peptide mass fingerprinting.

One peptide sequence (LLDSLQELYR – derived from band b at 80 kDa) corresponded to a protein known as G protein-coupled receptor kinase 2 (GRK2) (Fig. 20; Table III). GRK2 is a Ser/Thr kinase involved in the negative regulation of GPCRs (Reviewed in (97)). Western blot analysis of Q-Sepharose purifications revealed that the highest concentration of GRK2 eluted between 0.75 and 0.12 M NaCl, consistent with its identification by mass spectrometry (Fig. 21A). Fractions eluting in this range

corresponded to those fractions that contained the first peak of the GST-BRS-associated kinase activity (Fig. 18; Peak I). A small aliquot of the affinity column active fraction that was submitted for mass spectrometry analysis was also found to contain GRK2 by western blotting (Fig. 21B, *Lane 4*). These results verified that GRK2 was in fact present in the samples submitted for mass spectrometry that contained a significant amount of the BRS-associated kinase activity.

Many of the other proteins identified by mass spectrometry were DNA or RNA binding proteins (Table III). Several of these proteins, such as DEAD (Asp-Glu-Ala-Asp)-box polypeptide 5, have been shown to be involved in RNA processing and translation. Seven members of the heterogeneous nuclear ribonucleoprotein (hnRNP) family, including hnRNP A, B, D, I, K, L, and U, were also identified in five independent mass spectrometry submissions. Proteins belonging to this family are capable of playing diverse roles in cellular functions by regulating RNA processing, DNA repair, cell signaling (Reviewed in (127)). In terms of the immune system, heterogeneous nuclear ribonuclear protein L functions in CD45 isoform splicing (128, 129). Western blot analysis using an antibody directed against one hnRNP family member (hnRNP A1) verified that this protein could associate with GST-BRS (Fig. 22; *Lane 5*). However, hnRNP A1 did not co-precipitate with full-length CD3 ϵ (*Lane 2*). Analysis of the amino acid sequences of many of the DNA/RNA binding proteins identified by mass spectrometry, including several of the hnRNP family members, revealed that most of them contain a high number of negatively charged residues. We reasoned that the identification of these DNA/RNA-binding proteins by mass spectrometry may be due to their ability to non-specifically associate with the positively charge residues of the BRS.

However, it remains possible that interactions between the BRS of CD3 ϵ and these proteins might actually serve unidentified functions in TCR-mediated signaling events. The relevance of these protein interactions has yet to be investigated.

CD3 ϵ Can Interact with Endogenous GRK2

Having identified GRK2 as a candidate CD3 ϵ -associated Ser/Thr kinase, we next determined whether full-length CD3 ϵ could interact with GRK2. Experimentally, GRK2 was cloned from murine thymocytes and inserted into a pcDNA3.1/*myc*-HIS expression vector. HEK 293 T cells were co-transfected with plasmids containing Myc-tagged GRK2 and a Tac-fusion protein that consisted of the Tac extracellular and transmembrane domains fused to the cytoplasmic domain of CD3 ϵ (Tac- ϵ) (56). Forty-eight hours post-transfection, the cells were lysed, and Tac- ϵ was immunoprecipitated. Myc-GRK2 was co-precipitated with Tac- ϵ immunoprecipitates (Fig. 23A; *Lane 4*). It should be noted that GRK2 was not always detected in these co-expression studies (detected in 9 of 15 assays). Potential explanations for this variability will be addressed in the discussion of this chapter.

CD3 ϵ was also immunoprecipitated from primary human and murine thymocyte lysates. A faint GRK2 signal was detected, revealing that endogenous GRK2 could be co-precipitated with CD3 ϵ (Fig. 23B; *Lane 4*).

Interactions between CD3 ϵ and GRK2 Occur Predominantly within Subcellular Compartments in a pH-sensitive Fashion

As previously mentioned, the CD3 ϵ /kinase complex was mainly detected in intracellular compartments (Fig. 10B). To address whether surface-associated or intracellular pools of CD3 ϵ could interact with GRK2, sequential immunoprecipitations of CD3 ϵ were performed. Thymocytes or lymphocytes were stained using anti-CD3 ϵ or anti-CD28 mAbs. Surface stained proteins were then immunoprecipitated using Protein A. The remaining intracellular pools of CD3 ϵ or CD28 were subsequently immunoprecipitated. Associated proteins from both sets of immunoprecipitations were resolved by SDS-PAGE, followed by anti-GRK2 immunoblotting. These experiments revealed that when equivalent levels of CD3 ϵ were precipitated from the surface of the cell versus intracellular compartments, GRK2 preferentially associated with the pool of CD3 ϵ isolated from within the cell (Fig. 24). This trend held true in both primary thymocytes and lymphocytes (*Lanes 5 and 9*).

The cytosolic pH of a cell is generally in the range of 7.4, while subcellular compartments, such as lysosomes and endosomes, are more acidic (130). To determine whether the intracellular interaction between GRK2 and CD3 ϵ was affected by pH, GST-BRS pull-downs/GRK2 western blots were performed using thymocyte WCLs prepared at different pHs. To ensure the association of GST-BRS with glutathione was not disrupted at a lower pH, the fusion protein was covalently coupled to glutathione Sepharose beads. These experiments revealed that at a lower pH, GST-BRS was able to precipitate GRK2 (Fig. 25A; *Lane 7*). No GRK2 was detected in pull-downs using GST,

GST-PRS, or GST-ITAM (Fig. 25A). GST-BRS/GRK2 interactions were optimal at a pH ranging from 5.0 to 3.0 (Fig. 25B; *Lanes 4 – 6*). Some GRK2 was present in GST pull-downs performed at a pH of 4.0 (*Lane 10*). However, the amount detected was very low compared to that seen with GST-BRS pull-downs.

We next used purified, recombinant GRK2 (provided by J. Tesmer) to assess the effects of pH on direct interactions between the BRS and GRK2. GST-BRS precipitated recombinant GRK2 (rGRK2) at pH values of 5.0, 4.0, and 3.0 (Fig. 25C; *Lanes 5 – 7*). A small amount of rGRK2 associated with GST controls, suggesting that some non-specific binding can occur between GRK2 and GST at a low pH (*Lane 12*). Taken together, these assays reveal two important characteristics about the interaction between the BRS of CD3 ϵ and GRK2. First, the binding of GRK2 appears to occur predominantly within subcellular compartments. Second, BRS/GRK2-binding is enhanced in the pH range normally found in late endosomal (pH 5.4 to 6.0) or early lysosomal (pH 4.5 to 5.0) compartments (130, 131). The implications for this finding are presented in the discussion of this chapter.

The third connotation of these studies is that GRK2 and CD3 ϵ interact directly, without an intermediate protein. However, it remains possible that additional proteins may stabilize CD3 ϵ /GRK2 binding within a cell.

The Effect of GRK2 siRNA Treatment on the BRS/CD3 ϵ -associated Kinase Activity

Our next goal was to determine whether a reduction in GRK2 protein expression would have an effect on the level of the BRS-associated kinase activity. Since GRK2^{-/-}

mice are embryonic lethal, we utilized an siRNA approach to knock down GRK2 expression levels in a peripheral T cell line (95). Electroporation of Jurkat T cells with siRNAs directed against GRK2 consistently decreased GRK2 protein levels by 40% to 75% compared to control transfected cells (Fig. 26A; *Lane 2* and data not shown). Lysates from the siRNA treated cells were prepared, followed by GST-BRS pull-downs or CD3 ϵ immunoprecipitations and kinase reactions. As seen, the BRS-associated kinase activity was reduced by 16.8% when GRK2 siRNA treated cells were compared to control transfected cells (average of $14.6 \pm 7.3\%$; $n=4$ independent assays) (Fig. 26B). Although modest, the average decrease of $14.6 \pm 7.3\%$ was statistically significant (p value < 0.05). CD3 ϵ immunoprecipitations from cells in which GRK2 protein expression had been reduced by 75% exhibited at most a 4% decrease in the level of associating kinase activity and was not found to be statistically significant (data not shown). As detailed in the discussion of this chapter, there are several possibilities for why a more dramatic decrease in the associating kinase activity was not seen following GRK2 siRNA treatment.

SDF-1 α Treatment of Primary Thymocytes Significantly Reduces the CD3 ϵ -associated Kinase Activity

Kumar et al recently reported that when T cells are treated with stromal cell-derived factor-1 α (SDF-1 α), an inducible association between the TCR and the GPCR, CXCR4, takes place (61). This interaction allows CXCR4 to utilize the CD3 invariant chains and their associating proteins for its own signal transduction. Since CXCR4 is

known to both activate GRK2 and to be regulated by its catalytic activity, we examined the effects of SDF-1 α treatment on the CD3 ϵ -associated kinase activity. Murine thymocytes were incubated with recombinant SDF-1 α for 30 minutes. CD3 ϵ , CXCR4, PKC θ , or CD28 were then immunoprecipitated and subjected to kinase reactions (Fig. 27A). Following SDF-1 α treatment, the levels of CD3 ϵ - and CXCR4-associated kinase activities decreased by 33% and 36%, respectively (average of $24 \pm 13.7\%$ and $36 \pm 8.5\%$, respectively; $n=6$ independent assays; p value < 0.05) (Fig. 27A). Control immunoprecipitations using antibodies against PKC θ and CD28 revealed no significant variations in kinase activity.

Studies have shown that GPCR engagement induces the phosphorylation of GRK2 on tyrosine and/or Ser/Thr residues, thereby altering its intracellular trafficking, catalytic activity, and proteolytic degradation (132-137). To examine whether such post-translational modifications of GRK2 were responsible for the decrease in the CD3 ϵ -associated kinase activity, western blot analyses were performed. Thirty minutes of SDF-1 α treatment did not result in the degradation of CD3 ϵ or GRK2 as evidence by equivalent levels of both proteins in the WCLs of treated versus untreated cells (Fig. 27B; *upper and lower panels*). Additionally, immunoblotting revealed that the amount of GRK2 precipitating with CD3 ϵ remained comparable after thirty minutes of SDF-1 α treatment (Fig. 27B; *middle panel*). We did observe a modest increase in the phosphorylation of GRK2 on serine 670 (Ser670) after 5 minutes of treatment (Fig. 27C; *Lane 2*). Phosphorylation at this site has been demonstrated to inhibit the catalytic activity of GRK2 toward physiologically relevant substrates, such as light activated rhodopsin (137). However, the phosphorylation of Ser670 returned to background levels

after 30 minutes of stimulations, suggesting that changes at this site may not account for the decreased kinase activity seen in the CD3 ϵ immunoprecipitates. Overall, our experiments indicate that the regulation of GRK2 in association with CD3 ϵ may be a complex process, involving multiple post-translational modifications with varying kinetics.

Discussion

In our investigations of kinases capable of associating with the invariant chains of the TCR, we determined that the CD3 ϵ subunit couples with two Ser/Thr kinases, HPK1 and GRK2. The formation of a HPK1/CD3 ϵ complex required TCR engagement. Furthermore, the association of HPK1 with CD3 ϵ was not direct, indicating that it required the presence of an adaptor protein. A likely candidate for such an adaptor is Nck, since it can associate with both CD3 ϵ and HPK1 following TCR ligation (45, 138).

Unlike interactions with HPK1, associations between the cytoplasmic tail of CD3 ϵ and GRK2 were constitutively present in *ex vivo* T cells. Prior to identifying GRK2, we attempted to elucidate whether engagement of the TCR affected the level of associating kinase activity. These assays revealed that the kinase activity associating with CD3 ϵ was lost if the cells were allowed to rest prior to CD3 ϵ immunoprecipitations but increased in both *ex vivo* and rested T cells after TCR stimulations. There are several implications for these results. First, the finding that the kinase activity associating with CD3 ϵ dissipated when cells were sparsely cultured indicates that constitutive interactions between CD3 ϵ and at least one kinase requires TCR interactions with self-peptide/MHC complexes. Since GRK2 interactions with CD3 ϵ were found to occur predominantly within intracellular compartments, it is possible that ligand-induced endocytosis of the TCR may increase the intracellular pool of CD3 ϵ available for GRK2 binding, thus increasing the level of CD3 ϵ -associated kinase activity. Alternatively, the increase in kinase activity may reflect inducible associations between CD3 ϵ and other kinases, such as HPK1 and PKA. It is also possible that a combination of the two (an increase in TCR

internalization and, thus, GRK2 association, as well as an increase in contributions from HPK1 and PKA) are occurring. Attempts to determine whether GRK2 interactions with CD3 ϵ were affected by TCR engagement by western blotting were not conclusive (data not shown).

GRK2 was found to co-precipitate with CD3 ϵ in both transfected and primary cells. However, as previously mentioned, the interaction between GRK2 and CD3 ϵ was not always detected in transfected HEK293 T cells (present in 9 of 15 immunoprecipitations). There are several possible explanations for this variability. First, endogenous interactions between GRK2 with CD3 ϵ may utilize additional protein in order to stabilize their interaction. A candidate for such a stabilizing protein includes the G protein, $G\alpha_{q/11}$. $G\alpha_{q/11}$, a well-known binding partner of GRK2, has also been reported to interact with the cytoplasmic tail of CD3 ϵ (75, 139).

The finding that CD3 ϵ /GRK2 interactions occur largely within subcellular compartments may also have important implications for our initial co-precipitation studies. Since proteins located within intracellular organelles, including the endosomes or lysosomes, are difficult to extract, the solubilization conditions used in our earlier procedures may not have been ideal. Consequently, inconsistencies in the ability to co-precipitate CD3 ϵ and GRK2 may be ameliorated by modifying our original experimental conditions. For instance, one of the initial steps performed in our transfection of HEK293 T cells was the treatment of these cells with chloroquine, a reagent known to block acidification of endocytic vesicles (140). Although this step is important for preventing the acidification of plasmid DNA, inhibiting the ability of endosomes or lysosomes to maintain a low pH may have consequently interfered with the ability of

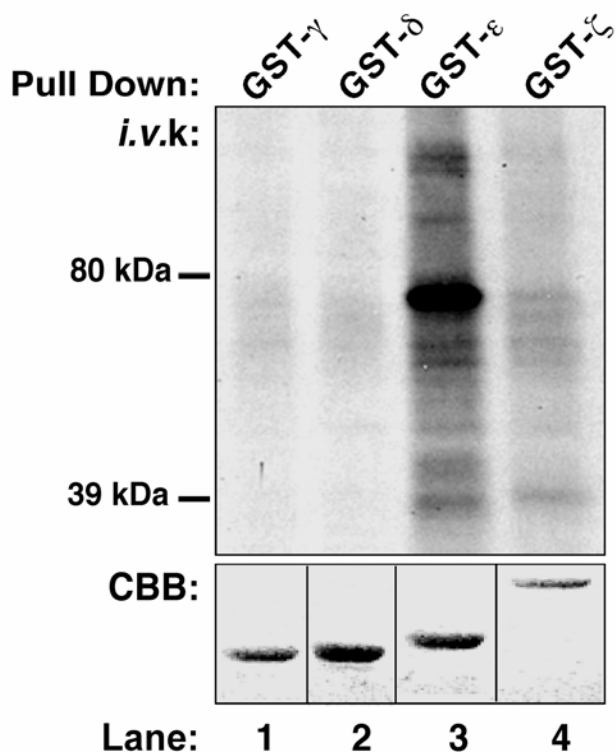
Myc-GRK2 to bind Tac- ϵ . A plausible solution for overcoming this occurrence may be to avoid chloroquine treatment of the cells, or to simply lower the pH of the buffer in which future precipitations are performed.

In our siRNA studies, we noted that an average $14.6 \pm 7.3\%$ decrease in the BRS-associated kinase activity was observed when GRK2 protein expression was reduced by 40% or more in Jurkat T cells. This modest decrease in kinase activity may also be due to several factors. First, it is possible that only a minute amount of GRK2 is needed to generate the CD3 ϵ -associated kinase profile. This is supported by our finding that while a substantial amount of GRK2 can be detected in the WCL of unstimulated thymocytes, only a small fraction appears to interact with CD3 ϵ (Fig. 23B). In this case, even a 75% reduction in GRK2 protein levels may not be sufficient to eliminate the CD3 ϵ -associated kinase activity. Alternatively, the possibility remains that interactions between CD3 ϵ and other kinases, such as HPK1 or PKA, might mask the effects of decreasing GRK2 expression in Jurkat T cells. Therefore, siRNAs directed against multiple Ser/Thr kinases may be necessary to decrease the CD3 ϵ -associated kinase activity substantially.

Since GRK2 regulates GPCRs, we sought to elucidate whether a functional link might be present between GPCR signaling and the CD3 ϵ -associated kinase activity. Accordingly, we undertook chemokine receptor stimulations and kinase reactions in murine thymocytes. SDF-1 α treatment of thymocytes resulted in a statistically significant decrease in the level of CD3 ϵ -associated kinase activity. This decrease did not appear to be due to a reduction in CD3 ϵ /GRK2 interactions or to an increase in the phosphorylation of GRK2 on Ser670 (a modification that has previously been shown to inhibit the catalytic activity of GRK2). However, it should be noted that these assays

were performed prior to the finding that CD3 ϵ /GRK2 interactions occurred largely within subcellular compartments. Consequently, in these experiments, the total pool of CD3 ϵ was precipitated from SDF-1 α treated cells, as opposed to intracellular pools. Under these conditions, obtaining a pronounced signal from associating GRK2 was admittedly difficult. In order to more clearly elucidate whether a reduction in CD3 ϵ /GRK2 interactions results from chemokine treatment, the intracellular pools of CD3 ϵ should be analyzed. Alternatively, alterations in GRK2 phosphorylation on residues other than Ser670, such as Ser29 or Ser685, may negatively effect GRK2 activity (136, 141). This possibility was not explored.

In summary, the identification of two Ser/Thr kinases capable of interacting with CD3 ϵ adds to the complex array of proteins contributing to TCR-mediated signaling both before and after receptor engagement. With regard to CD3 ϵ interactions with GRK2, several reports have shown that signals generated through GPCRs and the TCR share a number of signaling components, including $G\alpha_{q/11}$, ZAP-70, LAT, and SLP-76 (61, 63, 75). The finding that GRK2 associates with CD3 ϵ adds to the body of evidence that chemokine receptors and the TCR share molecules that enable them to crosstalk.



Invariant Chain	Amino Acid Sequence of Cytoplasmic Tail
CD3 γ	QDGVRQSRASDKQTLQNEQLYQPLKDREYDQYSHLQGNQLRKK
CD3 δ	HETGRPSGAAEVQALLKNEQLYQPLRDREDTQYSRLGGNWPRNKKS
CD3 ϵ	KNRKAKAKPVTRGTGAGSRPRGQNKERPPVPNPDYEPKRGQRDLYSGLNQRAV
CD3 ζ	RAKFSRSAETAANLQDPNQLYNELNLRREEYDVLEKKRARDPEMGGKQQRRRNP QEGVYNALQKDKMAEAYSEIGTKGERRRGKGHGGLYQGLSTATKDTYDALHMQTL APR

Figure 7. The cytoplasmic tail of CD3 ϵ uniquely associates with a kinase activity. GST-fusion proteins containing the cytoplasmic portion of CD3 γ , δ , ϵ , or ζ were prepared and quantified by Coomassie Brilliant Blue (CBB) staining (lower panel). Equivalent amounts of each GST-fusion protein were then incubated with thymocyte WCLs, followed by *in vitro* kinase (i.v.k) reactions in the presence of [γ - 32 P]ATP. Proteins were resolved by SDS-PAGE, and phosphoproteins were visualized by autoradiography (upper panel).

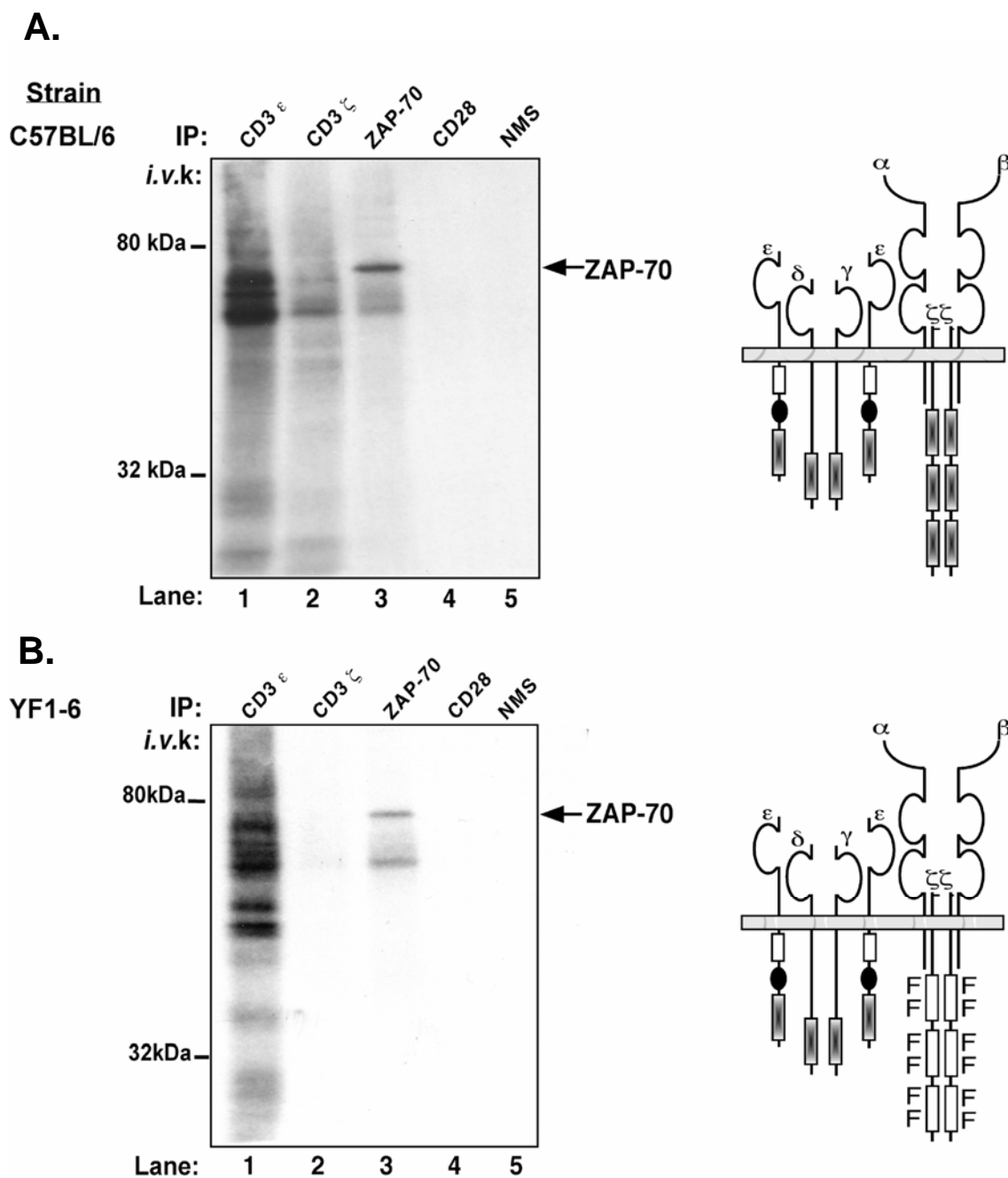


Figure 8. Full-length CD3 ϵ associates with a kinase in a CD3 ζ ITAM-independent manner. Thymocyte WCLs were prepared from C57BL/6 (A) or C57BL/6 YF1-6 (B) mice. TCR diagrams illustrate the number of tyrosine-to-phenylalanine substitutions that were made in the YF1-6 CD3 ζ ITAMs. Immunoprecipitations (IP) of the indicated molecules were performed in WCLs from each line, followed by *in vitro* kinase reactions, and SDS-PAGE. Autoradiography was used to visualize phosphoproteins. NMS = Normal mouse sera.

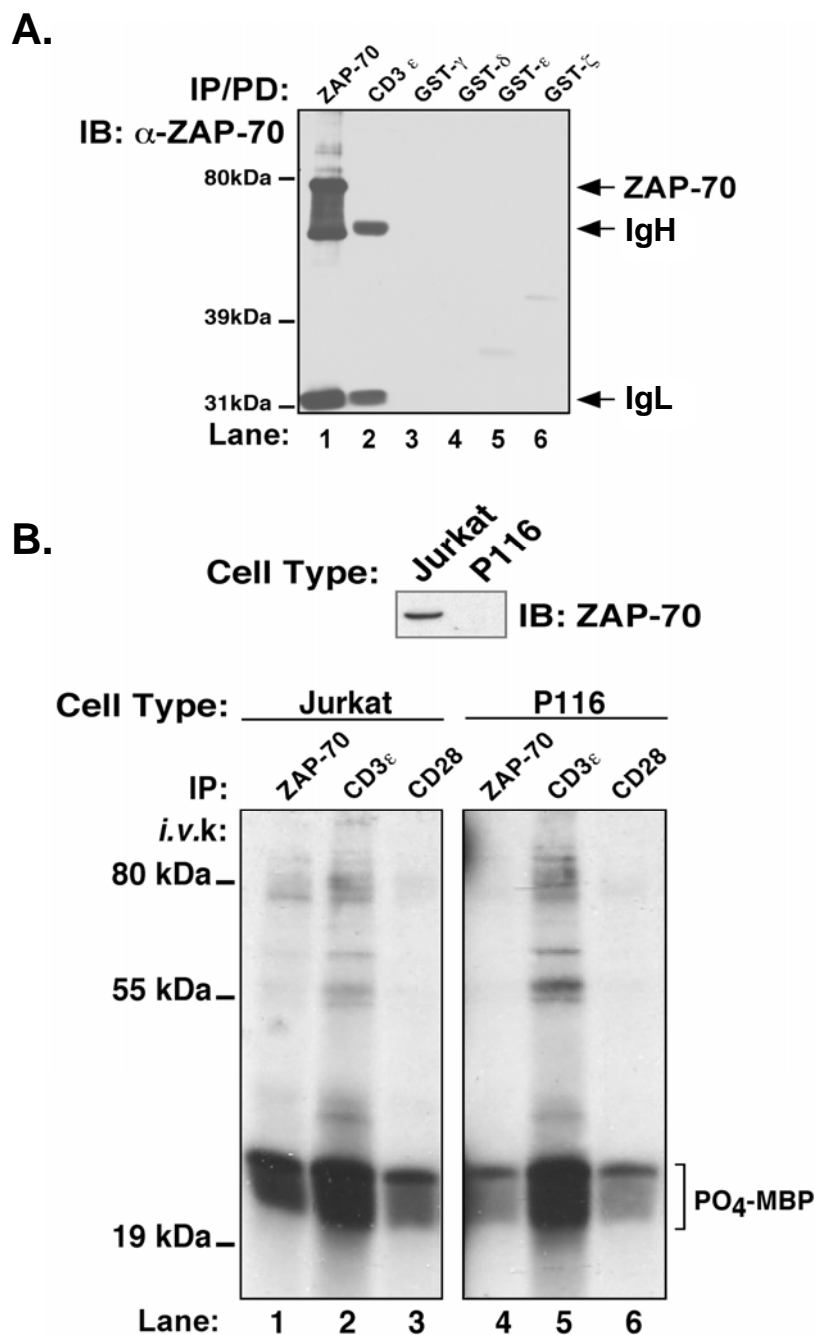
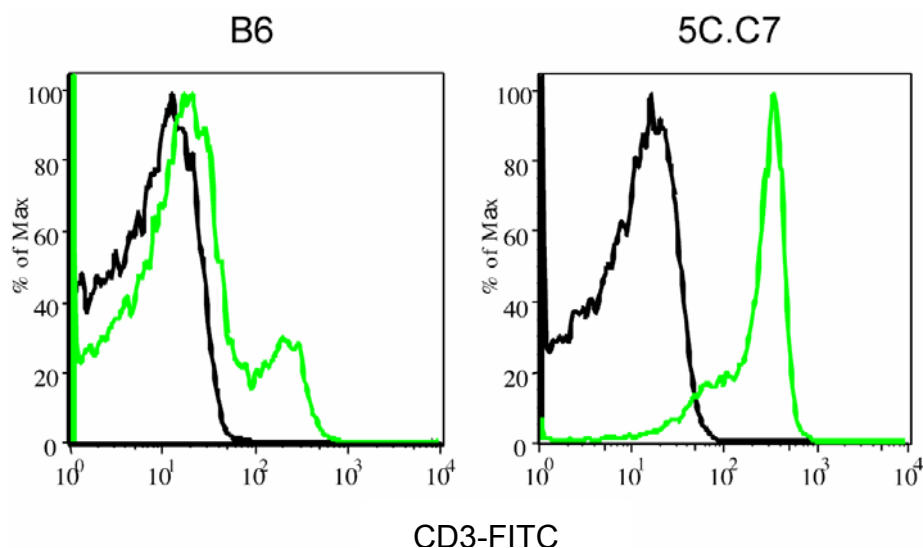


Figure 9. The CD3 ϵ -associated kinase is distinct and independent of ZAP-70. (A) Immunoprecipitations were performed in thymocyte WCLs using anti-ZAP-70 or anti-CD3 ϵ . Pull-downs were also performed using GST-fusion proteins containing the cytoplasmic tails of CD3 γ , δ , ϵ , or ζ . The presence of ZAP-70 was then assessed by western immunoblotting. (B) Upper Panel: Equivalent numbers of Jurkat T cells or P116 Jurkat T cells were lysed. WCLs were subjected to SDS-PAGE and α -ZAP-70 immunoblotting. Lower Panel: The indicated molecules were immunoprecipitated from either Jurkat T cell or P116 Jurkat T cell WCLs. Precipitates were incubated in a kinase reaction mix containing [γ -³²P]ATP and MBP. Phosphoproteins were visualized by autoradiography.

A.



B.

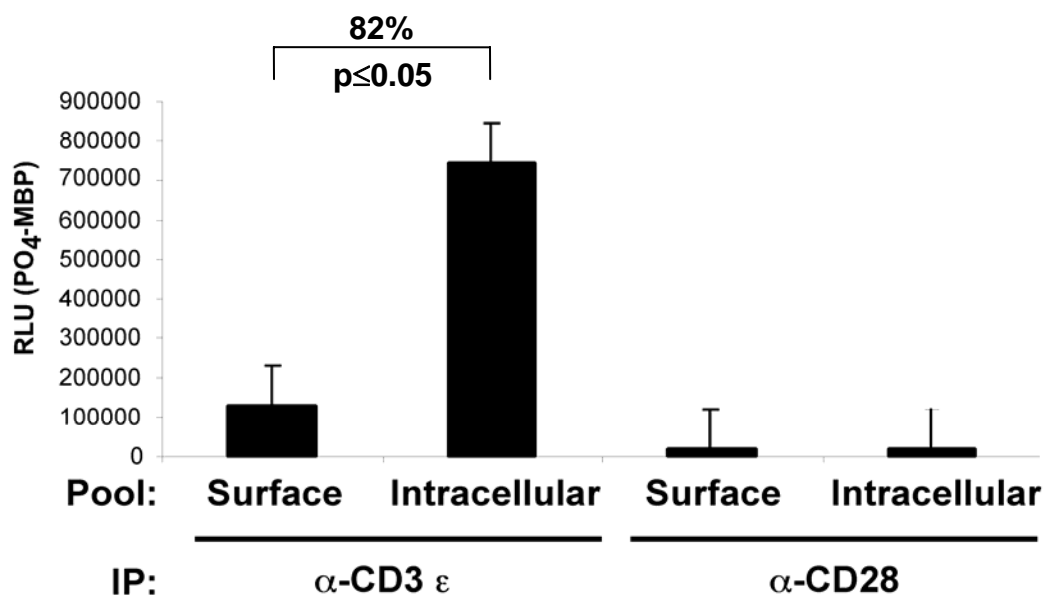


Figure 10. The CD3 ε-associated kinase activity is predominantly intracellular.

(A) Thymocytes were isolated from C57BL/6 or TCR transgenic 5C.C7 mice. Cells were stained using fluorescently labeled anti-CD3 ε (green line) or an isotype control (black line). Surface expression of CD3 ε was then assessed by flow cytometric analysis. (B) Primary murine thymocytes were stained using mAbs directed against the ectodomain of CD3 ε or CD28. The cells were washed and lysed. Surface stained CD3 ε or CD28 was then precipitated by the addition of Protein A Sepharose. Intracellular pools of the same molecules were subsequently immunoprecipitated. *In vitro* kinase reactions were performed using MBP as an exogenously added substrate. PO₄-MBP was quantified with a phosphorimager, and the level of associated kinase activity was represented as relative light units (RLU). Graph is representative of three independent reactions.

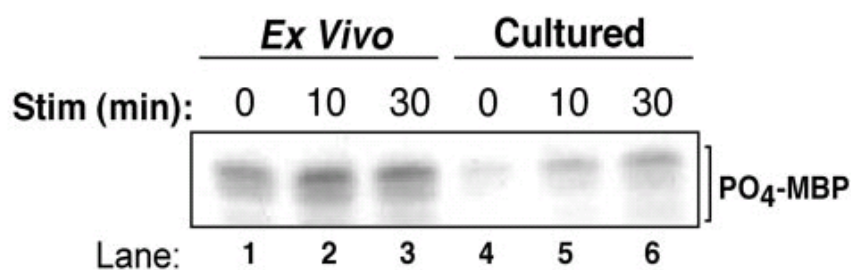


Figure 11. Interactions between CD3 ϵ and a kinase activity are constitutive in *ex vivo* thymocytes. Primary murine thymocytes were either untreated or stimulated *ex vivo* for 10 or 30 min with an anti-CD3 ϵ mAb (Lanes 1–3). Alternatively, the cells were cultured at 37 °C for 4 h, followed by anti-CD3 ϵ stimulations (Lanes 4–6). The cells were washed, lysed, and CD3 ϵ immunoprecipitates were subjected to *in vitro* kinase reactions in the presence of MBP. Associated kinase activity was assessed by quantifying the amount of ^{32}P -labeled substrate (MBP).

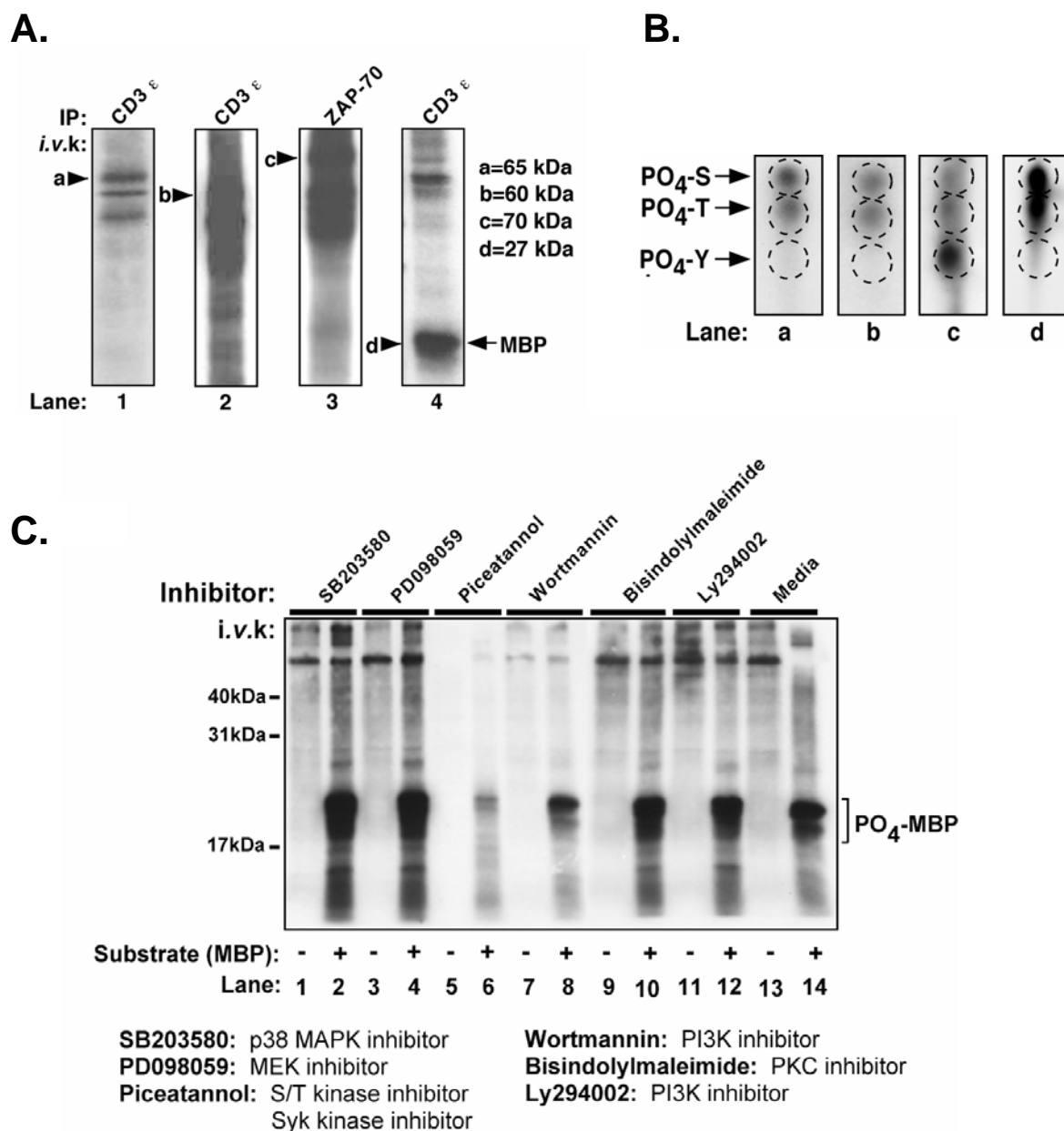


Figure 12. CD3 ϵ associates with a serine/threonine kinase. (A) The indicated molecules were isolated from primary thymocytes (Lanes 1 and 4) or primary lymphocytes (Lanes 2 and 3) and assayed by *in vitro* kinase (*i.v.k*) reactions. In Lane 4, MBP was added as a substrate prior to performing the kinase reaction. (B) The indicated ^{32}P -labeled bands (a–d) were extracted and subjected to phosphoamino acid analysis ($n = 5$ assays). (C) CD3 ϵ was immunoprecipitated from murine thymocyte lysates. The samples were incubated with the indicated kinase inhibitors or media alone (Lanes 13–14) for 10 min at room temperature. Kinase reactions were then performed in the presence or absence of MBP. Phosphoproteins were visualized by autoradiography (piceatannol inhibition; $n = 4$ assays).

CD3 ϵ : KNRKAKAKPVTRGTGAGSRPRGQNKERPPPVPNPDYEPIRKGQRDLYSGLNQRAV

BRS: KNRKAKAKPVTRGTGAGSRPRGQNK

PRS: ERPPPVPNPDYE

ITAM: NPDYEPPIRKGQRDLYSGLNQRAV

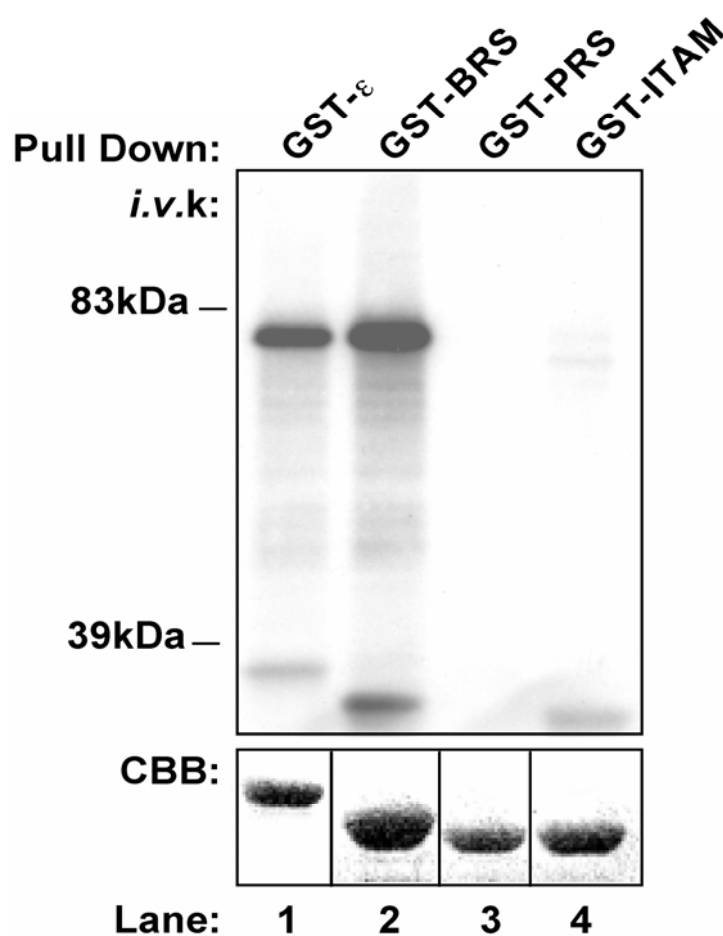


Figure 13. The basic-rich stretch of CD3 ϵ mediates the kinase association. GST-fusion proteins containing the listed amino acid sequences were prepared and quantified by Coomassie Brilliant Blue (CBB) (lower panel). Equivalent amounts of the indicated fusion proteins were then incubated with thymocyte WCLs. Following kinase reactions (*i.v.k.*), phosphoproteins were visualized by SDS-PAGE/autoradiography (upper panel). Associations between a kinase activity and the BRS are representative of over a dozen independent experiments.

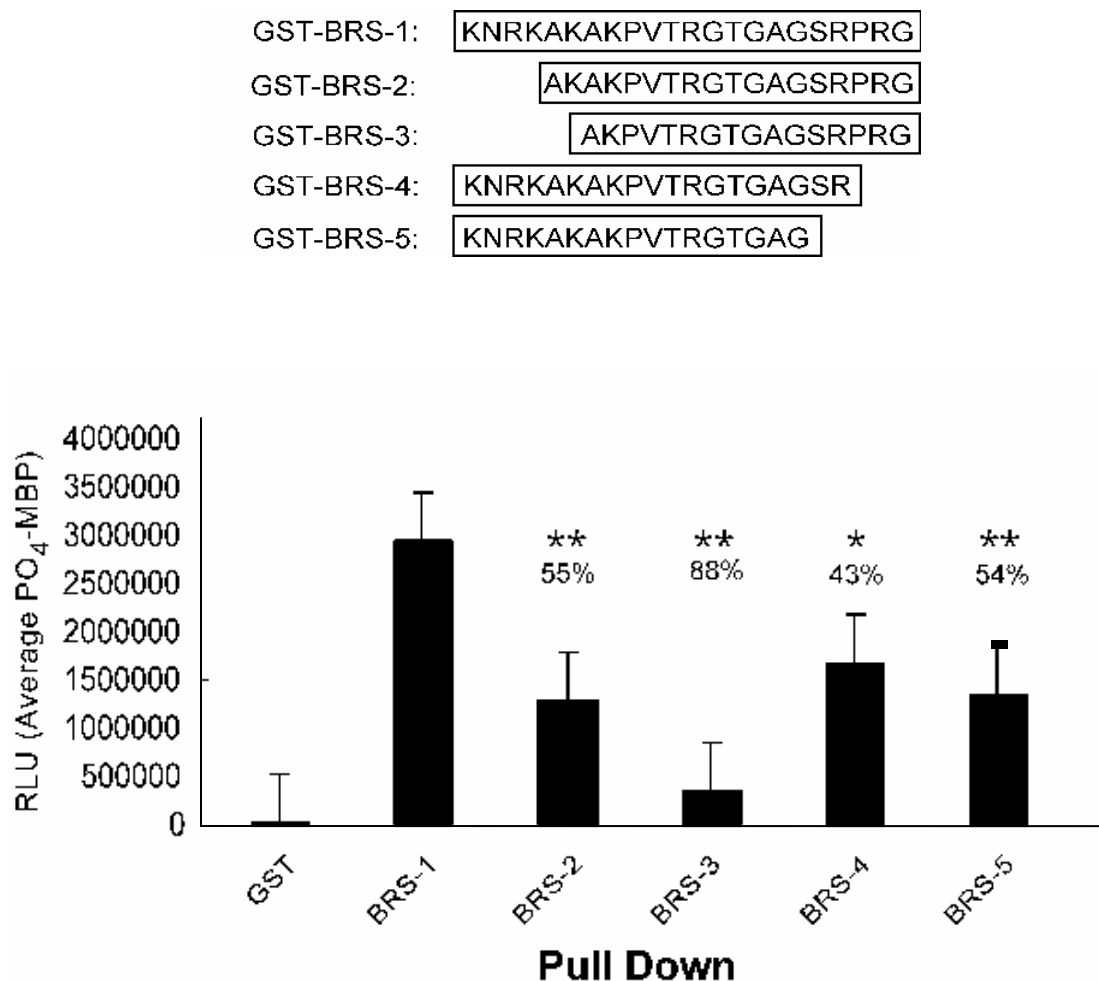


Figure 14. The full-length BRS is required to precipitate the optimal amount of the CD3 ϵ -associated kinase activity. GST-fusion proteins containing the listed amino acid sequences were used as affinity ligands in WCLs. The pull-downs were subjected to *in vitro* kinase reactions in the presence of [γ -³²P] ATP and MBP. The level of PO₄-MBP generated in three independent assays was quantified using a phosphoimager, averaged, and represented as relative light units (RLU). Percentage values indicate the average decrease in the percent of kinase activity associated with each of the GST-fusion proteins when compared to GST-BRS-1. (*) = $p \leq 0.05$. (**) = $p \leq 0.001$.

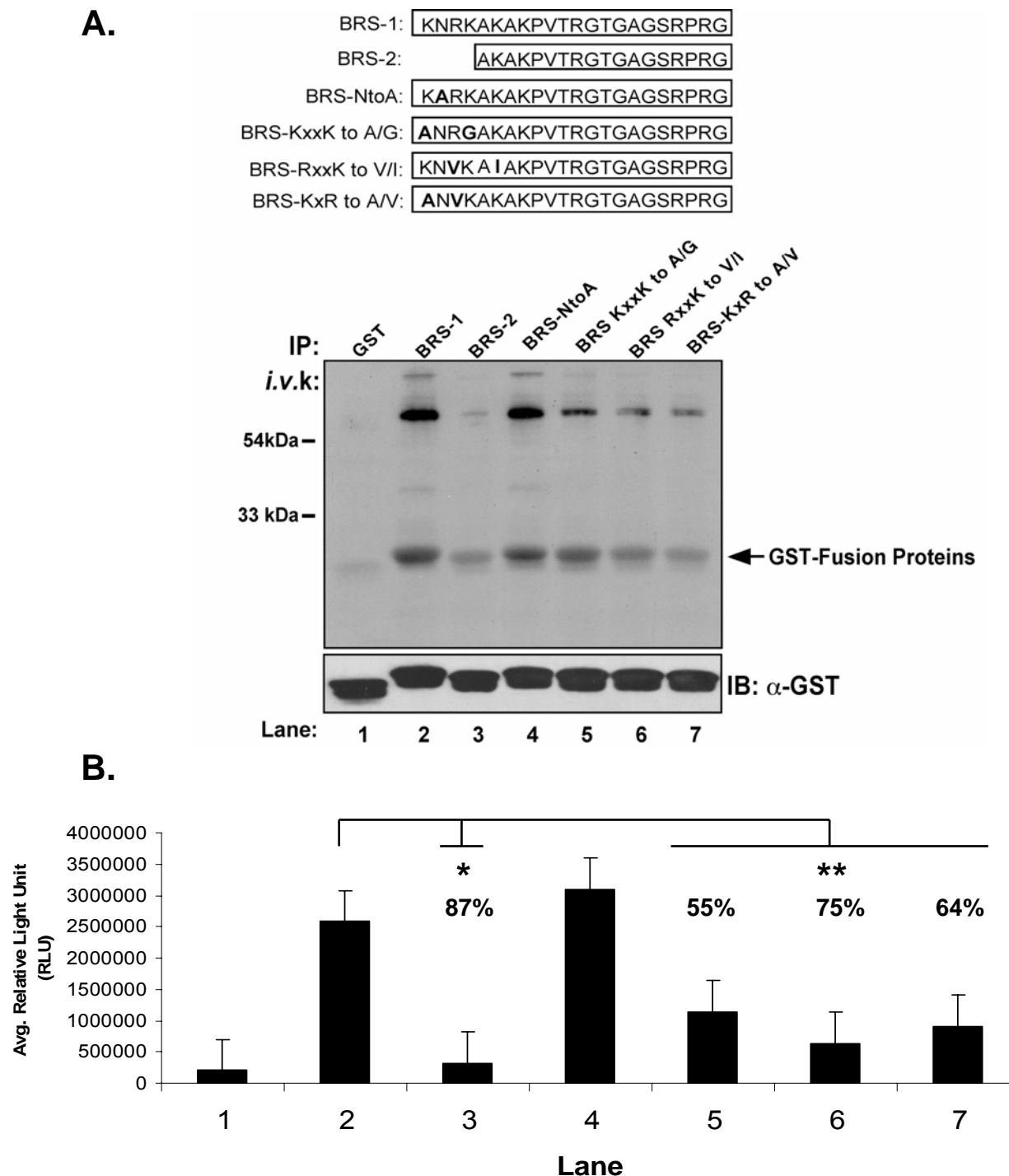


Figure 15. The positively charged residues within the BRS mediate a kinase association and/or activity. (A) GST-fusion proteins containing the listed amino acid sequences were used to pull down proteins from murine thymocyte WCLs. Upper panel: *In vitro* kinase reactions were performed on each sample, and phosphoproteins were visualized by autoradiography. Lower panel: Immunoblotting of the autoradiograph was carried out using an anti-GST mAb to verify equivalent levels of each GST-fusion protein had been used. (B) The amount of kinase activity found to associate with each GST-fusion protein in four independent assays was quantified by phosphoimaging, averaged, and graphed as relative light units (RLU). Percent values indicate the average decrease in the associating kinase activity as compared to GST-BRS-1. (*) = $p \leq 0.05$ (**) = $p \leq 0.001$.

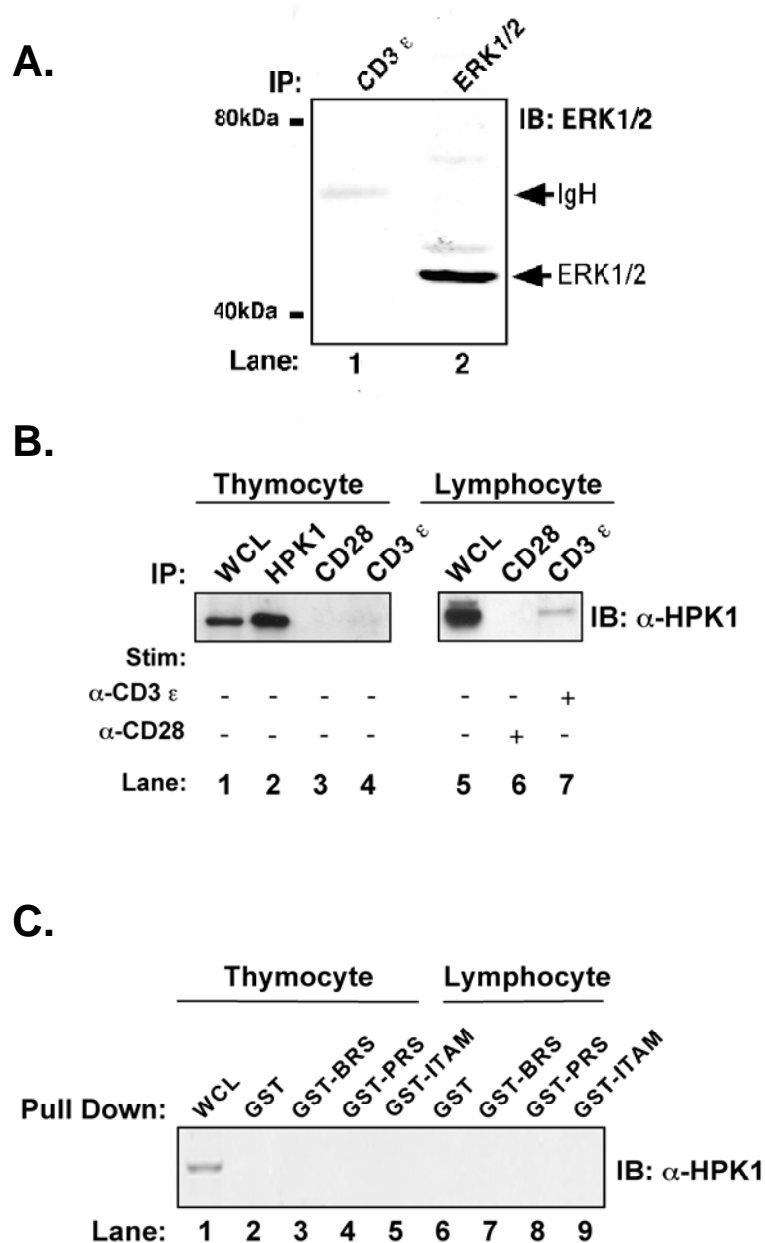


Figure 16. The BRS of CD3 ϵ associates with a Ser/Thr kinase other than ERK1/2 and HPK1. (A) CD3 ϵ and ERK1/2 immunoprecipitates were isolated from thymocyte WCLs, followed by anti-ERK1/2 western blotting. (B) Thymocytes or lymphocytes were incubated at 37°C for 30 min in the presence of the indicated mAbs. The cells were then washed, lysed, and HPK1, CD28, or CD3 ϵ were immunoprecipitated and analyzed by immunoblotting with an anti-HPK1 mAb. (C) The indicated GST-fusion proteins were used in pull-down assays with lysates prepared from thymocytes (lanes 2–5) or lymphocytes (lanes 6–9). The pull downs were immunoblotted with anti-HPK1.

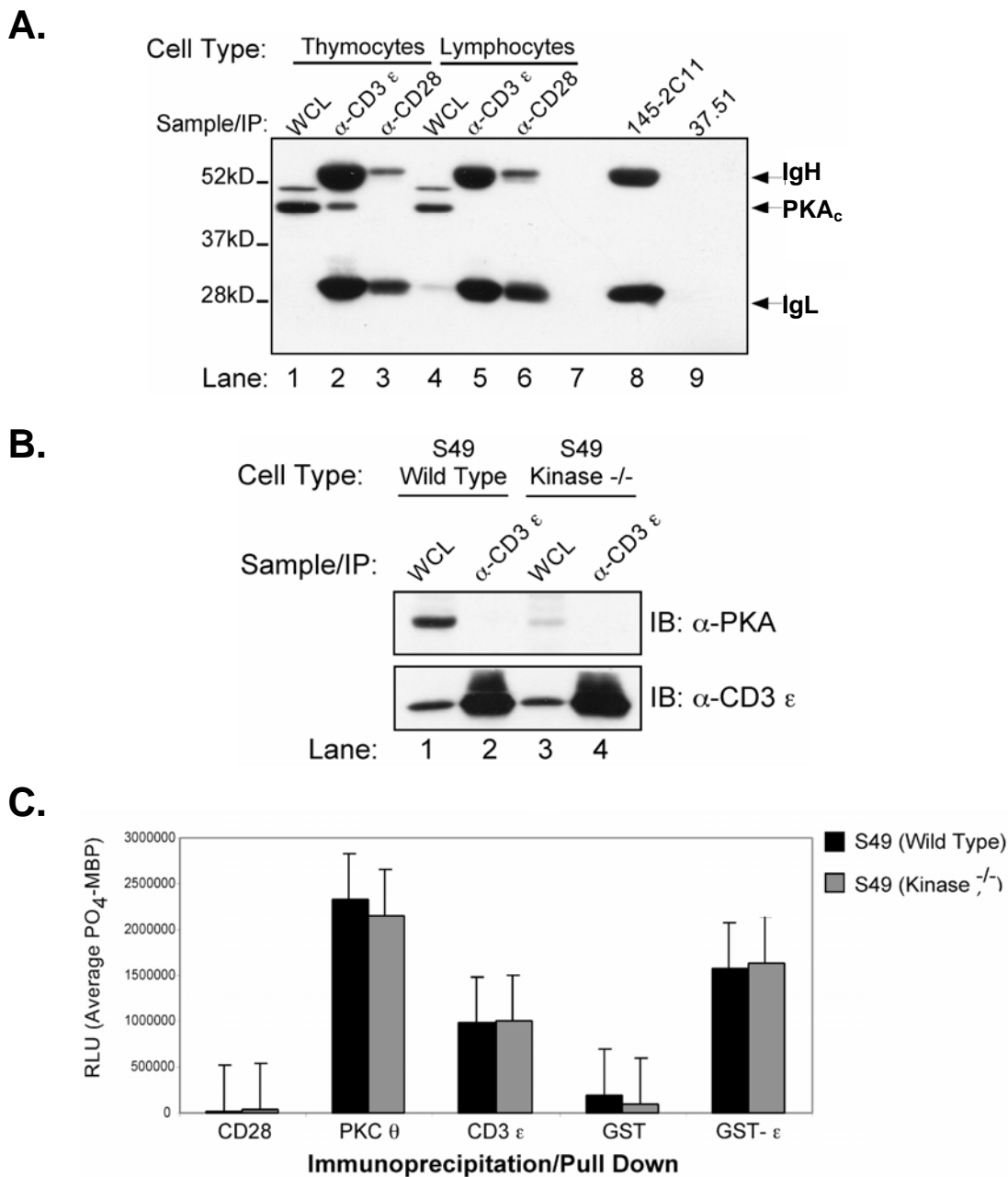
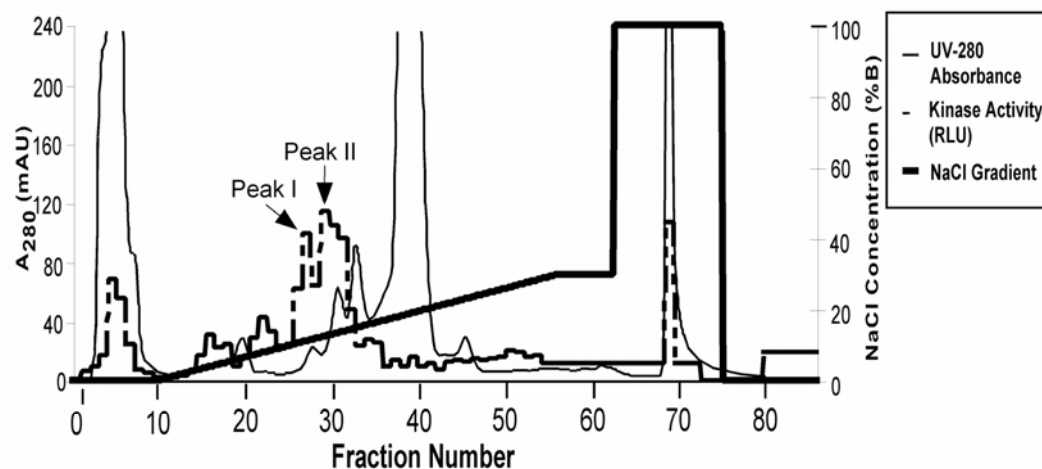


Figure 17. PKA does not constitutively associate with CD3 ϵ in peripheral T cells. (A) Murine thymocyte or lymphocyte extracts were prepared in a 0.25% Triton X-100 containing lysis buffer. Anti-CD3 ϵ or anti-CD28 immunoprecipitations (IP) were performed, followed by western blotting using an Ab directed against the catalytic α subunit of (PKA α). In Lanes 8 & 9, anti-CD3 ϵ (145-2C11) or anti-CD28 (37.51) alone was resolved as negative controls. (B) Anti-CD3 ϵ IPs were performed in WCLs derived from equivalent numbers of S49 Wild Type or S49 Kinase $^{-/-}$ cells. Western blotting was performed using anti-PKA α (upper panel) or anti-CD3 ϵ (lower panel) mAbs. (C) IPs/pull-downs were performed using the indicated mAbs/GST-fusion proteins. *In vitro* kinase reactions were then performed with both [γ - 32 P]ATP and MBP. The average level of PO $_4$ -MBP from three independent assays was quantified and graphed as relative light units (RLU).

A.



B.

Pull Down: GST-BRS
Substrate: MBP

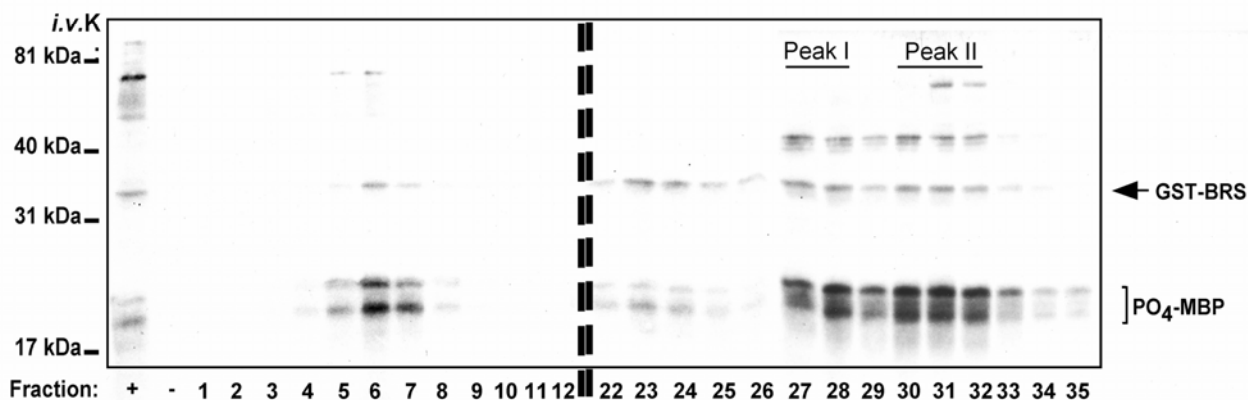
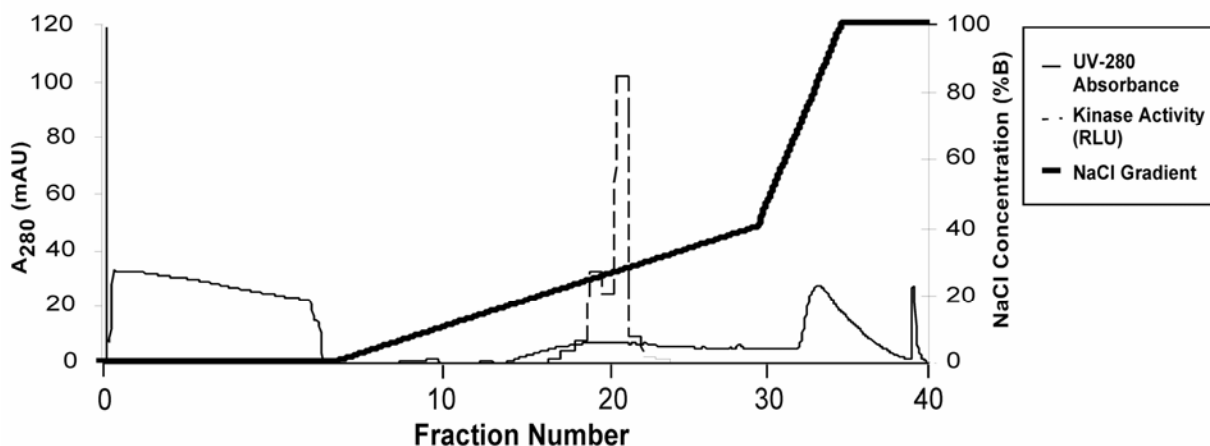


Figure 18. Isolation of the CD3 ϵ -associated kinase activity by anion-exchange chromatography.

(A) Thymocyte homogenates were applied to an anion-exchange column. Proteins retained on the column were eluted with a linear salt gradient (thick line) and collected in 10-ml fractions. Proteins eluting off the column were detected by UV absorbance (thin black line). The kinase activity contained in each fraction (dashed line) was determined as in (B). (B) An aliquot from each fraction was subjected to GST-BRS pull-downs and kinase reactions in the presence of MBP. The amount of activity present in each fraction was visualized by autoradiography and a Phosphoimager. + = GST-BRS pull-downs from whole cell homogenate; - = GST pull-downs from whole cell homogenate; *i.v.k.*, *in vitro* kinase.

A.**B.**

Pull Down: GST-BRS
 Substrate: MBP

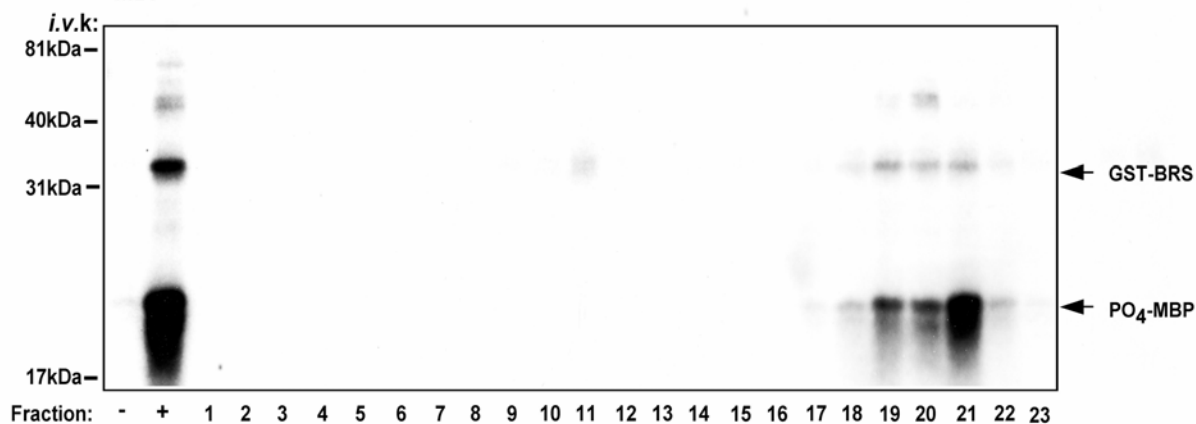


Figure 19. Purification of the CD3 ϵ -associated kinase activity using affinity chromatography. (A) Fractions 27-32 generated by Q-Sepharose fractionations (Figure 18) were applied to an affinity column consisting of GST-BRS. Proteins retained on the column were eluted with a linear salt gradient (thick line) and collected in 5-ml fractions. Proteins eluting off the column were detected by UV absorbance (thin black line). Dashed line, kinase activity contained in each fraction as determined in (B). (B) An aliquot from each fraction was subjected to GST-BRS pull-downs and kinase reactions in the presence of MBP, with the amount of activity visualized by autoradiography and a phosphoimager. + = GST-BRS pull-downs from whole cell homogenate; - = GST pull-downs from whole cell homogenate; i.v.k, *in vitro* kinase.

Table II. Purification of the CD3 ϵ associated Ser/Thr kinase from murine thymocytes

Purification Step	Specific Activity (pmols/min/μg)	Protein Concentration ^c (mg/ml)	Total Activity (pmols/min)	Fold Enrichment
Thymocyte Homogenates	5.11×10^{-7}	0.9	2.3×10^{-5}	
Anion Exchange (Peak I) ^a	3.5×10^{-7}	0.05	8.75×10^{-7}	0.68
Affinity Chromatography (Peak I) ^b	1.29×10^{-5}	0.05	2.58×10^{-7}	25
Anion Exchange (Peak II) ^a	2.82×10^{-7}	4.0×10^{-4}	7.05×10^{-7}	0.55
Affinity Chromatography (Peak II) ^b	7.0×10^{-5}	6.0×10^{-4}	2.1×10^{-6}	137

^a This preparation exhibited a robust amount of kinase activity following a single freeze-thaw cycle.

^b This preparation exhibited a robust amount of kinase activity following two freeze-thaw cycles.

^c Protein concentration was determined by spectrophotometric analysis.

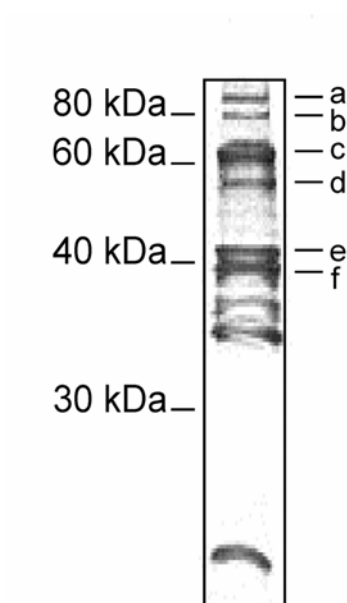


Figure 20. Silver stain of proteins isolated by sequential chromatography purifications of murine thymocyte lysates. Fractions 19-21 generated using the BRS-affinity column (Fig. 19) were acetone-precipitated, resolved by SDS-PAGE, and silver stained. The indicated bands (a-f) were then excised for mass spectrometry analysis.

Table III. Representative table of proteins identified by mass spectrometry analysis of affinity-purified fractions. The silver stained proteins indicated in Fig. 20 were extracted, digested with trypsin, and submitted to the UTSW protein core facility for mass spectrometry analysis. The sequences identified by mass spec as well as the corresponding protein name, function, and molecular weight are listed.

Band	Protein Name	MW (kDa)	Sequence Identified	Function
a	PTB-associated Splicing Factor	83	MGGGGTMNMGDPYGGGQK	Pre-mRNA Splicing Factor
b	G Protein-Coupled Receptor Kinase 2	80	LLDSDQELYR	Serine/Threonine Kinase
b	DEAD Box Polypeptide 5	69	MLDMGFEPQIR	RNA Helicase
c	Heterogeneous Nuclear Ribonucleoprotein L	60	SKPGAAMVEMADGYAVDR	RNA Binding Protein
d	Regulator of Differentiation 1	56	NNQFQALLQYADPVNAQYAK	RNA Binding Protein
e	Pigpen	52	TGQPMINLYTDR	DNA Stabilizing Protein
f	Farnesyl Diphosphate Synthetase	40	QILEENYGQKDPEK	Synthetase

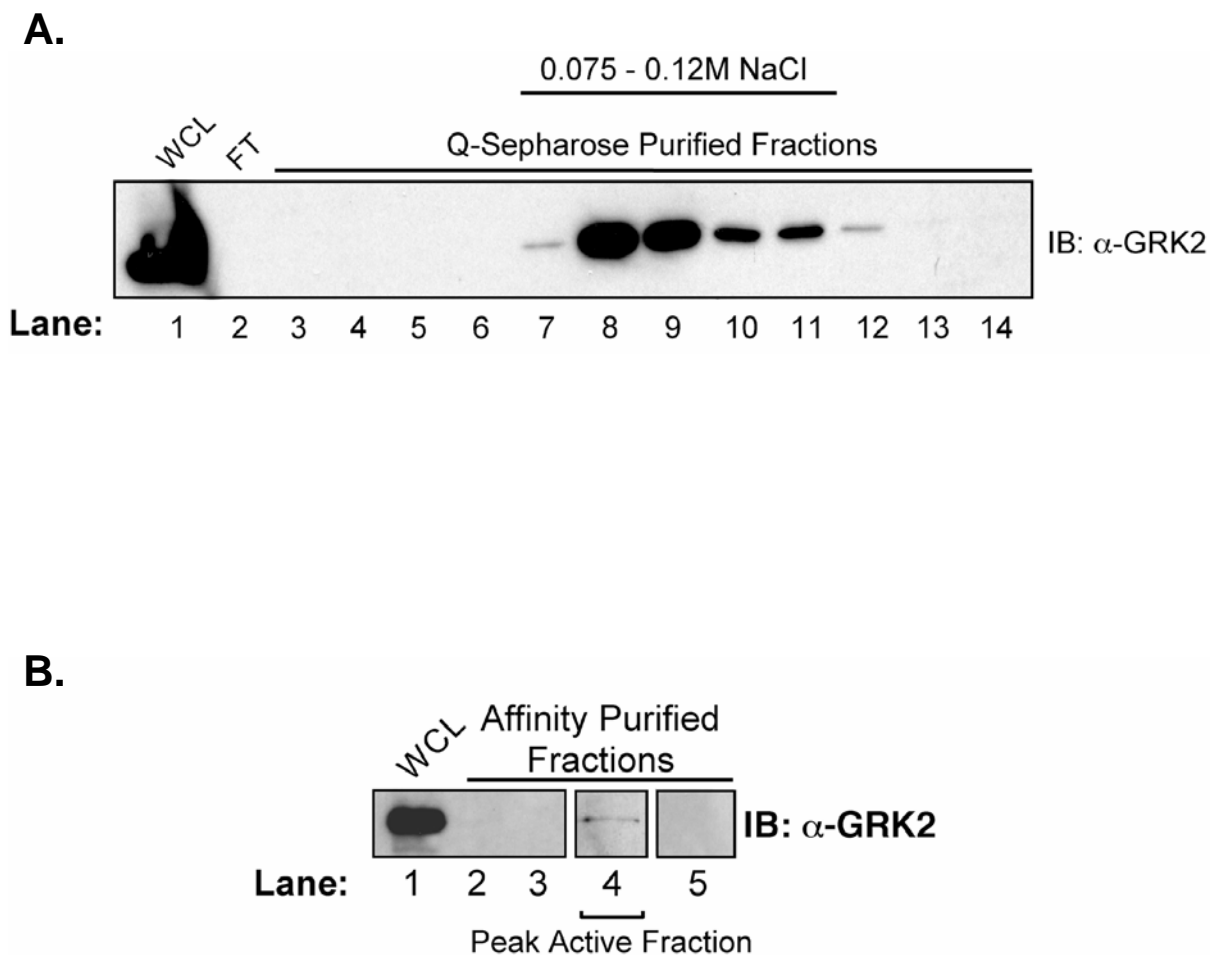


Figure 21. GRK2 elutes in the Q-Sepharose and affinity purified fractions that also contain the BRS-associated kinase activity. (A) An aliquot from Q-Sepharose purified fractions corresponding to those that contained the GST-BRS-associated kinase activity were resolved by SDS-PAGE and immunoblotted with an anti-GRK2/3 antibody. (B) Fractions generated by GST-BRS affinity chromatography were immunoblotted with an anti-GRK2/3 mAb. The peak active fraction (Lane 4) indicates the fraction that both contained the greatest amount of BRS-associated kinase activity and was submitted for mass spectrometry analysis. WCL = Whole cell lysate; FT = Flow through.

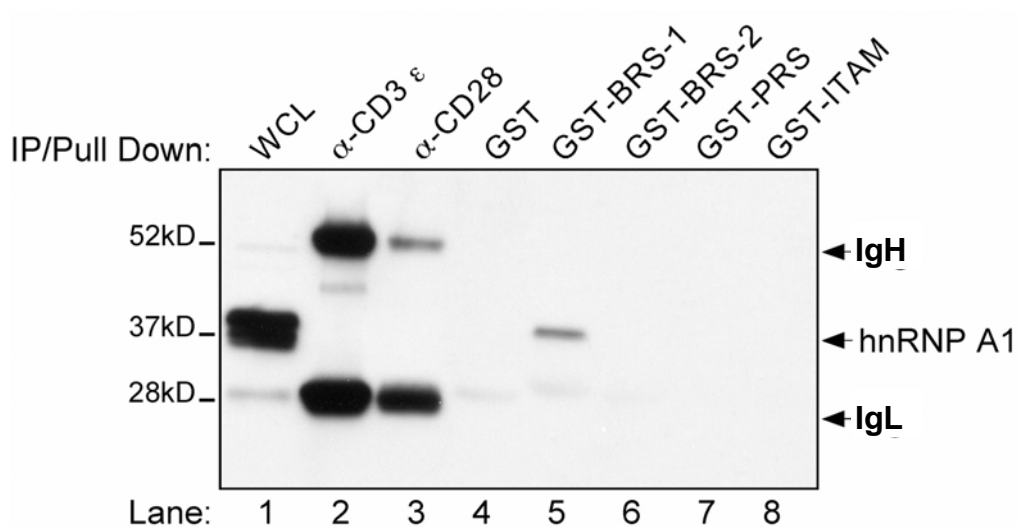


Figure 22. HnRNP A1 can co-precipitate with GST-BRS. Primary murine thymocyte extracts were subjected to immunoprecipitations or pull-downs using the indicated mAbs or GST-fusion proteins, respectively. Precipitated proteins were resolved by 12.5% SDS-PAGE and western blotted using an anti-hnRNP A1 mAb.

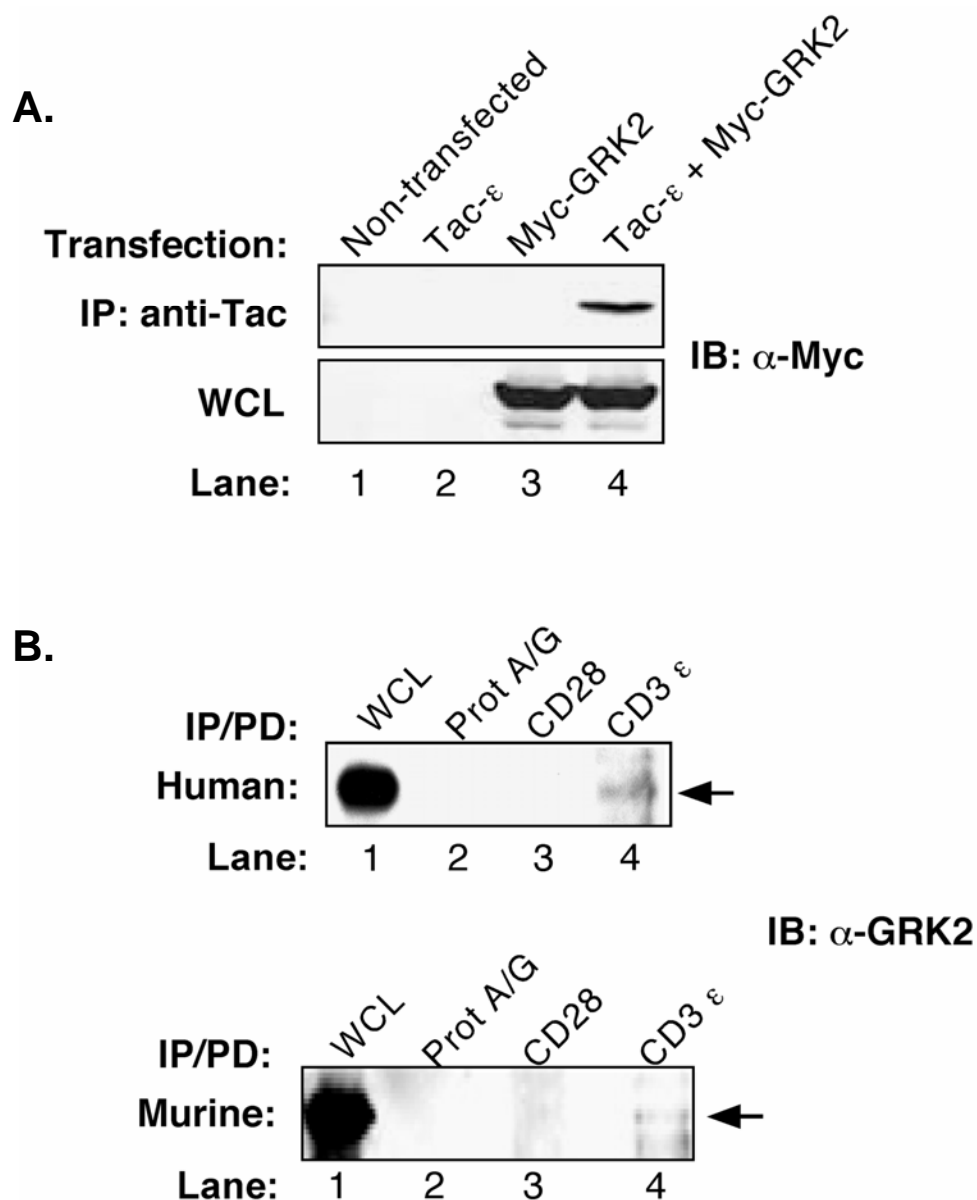


Figure 23. GRK2 is capable of interaction with CD3 ϵ . (A) HEK 293 T cells were transfected with the indicated constructs. Cells were lysed and Tac- ϵ was immunoprecipitated (IP) using an anti-Tac mAb. The precipitates were washed, resolved by 8% SDS-PAGE, and western blotted with anti-Myc. This figure is representative of nine of fifteen immunoprecipitations. (B) 3.0×10^8 primary murine or human thymocytes were lysed and subjected to immunoprecipitations with the indicated mAbs. Immunoprecipitates were stringently washed using a 1 M NaCl buffer. Western blots were performed with an anti-GRK2/3 antibody. Each blot is representative of two independent experiments.

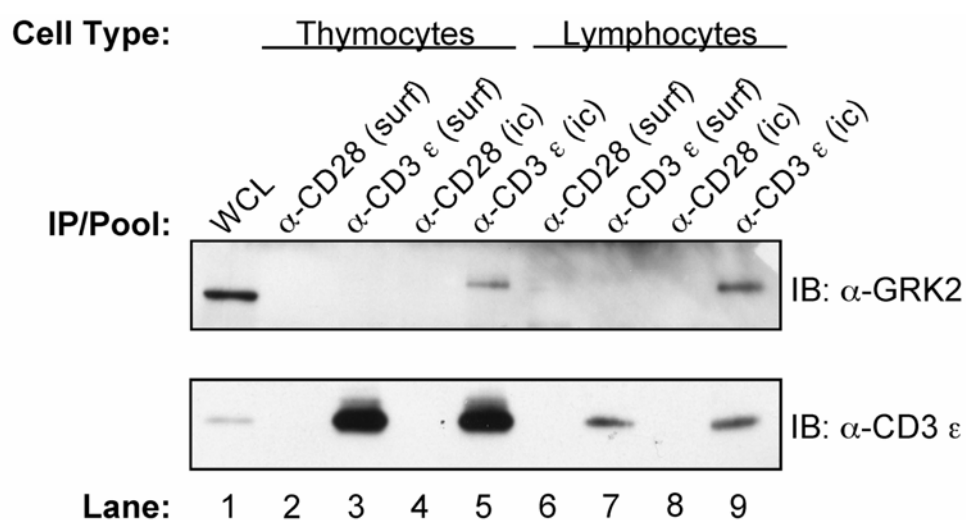


Figure 24. The intracellular pools of CD3 ϵ interact with GRK2. Primary murine thymocytes (Lanes 2 - 5) or lymphocytes (Lanes 6 - 9) were stained with mAbs capable of recognizing the extracellular portions of either CD28 or CD3 ϵ . The cells were washed, lysed, and incubated with Protein A-Sepharose to precipitate Ab-bound molecules. WCLs that had been cleared of surface stained CD28 or CD3 ϵ were subsequently incubated with anti-CD28 or anti-CD3 ϵ . All samples were resolved by SDS-PAGE and western blotted using Abs against GRK2/3 (upper panel) or CD3 ϵ (lower panel). surf = surface immunoprecipitation; ic = intracellular immunoprecipitation.

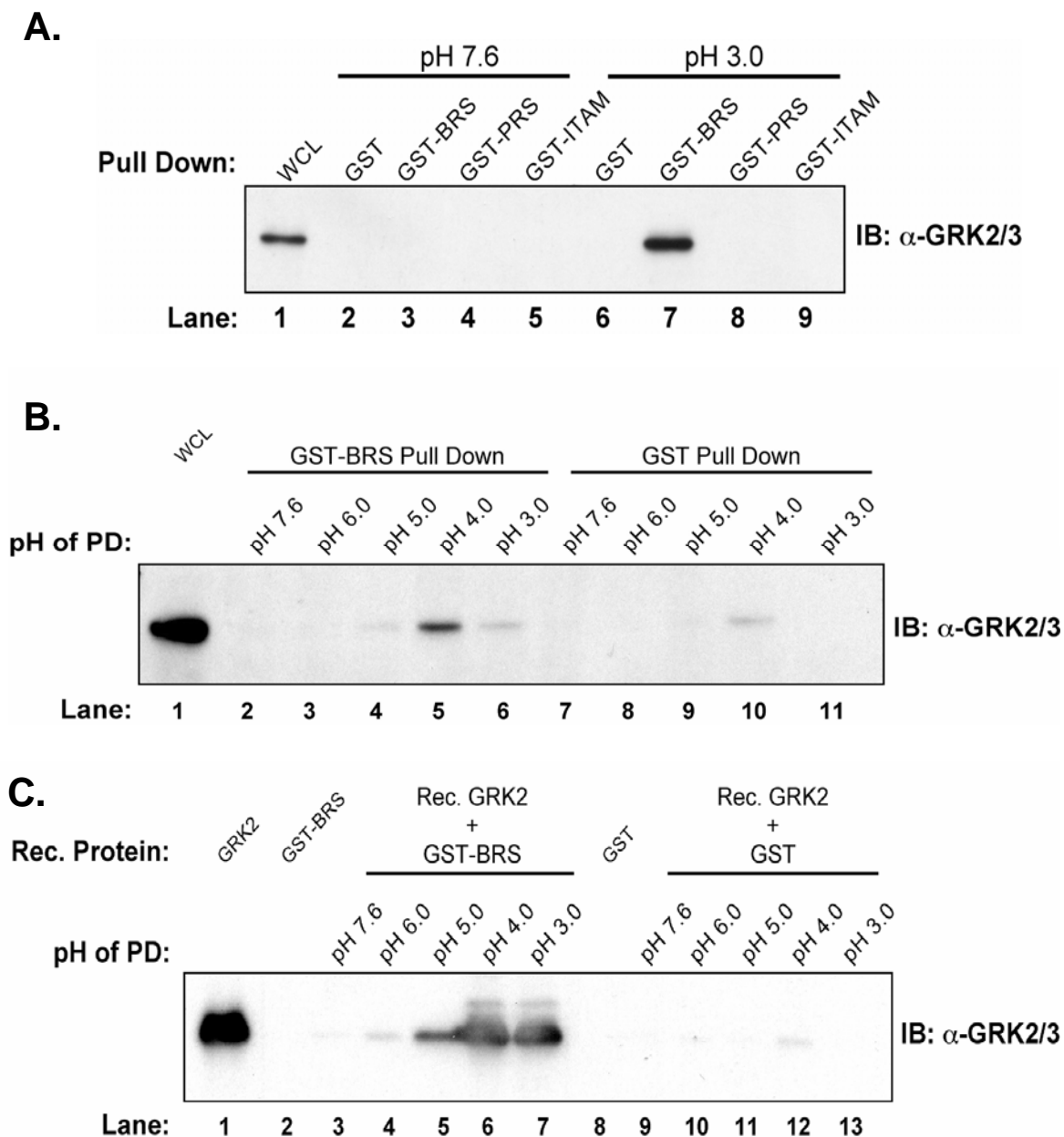


Figure 25. Interactions between the BRS and GRK2 are optimal at a low pH. (A) Primary thymocytes were lysed in a 1% Triton X-100 lysis buffer adjusted to a pH of 7.6 or 3.0. GST-fusion protein pull-downs were then performed, followed by SDS-PAGE and anti-GRK2/3 western blotting. (B) Murine thymocyte WCLs were generated at the indicated pH. GST or GST-BRS pull-downs were performed and associating proteins were resolved by SDS-PAGE. Interactions with GRK2 were investigated by anti-GRK2 immunoblotting. (C) Glutathione Sepharose absorbed GST or GST-BRS were incubated with 1 μ g of recombinant GRK2 in buffers adjusted to the indicated pH. The samples were washed at the same pH in which the pull-downs had been carried out and resolved by SDS-PAGE. Immunoblotting (IB) was performed using an anti-GRK2/3 Ab. PD = pull-down.

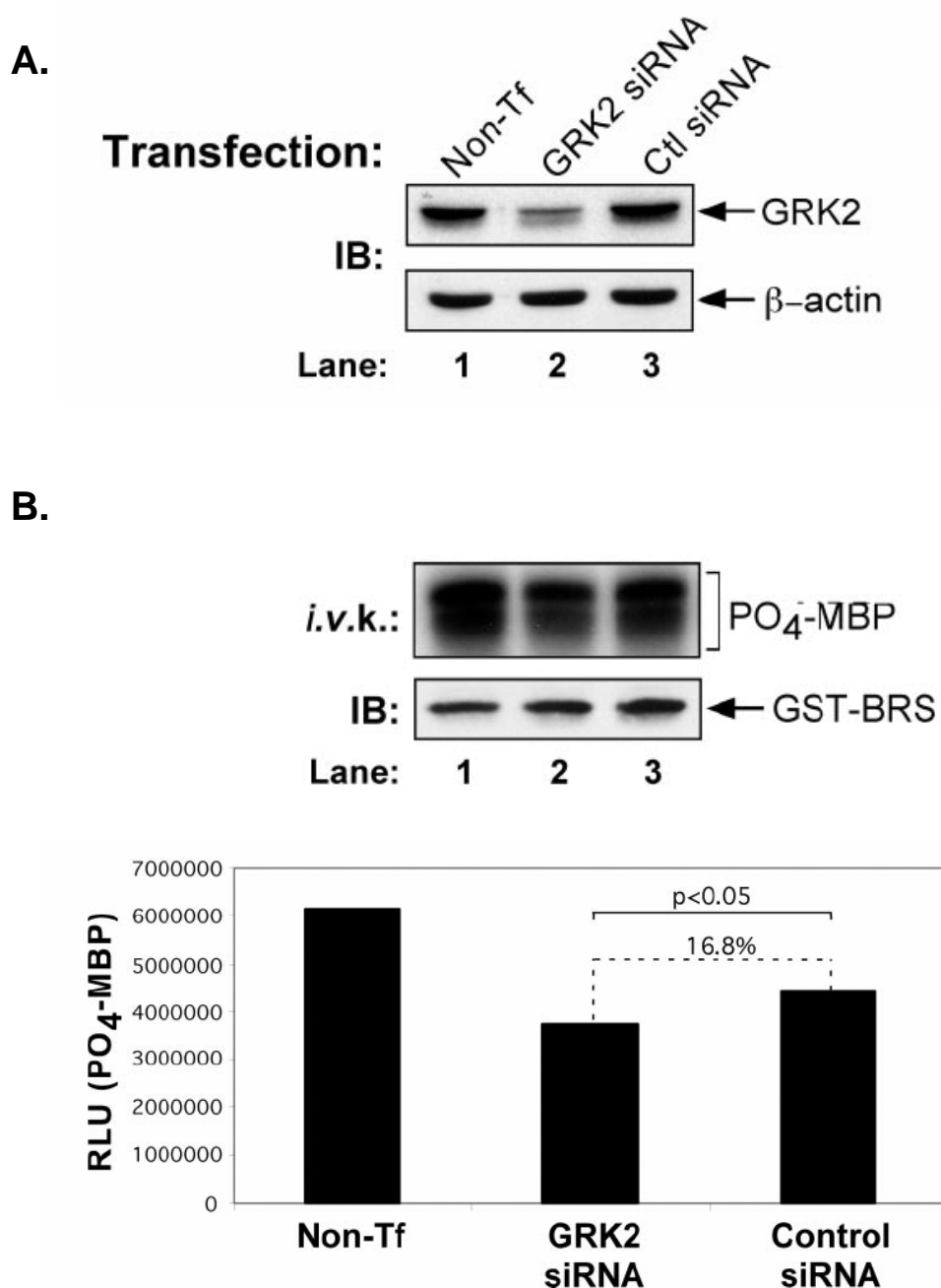


Figure 26. Reduced expression of GRK2 decreases the BRS-associated kinase activity. (A) Jurkat T cells were left untreated or were transfected with siRNAs specific for human GRK2 or luciferase (control). The cells were lysed, and GRK2 knockdown was assessed by western blot analysis of WCLs. (B) GST-BRS pull-downs were performed as described previously from the WCLs of Jurkat T cells transfected with the indicated siRNA. Kinase reactions were then performed in the presence of MBP. PO₄-MBP was visualized by autoradiography (upper panel) and quantified using a phosphoimager (RLU, relative light units). Immunoblotting (IB) against GST was performed to ensure equivalent levels of GST-BRS were used in each pull-down (lower panel).

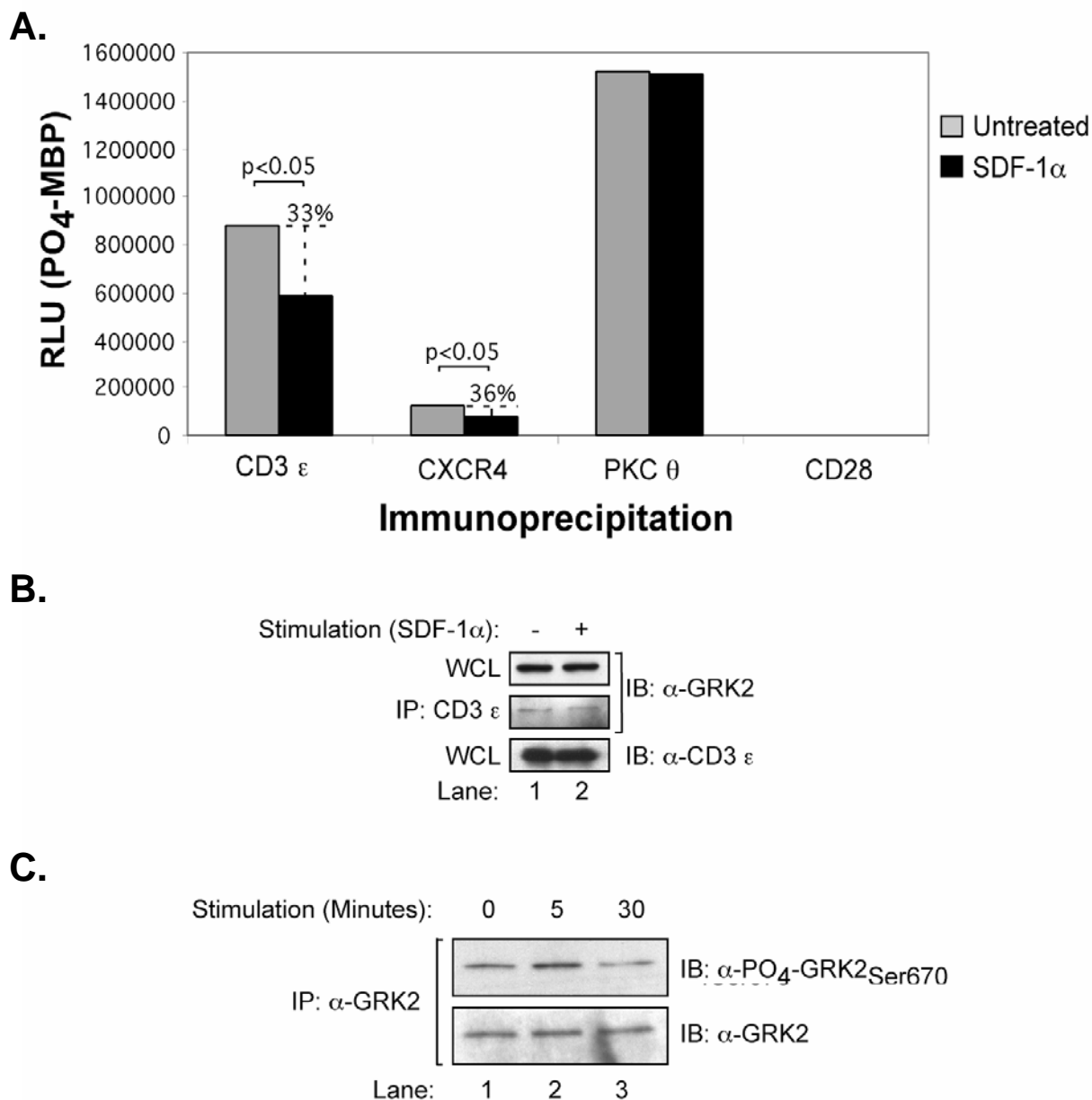


Figure 27. SDF-1 α treatment of primary thymocytes significantly decreases the amount of CD3 ϵ -associated kinase activity. (A) Thymocytes were incubated at 37°C with or without 5 x 10⁻⁸ M recombinant murine SDF-1 α for 30 min. The indicated molecules were isolated and subjected to *in vitro* kinase reactions. PO₄-MBP was quantified with a phosphoimager. Data are presented as relative light units (RLU) and are representative of six independent assays. (B) SDF-1 α treatments were performed as in (A). WCLs or CD3 ϵ immunoprecipitates (IP) from treated or untreated cells were then western blotted using the indicated antibodies. Results are representative of three experiments. (C) Thymocytes were treated with SDF-1 α for the indicated time points. GRK2 immunoprecipitates were then resolved and western blotted using an antibody directed against PO₄-GRK2 (Ser-670). The membrane was subsequently stripped and re-blotted using anti-GRK2. Results represent two independent assays.

CHAPTER IV

CHARACTERIZATION OF THE MEMBRANE-PROXIMAL BASIC-RICH STRETCH OF CD3 ϵ IN T CELL FUNCTIONS

Introduction

The cytoplasmic tail of CD3 ϵ contains three distinct signaling motifs (the BRS, PRS, and ITAM). Each of these subregions has been demonstrated to interact with a unique repertoire of adaptor/effector molecules that are important for signaling through the TCR (57). Additionally, the conformational change that occur within the cytoplasmic tail of CD3 ϵ following TCR ligation is a pre-requisite for T cell activation (22). Since independent mutations within the PRS or ITAM of CD3 ϵ have no effect on T cell development and/or TCR-mediated signaling, we wanted to assess the role of the BRS in these pathways (19, 50). An intriguing feature of the BRS is its similarity to polybasic clusters found in a number of other transmembrane proteins and certain signaling molecules. These patches of positively charged residues interspersed with hydrophobic amino acids have been identified in a variety of cytoskeletal proteins, clathrin adaptor proteins, and approximately 37 small GTPases (42, 142, 143). Such polybasic clusters allow proteins to electrostatically interact with negatively charged phosphoinositides (PtdIns), such as phosphatidylinositol-3-phosphate (PI(3)P) and phosphatidylinositol-4,5-bisphosphate (PI(4,5)P₂) (43). As a result of this charge-mediated binding, signaling molecules containing polybasic clusters are localized to various intracellular membranes, including the inner leaflet of the plasma membrane, the Golgi, and endosomes (42, 43). In the case of the epidermal growth factor receptor (EGFR), electrostatic interactions

between the positively charged residues within its membrane-proximal portion and negatively charged PtdIns concentrated on the surface of the plasma membrane are thought to regulate the catalytic activity of its cytoplasmic tail (44). In the context of the immune system, there are several transmembrane receptors in addition to CD3 ϵ that also contain polybasic motifs in their juxtamembrane portion. These include CD43, CD44, and ICAM-1/2 (144-146). Given the importance of polybasic clusters in mediating protein localization or signal initiation, we hypothesized that the BRS may contribute to TCR signaling and/or T cell development.

Thymocyte development begins when T cell progenitors, lacking both CD4 and CD8 (double negative (DN)), migrate into the thymus from the bone marrow. In the cortex of the thymus, these pre-T cells will progress through four developmental stages defined by their expression of CD25 and CD44. These stages are termed the DN1 stage (CD25⁻CD44⁺), DN2 stage (CD25⁺CD44⁺), DN3 stage (CD25⁺CD44⁻), and DN4 stage (CD25⁻CD44⁻) (147). During the DN3 stage of development, a number of enzymes, including RAG-1 and -2, rearrange the V-D-J gene segments encoding the variable portion of the β subunit (V β) (148). Productive β gene rearrangement results in the expression of a pre-TCR, while cells unable to produce a properly folded β chain will die of apoptosis. Thymocytes that manage to produce a properly assembled TCR must still go through positive and negative selection events (Reviewed in (149)). These developmental checkpoints are necessary to ensure that T cells released into the periphery are capable of recognizing peptide in the context of self-MHC but are not reactive to self-antigens. The outcome of positive and negative selection is thought to be regulated by the strength of TCR signaling (150, 151).

In the absence of CD3 ϵ , thymopoiesis is blocked at the CD44⁺/CD25^{low}, DN 3 stage (19, 152, 153). Consequently, CD3 $\epsilon^{-/-}$ mice exhibit a significant reduction in their overall thymic cellularity and possess no detectable peripheral T cells. The developmental block at the DN3 stage is due to the fact that mice lacking the CD3 ϵ subunit cannot assemble the pre-TCR complex (153-155). However, it should not be discounted that the cytoplasmic tail of CD3 ϵ may also play an important role in TCR signaling and development. Herein we present evidence that the BRS of CD3 ϵ complexes particular charged phospholipids. We further demonstrate that modifying the BRS in a manner that prevents these interactions significantly alters the ability of T cells to carry out normal T cell development.

Results

The BRS of CD3 ϵ Allows for Interactions with Select Phospholipids

To determine whether the BRS could interact with specific phospholipids, hydrophobic membranes spotted with lipids (PIP strips) were incubated with GST-fusion proteins containing the full-length cytoplasmic tail of CD3 ϵ (GST- ϵ) or the various subdomains of CD3 ϵ (GST-BRS, -PRS, or -ITAM) (Fig. 28A). GST alone served as a negative control. Ant-GST western blotting revealed that GST- ϵ could interact with several phosphorylated lipids, including phosphatidylinositol-3-phosphate (PI(3)P), phosphatidylinositol 4-monophosphate (PI(4)P), phosphatidylinositol 5-phosphate (PI(5)P), and phosphatidic acid (PA) (Fig. 28B). Less intense spots were also detected with phosphatidylinositol-3,4-bisphosphate (PI(3,4)P₂), phosphatidylinositol-4,5-bisphosphate (PI(4,5)P₂), and phosphoinositide-3,4,5-trisphosphate (PI(3,4,5)P₃). The ability of the CD3 ϵ 's cytoplasmic tail to mediate phospholipid interactions was mapped to the BRS since GST-BRS could complex the same phospholipids as GST- ϵ , while GST, GST-PRS, and GST-ITAM could not.

To determine whether the positively charged amino acids of the BRS were important for phospholipid binding, two additional GST-fusion proteins were generated. One had a truncation at the NH₂-terminal of the BRS, while the second had several of the positively charged residues substituted for uncharged amino acids (GST-BRS-Truncate and GST-BRS-Substitute) (Fig. 28A). Loss of these basic amino acids prevented lipid binding (Fig. 28B). These findings strongly supported the hypothesis that the basic

residues within the membrane-proximal portion of CD3 ϵ could mediate phospholipid associations.

We next addressed whether the BRS could complex phospholipids in an intact lipid bilayer. Experimentally, GST-BRS was incubated with sucrose-loaded liposomes composed of 100% phosphatidylcholine (PC) or 80% PC and either 20% PI, PI(4)P, or phosphatidylserine (PS). The liposomes were then pelleted, washed, and associating proteins were resolved by electrophoresis. Immunoblotting against GST revealed that liposomes containing PI(4)P were uniquely capable of precipitating GST-BRS (Fig. 29). Since little binding was observed with liposomes containing PS, BRS interactions with phospholipid exhibited specificity (*Lane 7*). Taken together, these findings suggested that the BRS of CD3 ϵ may play a previously unrecognized role in TCR-mediated signaling events by interacting with charged phospholipids.

Modifications within the BRS of CD3 ϵ Do Not Interfere with CD3 ϵ Protein Expression or TCR Assembly in Transfected Cells

To characterize the BRS, we generated five distinct modifications within it. These modifications were designed to eliminate several of its basic amino acids by truncating its NH₂-terminus (BRS-Truncate) or substituting two or more of the basic residues with uncharged, non-polar amino acids (BRS-Substitute and BRS-Mutate) (Fig. 30). In one construct, the first twenty-one amino acids of the BRS were relocated to the membrane-distal portion of the molecule (BRS-Displace).

Western blotting revealed that all of the CD3 ϵ constructs were expressed as full-length proteins in transfected cells (Fig. 31A). Of note, the BRS-Substitute, BRS-Truncate, and BRS-Mutate proteins had a slightly faster mobility when subject to electrophoresis.

The CD3 ϵ subunit must pair with CD3 γ or CD3 δ in order for proper TCR assembly to occur. To determine if modifying the BRS affected CD3 γ or CD3 δ pairing, HEK293 cells were transfected with full-length CD3 γ or CD3 δ alone or in combination with the different CD3 ϵ -BRS constructs (Fig. 31B). CD3 ϵ was then immunoprecipitated and analyzed for the presence of CD3 γ or CD3 δ as co-precipitating molecules. These assays determined that all of the CD3 ϵ BRS-modified constructs retained their ability to pair with CD3 γ and CD3 δ (*Lanes 2-6*).

Distinct Modifications within the BRS Interfere with Nck Binding and ITAM

Phosphorylation

When CD3 ϵ is expressed in non-T cells in the absence of the other TCR/CD3 chains, the PRS is constitutively available for Nck binding (45). To determine whether modifications within the BRS could interfere with PRS/Nck binding, Nck pull-downs/western blotting assays were performed using HEK293 T cells. CD3 ϵ BRS-Wild Type, -Substitute, -Truncate, and -Mutate were all detected in the GST-Nck pull-downs (Fig. 32; *middle panel; Lane 2-4 and 6*). In contrast, CD3 ϵ BRS-Displace could not associate with Nck. This may indicate that the location of the BRS within the cytoplasmic tail of CD3 ϵ is important for Nck binding. Alternatively, the failure of Nck

to associate might relate to the relocalization of the PRS into such close proximity with the plasma membrane.

The membrane-distal portion of CD3 ϵ contains an ITAM. To determine whether modifications of the BRS could affect the tyrosine phosphorylation of this motif, the different CD3 ϵ constructs were co-transfected in HEK293T cells with Lck and analyzed for their phosphorylation state (Fig. 33A). CD3 ζ was utilized as a positive control (106). Wild type CD3 ϵ was difficult to detect as a phosphorylated protein, consistent with studies in intact T cells (*Lane 2*). This was also true for the BRS-Displace and BRS-Mutate constructs (*Lanes 5 and 6*). Interestingly, phosphorylated CD3 ϵ was detected in the BRS-Substitute and BRS-Truncate molecules. To ensure that all the BRS-modified constructs could be phosphorylated, the transfected cells were treated with pervanadate (an irreversible protein tyrosine phosphatase inhibitor). Using this reagent, all of the CD3 ϵ BRS constructs were detected as tyrosine phosphorylated proteins (Fig. 33B). These experiments suggested that the basic charge of the BRS interferes with the ability of the CD3 ϵ ITAM to be phosphorylated, perhaps by regulating the accessibility and/or the conformation of the CD3 ϵ cytoplasmic tail.

Expression of a Transgene Encoding Mutations in the BRS Restores CD3 ϵ Protein

Expression in CD3 ϵ -Deficient Mice

There are currently no CD3 $\epsilon^{-/-}$ T cell lines that could be used to explore the function of the BRS through CD3 ϵ reconstitutions. Consequently, we used a transgenic approach to assess the role of the BRS in TCR-mediated signaling. This strategy would

also allow us to identify contributions of the BRS to T cell development. To generate BRS transgenic mice, CD3 ϵ cDNAs containing the BRS-Wild Type, BRS-Substitute, BRS-Truncate, and BRS-Displace constructs were subcloned into the VA-CD2 transgenic cassette (105, 106). The DNA was submitted to the Transgenic Technology Center at UT Southwestern in order to generate C57BL/6 transgenic lines. BRS transgenic founders were identified by Southern blotting and backcrossed onto a CD3 ϵ null background (Fig. 6). At least three different transgenic founders per construct were analyzed in these studies. CD3 ϵ protein expression in the lymphoid tissues of several of the transgenic lines was verified by western blot analysis (Fig. 34A). In spite of a restoration in the expression of CD3 ϵ protein, certain lines exhibit a significant decrease in their overall thymic cellularity. There was a slight decrease in the average thymic cellularity of mice encoding the BRS-Wild Type transgene when compared to C57BL/6 mice (Fig. 34B; $p \leq 0.05$). This is possibly due to the fact that a high copy number of the CD3 ϵ gene can dysregulate the recruitment of signaling molecules to the TCR complex (156). For this reason, mice bearing mutations within the BRS were analyzed in comparison to both C57BL/6 mice and the BRS-Wild Type transgenic line. Mice possessing the BRS-Substitute, -Truncate, and -Displace transgenes had a statistically significant reduction in thymic cellularity when compared to BRS-Wild Type mice (Fig. 34B). The BRS-Displace resembled CD3 $\epsilon^{-/-}$ mice, as their average thymic cellularity was 100 fold less than that of C57BL/6 mice ($p \leq 0.001$). It is important to note that the BRS-Substitute, -Truncate, and -Displace mice had comparable CD3 ϵ protein expression as BRS-Wild Type mice (Table I). These findings clearly show that the reduced thymic cellularity was not a consequence of protein overexpression.

Select modifications of the BRS Block T Cell Development in Transgenic Mice

T cell development can be characterized by the cell surface expression of the co-receptors, CD4 and CD8. The BRS-Wild Type transgene fully restored T cell development in CD3 $\epsilon^{-/-}$ mice, as normal percentages of CD4⁻CD8⁻ (double negative-DN), CD4⁺CD8⁺ (double positive-DP), CD4⁺CD8⁻ and CD4⁻CD8⁺ (single positive-SP) cells were detected (Fig. 35A). Mice expressing the BRS-Substitute transgene also had normal percentages of DP and SP thymocytes, while those expressing the BRS-Truncate transgene exhibited an average 10% decrease in the DP population (Fig. 35B). The BRS-Displace transgenic mice had a complete block at the DN stage of development with less than 1% DP thymocytes.

To define whether pre-T cell development was affected by the BRS-modifications, we analyzed Thy1.2⁺CD4⁻CD8⁻ cells for their expression of CD25 and CD44. Thymic development is blocked at the DN3 stage in CD3 $\epsilon^{-/-}$ mice (Fig. 36A) (19, 152, 153). The BRS-Displace mice had a similar block at the DN3 stage, with more than 90% of the cells being CD44⁻CD25⁺ (Fig. 36A). Mice bearing the BRS-Substitute and -Truncate transgenes also exhibited an intermediate developmental block in the DN3 to DN4 transition. Consequently, the percentage of cells in the DN4 stage from these lines was significantly reduced in comparison to C57BL/6 mice (Fig. 36B; $p \leq 0.001$). The BRS-Wild Type mice revealed no significant variations in the percentages of cells in the DN stages.

We next examined the peripheral populations of cells in the BRS-transgenic lines. Cells were isolated from the lymph nodes or spleens of various transgenic mice, stained

with mAbs against CD3, CD4, CD8, and B220 and analyzed by flow cytometry. The BRS-Wild Type, -Truncate, and -Substitute exhibited no significant variation in the percentages of CD4⁺, CD8⁺, CD3⁺, or B220⁺ cells when compared to C57BL/6 controls (Fig. 37-40). Conversely, the BRS-Displace mice had a significant reduction in the percentage of both of CD4⁺ and CD8⁺ SP T cells (<10% of normal) when compared to control animals (Fig. 37 and 38). Although the BRS-transgenics generally expressed twice as much CD3 ϵ at the protein level as wild type C57BL/6 mice, CD3 staining revealed that the BRS-Wild Type, -Truncate, and -Substitute mice had relatively equivalent TCR surface expression (Table I; Fig. 39 and 40). Cells isolated from the BRS-Displace mice resembled those from CD3 ϵ deficient animals in that there were no CD3⁺ T cells in the periphery (Fig. 39 and 40). The lack of CD3⁺ cells in these mice coincided with an increase in the percentage of B220⁺ cells in their lymph nodes (Fig. 39). An increase in the percentage of B220⁺ cells was also observed in the spleens of CD3 ϵ ^{-/-} mice, while the percentage of these cells remained normal in the spleens of the BRS-Displace mice (Fig.40). Collectively, these results suggest that modifying the number of positively charged residues within the BRS or relocating the BRS distal from the plasma membrane has a significant impact on T cell development.

TCR β Gene Rearrangement and Invariant Chain Pairing Occur Normally in the BRS-Displace Mice

During thymic development, the gene segments encoding the TCR β subunit will undergo a rearrangement process. Productive rearrangement of the TCR β gene is

detected by the expression of a pre-TCR complex, which consists of the TCR β chain, a pre-T α polypeptide, and the CD3 subunits. Signals generated through the pre-TCR result in the differentiation of DN cells into DP thymocytes. The block in T cell development at the DN3 stage in the BRS-Displace mice suggested a defect in pre-TCR signaling. To examine this possibility, we first wanted to verify pre-TCR expression in the BRS-Displace transgenic line. We began by investigating whether the TCR β gene segments were undergoing rearrangement. Genomic DNA, isolated from the thymus of C57BL/6 or BRS-Displace transgenic mice, was analyzed by PCR with primers directed against the V β 8 gene segment. Multiple bands of varying molecular weights were observed in samples containing thymic DNA from either wild type or BRS-Displace mice, while no product was visualized in control samples containing tail DNA (Fig. 41A). The presence of multiple bands indicated different sized TCR β genes, a result that confirms the presence of recombination at the TCR β locus in the BRS-Displace mice.

To further ensure that a pre-TCR could be assembled, CD3 ϵ was immunoprecipitated from C57BL/6 or BRS-Displace mice, followed by western blot analysis using antibodies directed against CD3 γ or δ (Fig. 41B). Both CD3 γ and δ co-precipitated with CD3 ϵ in the BRS-Displace transgenics (*Lane 2*). These experiments strongly suggest that the pre-TCR is assembled in BRS-Displace mice but is unable to signal. To assess this possibility, we examined whether the *in vivo* injection of anti-CD3 ϵ antibodies could induce the differentiation and expansion of DN thymocytes into CD4⁺CD8⁺ DP cells. In mice lacking expression of the RAG recombinases or the TCR- β subunit, injections of anti-CD3 causes a dramatic upregulation of CD4 and CD8, concomitant with a 10-50 fold expansion of the DP population (157-159). This results

from the engagement of CD3 γ/ϵ and δ/ϵ clonotypic-independent complexes (CIC) that are expressed at low levels on the surface of a T cell (160). The injection of anti-CD3 ϵ into the BRS-Displace mice did not result in the expansion of thymocyte cell numbers (Fig. 42A). Furthermore, flow cytometric analysis of these animals revealed that their thymocytes did not differentiate effectively to the DP stage (Fig. 42B). Taken together, these experiments indicate that while the pre-TCR assembles in the BRS-Displace line, it is unable to generate appropriate intracellular signals.

The Induction of Phosphoproteins and CD69 Expression is Normal in the BRS-Substitute and -Truncate Transgenic Mice

To examine whether the signaling properties of the TCR complex were altered in the BRS-Substitute or -Truncate lines, peripheral lymphocytes were analyzed for the appearance of multiple tyrosine-phosphorylated proteins before and after TCR cross-linking with anti-CD3 ϵ . Phospho-tyrosine western blotting revealed that lymphocytes from the BRS-Wild Type and -Substitute mice possessed normal levels of p21 (phospho-CD3 ζ) prior to receptor engagement (Fig. 43). The induction of p23 (phospho-CD3 ζ) in these lines was also comparable to wild type controls following TCR stimulation. Additionally, the tyrosine-phosphorylation of ZAP-70 was equivalent in the various transgenic mice, indicating that the activation of early effector proteins is not effected by substituting basic residues within the BRS. Similar results were obtained when lymphocytes from BRS-Truncate mice were analyzed (data not shown).

To address whether the BRS might regulate more distal TCR-mediated signaling events, we compared lymphocytes from the different transgenic mice for their ability to upregulate CD69. Both before and after T cell activation, the BRS transgenic lines exhibited a comparable level of CD69 expression on the surface of both CD4⁺ and CD8⁺ when compared to C57BL/6 controls (Fig. 44 and 45). These experiments indicate that the BRS is not required for signaling in response to strong stimuli, such as anti-CD3 ϵ mAbs.

Discussion

The cytoplasmic tail of CD3 ϵ consists of three distinct subregions (the BRS, PRS, and ITAM). Herein, we have provided evidence that the BRS of CD3 ϵ functions as a critical motif in developing T cells. In addition to mediating interactions with the Ser/Thr kinase GRK2, we have found that this domain binds to particular charged phospholipids, including PI(4)P and PI(4,5)P₂. Reducing the number of positively charged residues within the BRS interfered with the ability of GST-fusion proteins containing the BRS to bind phospholipids embedded in hydrophobic membranes. These results are consistent with reports demonstrating that the basic amino acids of certain transmembrane receptors are important for phospholipid binding (44).

Different phospholipid species are expressed on distinct intracellular membranes. For example, some PI(4)P is located at the plasma membrane (161). However, the majority of this phospholipid is concentrated on the Golgi complex. PI(4,5)P₂ is found primarily at the plasma membrane and serves as a precursor for IP₃ and DAG (Reviewed in (162)). The finding that the BRS could mediate interactions with distinct phospholipids might have important implications for its role in T cells. For instance, if the BRS predominantly binds PI(4)P, it may serve to regulate the translocation of the TCR from the ER to the plasma membrane. Alternatively, interactions between the BRS and phospholipids, such as PI(3)P or PI(3,5)P₂, might allow this motif to mediate the endocytosis of the TCR after ligand engagement. As previously described, interactions between a polybasic cluster located in the juxtamembrane of the EGFR and PI(4,5)P₂ at the plasma membrane are thought to regulate the initiation of signaling events through

this receptor. Consequently, it is also possible that interactions between the BRS and PI(4,5)P₂ might serve a similar role in the initiation of TCR signals. This hypothesis is particularly appealing since it would provide a mechanistic basis for how the conformational change that occurs within the cytoplasmic tail of CD3 ϵ takes place following TCR engagement. Two distinct models for this hypothesis are presented in greater detail in Chapter V.

Analysis of transgenic mice bearing mutations within the BRS revealed that this polybasic motif was necessary for proper T cell development. Eliminating five of the positively charged residues within the BRS through truncations or substitutions resulted in a significant reduction in the percentage of cells progressing to the DN4 stage when compared to C57BL/6 controls. Mice in which the BRS had been relocated to the membrane-distal end of CD3 ϵ 's cytoplasmic tail exhibited an even greater block in T cell development, with >90% of their thymocytes arrested in the DN3 stage. The developmental block in the BRS-mutant mice coincided with a significant reduction in their overall thymic cellularity. Such defects occurred in spite of the fact that similar TCR levels and CD3 ϵ protein expression were exhibited in the BRS-mutant mice when compared to BRS-Wild Type transgenic controls.

In terms of why a developmental defect occurs in the BRS-mutant mice, it is possible that mutating the BRS interferes with the ability of this motif to bind phospholipids, thereby leading to a dysregulation in TCR signaling. This hypothesis was supported by our findings that the phosphorylation of the BRS-Substitute and -Truncate CD3 ϵ chain was altered in transfected HEK293 T cells. Interestingly, TCR signal transduction in peripheral T cells from the BRS-Wild Type, -Substitute, and -Truncate

mice indicated that the phosphorylation of early signaling proteins was comparable to wild type controls. The induction of CD69 expression was also intact in these BRS-transgenics. Although a pronounced defect in TCR signaling was not observed in these assays, a number of factors should be taken under consideration. First, these assays only looked at a single stimulation time point (10 minutes). It is possible that the kinetics of signaling may vary among the BRS-transgenic animals. Consequently, both earlier and later time points should be analyzed to determine if eliminating the positively charged residues of the BRS through truncations or substitutions modifies the initiation of TCR-mediated signaling or its sustainability.

It should also be noted that lymphocytes stimulations were performed using a very potent stimulus (α -CD3 ϵ plus α -CD28). Engagement of the TCR with a more physiologically relevant ligand, such as peptide-MHC, could yield different results. Since the BRS-transgenic mice are currently on a C57BL/6 background, they possess a diverse α/β repertoire. Consequently, peptide-MHC stimulations may not be possible on this background. However, superantigens, such as staphylococcal enterotoxin B, might be useful. This is due to the fact that superantigens function by “gluing” the β subunit of the TCR to MHC molecules expressed on antigen presenting cells. Although this approach would still bypasses the specificity of the peptide presented in the MHC, the fact that signals will be generated through the engagement of the TCR as opposed to antibody ligations of the CD3 ϵ subunit might uncover differences in signaling within the BRS transgenics. For an even more physiological approach, the BRS-transgenic mice could be mated with a TCR transgenic line, such as the HY or OTII transgenics. This technique would give rise to mice bearing an antigen specific TCR with distinct

mutations in the BRS. The benefit of using such mice is address in more detail in Chapter V.

Of all the BRS-transgenics, the BRS-Displace mice exhibited the greatest defect in T cell development. Given that CD3 pairing and TCR β gene rearrangement appeared normal in these mice, it is likely that pre-TCR expression was intact in the BRS-Displace thymocytes. These results coupled with the finding that anti-CD3 injections did not allow for a DN to DP transition indicates that signaling through the BRS-Displace pre-TCR is defective. Signaling errors might be due to the fact that relocating the BRS to the membrane distal portion of CD3 ϵ removes it from the phospholipids expressed on intracellular membranes. Consequently, the TCR in these mice may no longer be able to initiate signaling events necessary to drive the differentiation of developing T cells. As one might expect from the severe defect in the BRS-displace thymic development, mature single positive T cells were significantly reduced in the peripheral tissues of these mice. This coincided with an increase in the percentage of B220⁺ cells in the lymph node of this transgenic strain. Interestingly, a similar increase was not observed in the spleen of these animals. This phenomenon may reflect the increase of another non-B cell population, such as monocytes and macrophages, within the BRS-Displace spleens. The expression of NK cells may also be affected in these animals since their development can be influenced by CD3 ϵ expression. NK cells are known to produce CD3 ϵ , although its expression is not detected on the surface of the cells. As of yet, the function of CD3 ϵ in NK cells remains unknown. If a defect is identified in the NK cells of BRS transgenic mice, further analyses might be warranted in order to elucidate the function of CD3 ϵ within this white blood cell population.

A.

CD3 ϵ : **KNRKAKAKPVTRGTGAGSRPRGQNKERPPPVPNPDYEPiRKGQRDLySGLNQRAV**
 BRS: **KNRKAKAKPVTRGTGAGSRPRGQNK**
 BRS-Substitute: **ANVGA / AKPVT LGTGAGSRPRGQNKERPPPVPNPDYEPiRKGQRDLySGLNQRAV**
 BRS-Truncate: **PVTRGTGAGSRPRGQNKERPPPVPNPDYEPiRKGQRDLySGLNQRAV**
 PRS: **ERPPPVPNPDYE**
 ITAM: **NPDYEPiRKGQRDLySGLNQRAV**

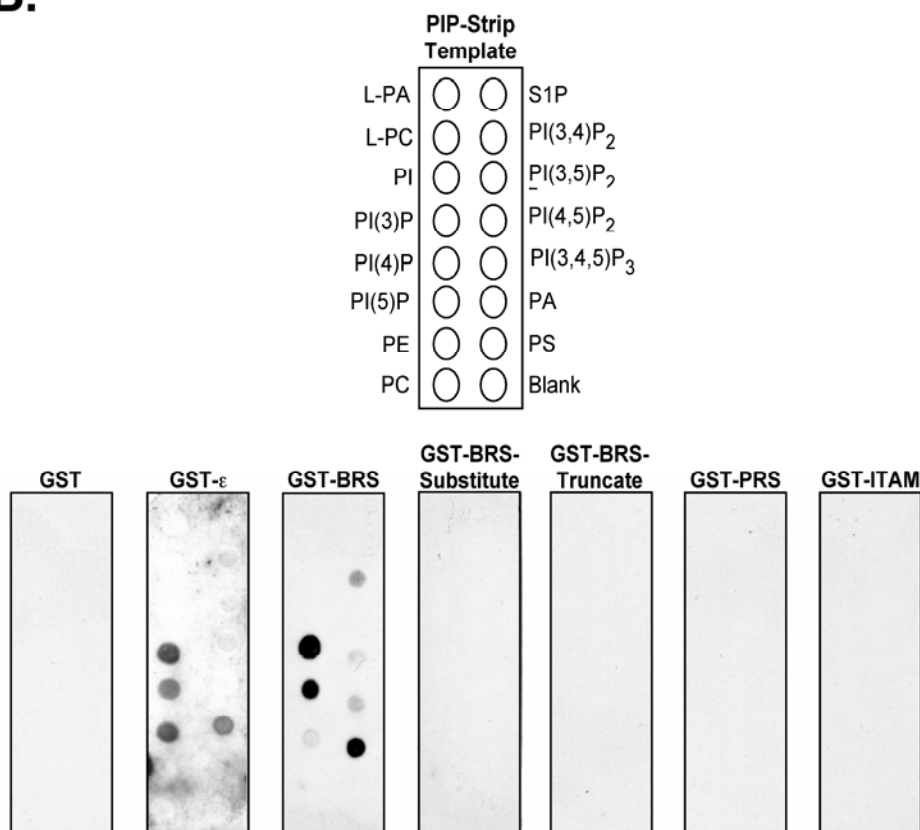
B.

Figure 28. The BRS of CD3 ϵ mediates phospholipid binding. (A) Schematic representation of GST-fusion proteins containing the full-length cytoplasmic tail of CD3 ϵ , the three subregions of CD3 ϵ (BRS, PRS, and ITAM), or the full-length tail of CD3 ϵ with select mutations within the BRS (BRS-Substitute and -Truncate). (B) Membranes spotted with various lipids were incubated with GST-fusion proteins containing the amino acid sequences shown in (A). The membranes were then washed and western blotting with an anti-GST mAb. Lipid bound proteins were detected by chemiluminescents.

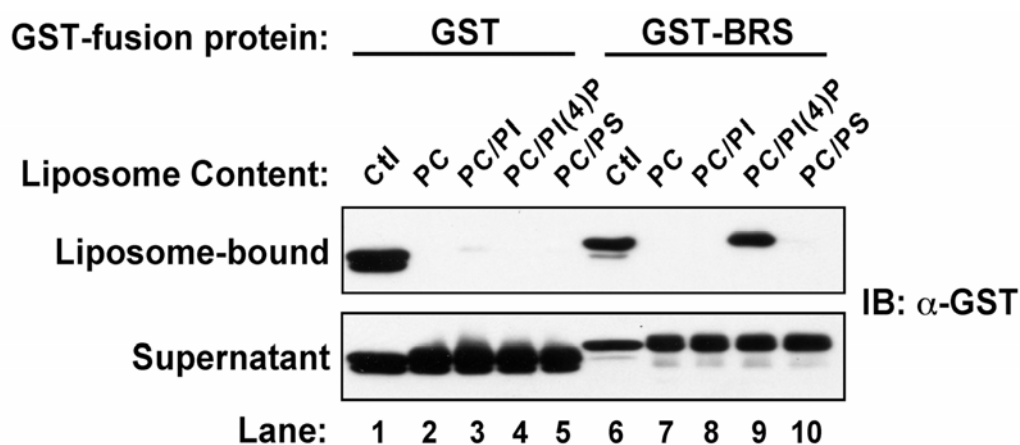


Figure 29. The BRS of CD3 ϵ can bind phospholipid in the context of a bilayer. Sucrose-loaded liposomes containing 100% phosphatidylcholine (PC) or 80% PC and 20% phosphatidylinositol (PI), phosphatidylinositol-4-phosphate (PI(4)P), or phosphatidylserine (PS) were incubated with purified GST or GST-BRS. The liposomes were then pelleted and an aliquot of supernatant from each sample was retained. The liposomes were washed and resuspended in SDS-sample buffer. Liposome-bound proteins (upper panel) as well as the aliquot of unbound protein contained in the supernatants (lower panel) were resolved by SDS-PAGE and western blotted using an anti-GST mAb. Ctl = purified GST (Lane 1) or GST-BRS (Lane 6).

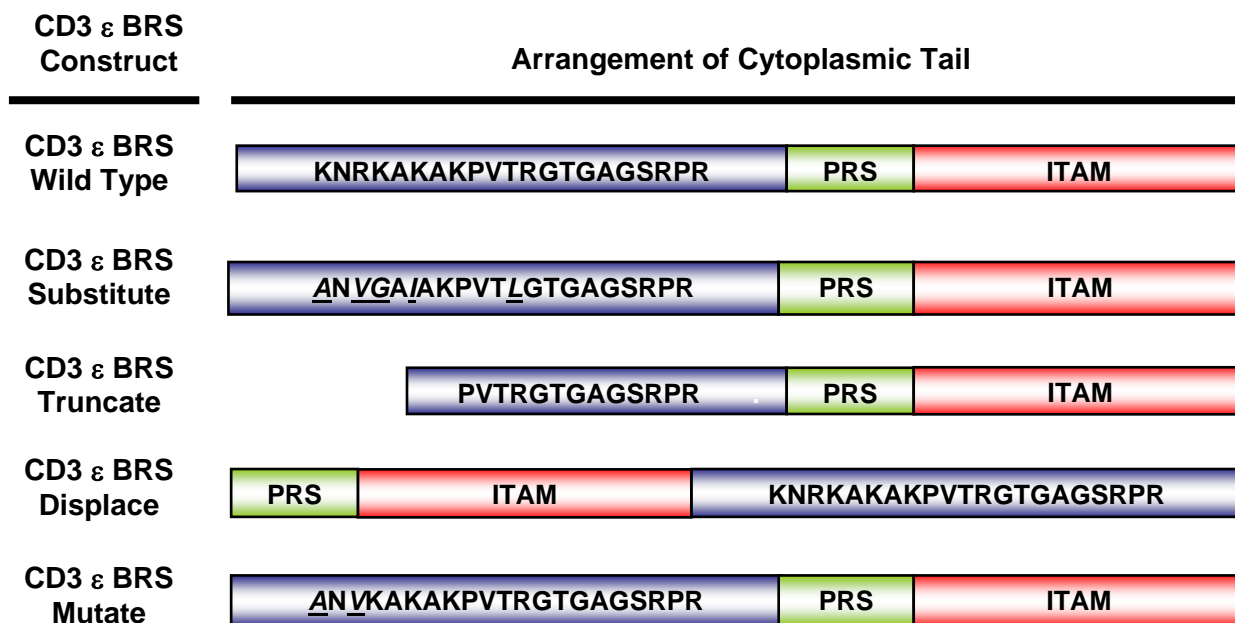


Figure 30. Schematic representation of the CD3 ϵ BRS transgenic constructs. Expression vectors were generated to encode the full-length CD3 ϵ protein (including the extracellular and transmembrane domains) with the indicated modifications within the cytoplasmic tail of the protein.

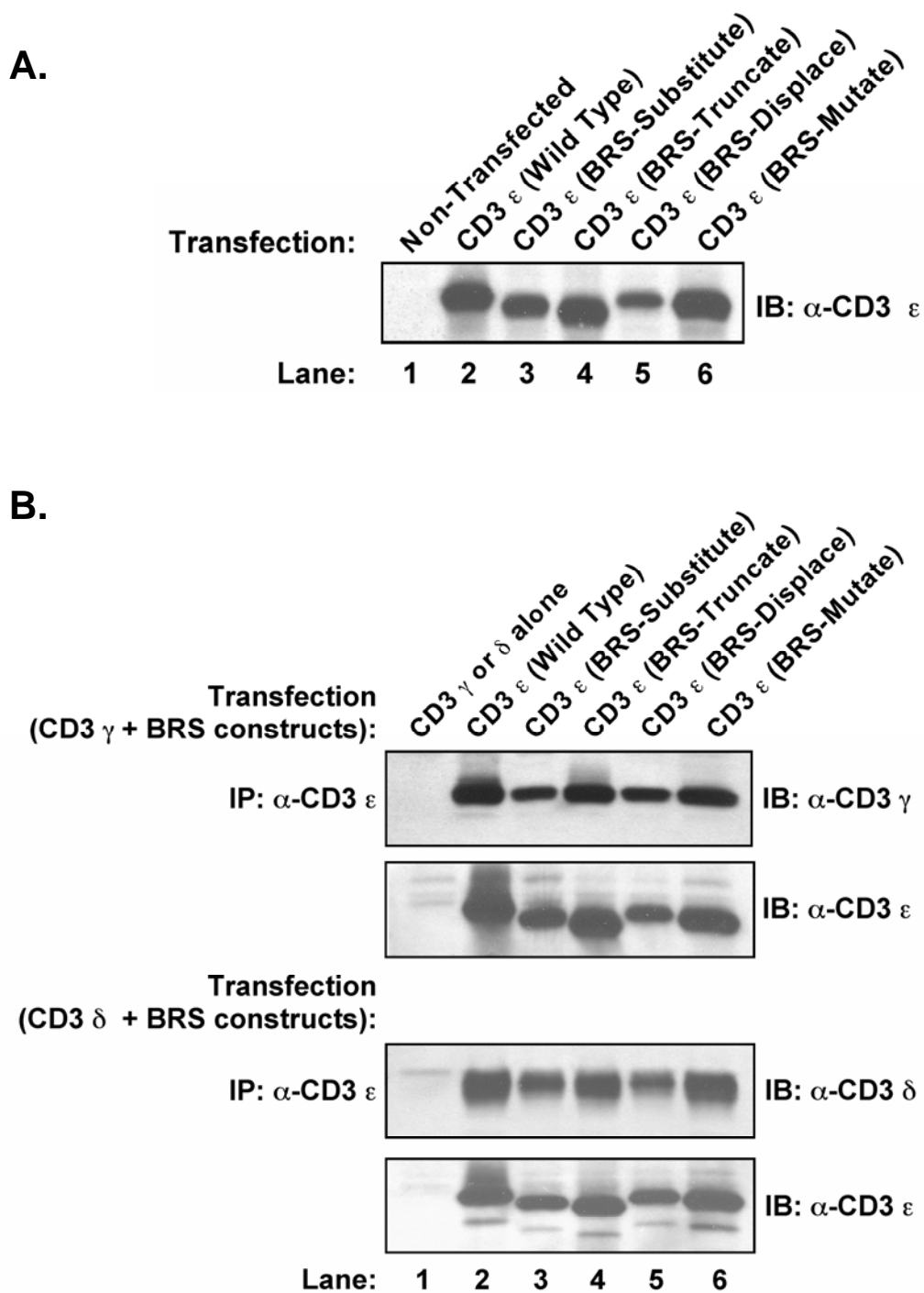


Figure 31. CD3 ϵ protein expression and pairing with CD3 γ or δ are not disrupted by mutations within the BRS. (A) HEK293 T cells were transfected with the indicated CD3 ϵ BRS constructs. Forty-eight hours later, the cells were lysed, WCLs were resolved by SDS-PAGE, and anti-CD3 ϵ immunoblotting was performed. (B) HEK293 T cells were transfected with the indicated CD3 ϵ BRS constructs in combination with either CD3 γ (two upper panels) or CD3 δ (two lower panels). CD3 ϵ immunoprecipitations were then performed and blotted for CD3 γ or CD3 δ . The membranes were then stripped and re-probed with anti-CD3 ϵ .

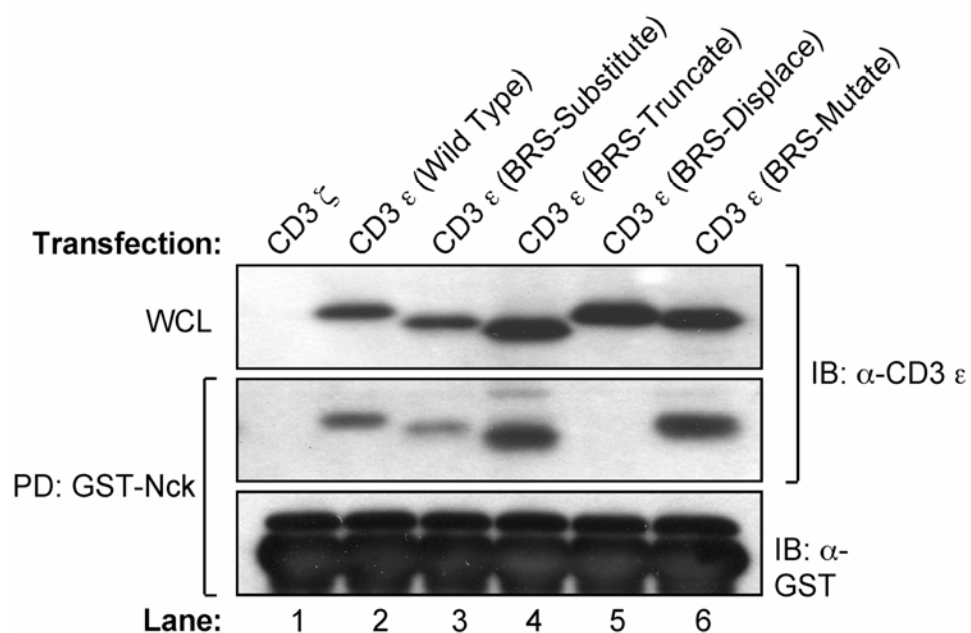


Figure 32. Displacing the BRS interferes with Nck binding in transfected cells. HEK293 T cells were transiently transfected with the indicated constructs. The cells were lysed, and pull-downs were performed using a GST-fusion protein containing the first SH3 domain of Nck (GST-Nck). WCLs and precipitated proteins were resolved by SDS-PAGE, followed by anti-CD3 ϵ immunoblotting (upper and middle panel). The membrane was subsequently re-probed using an anti-GST antibody to ensure equivalent levels of GST-Nck had been used in each pull-down. Results are representative of three independent assays.

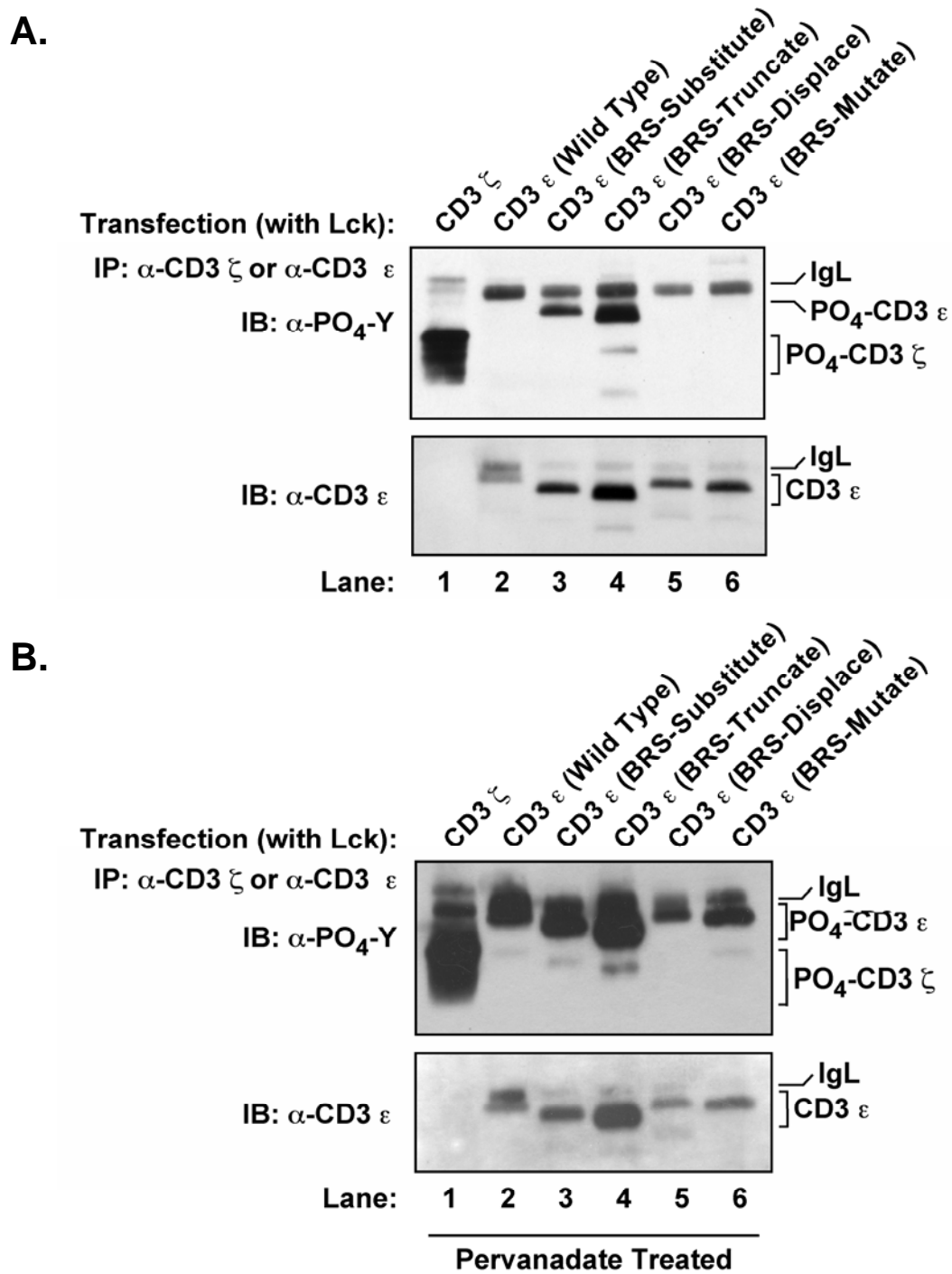
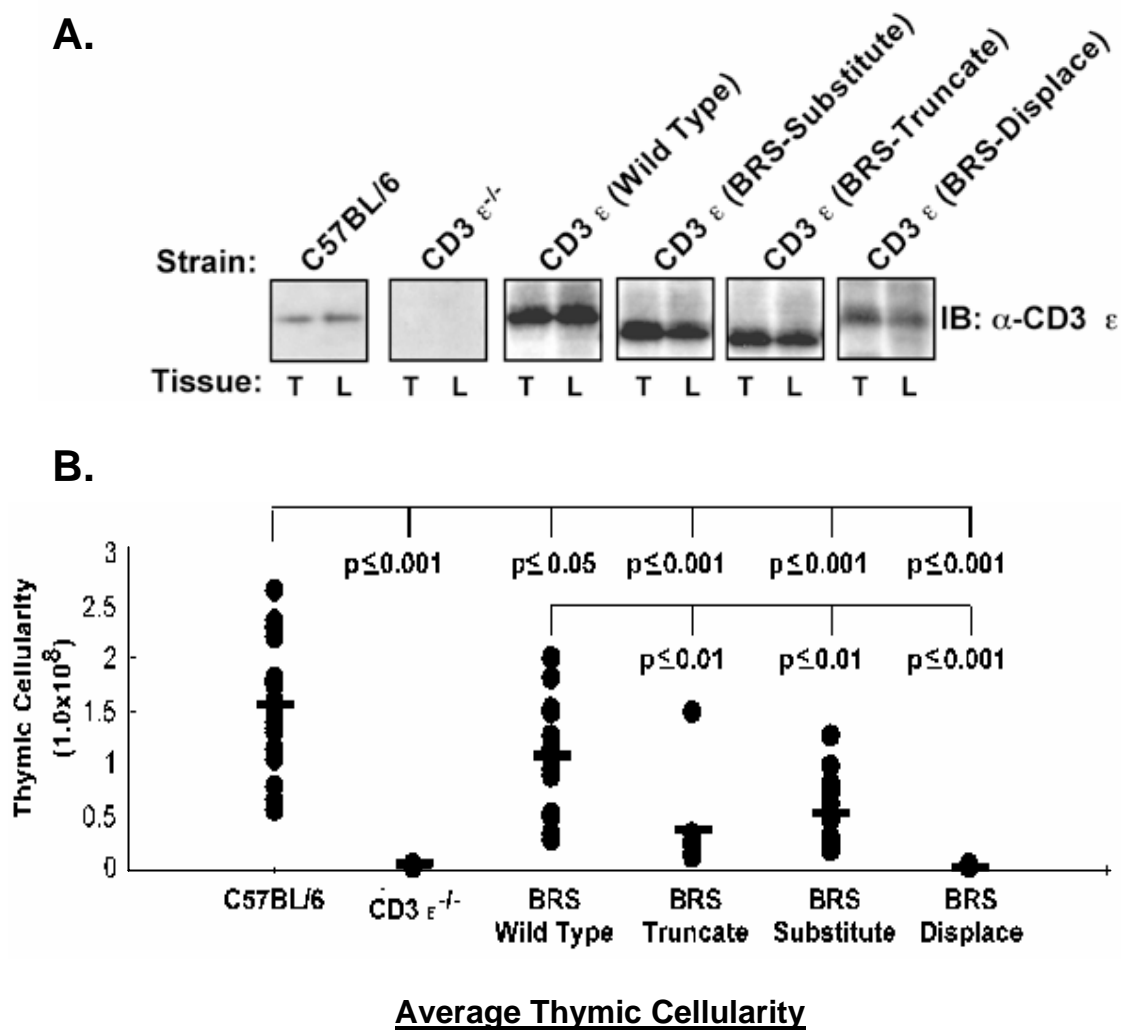
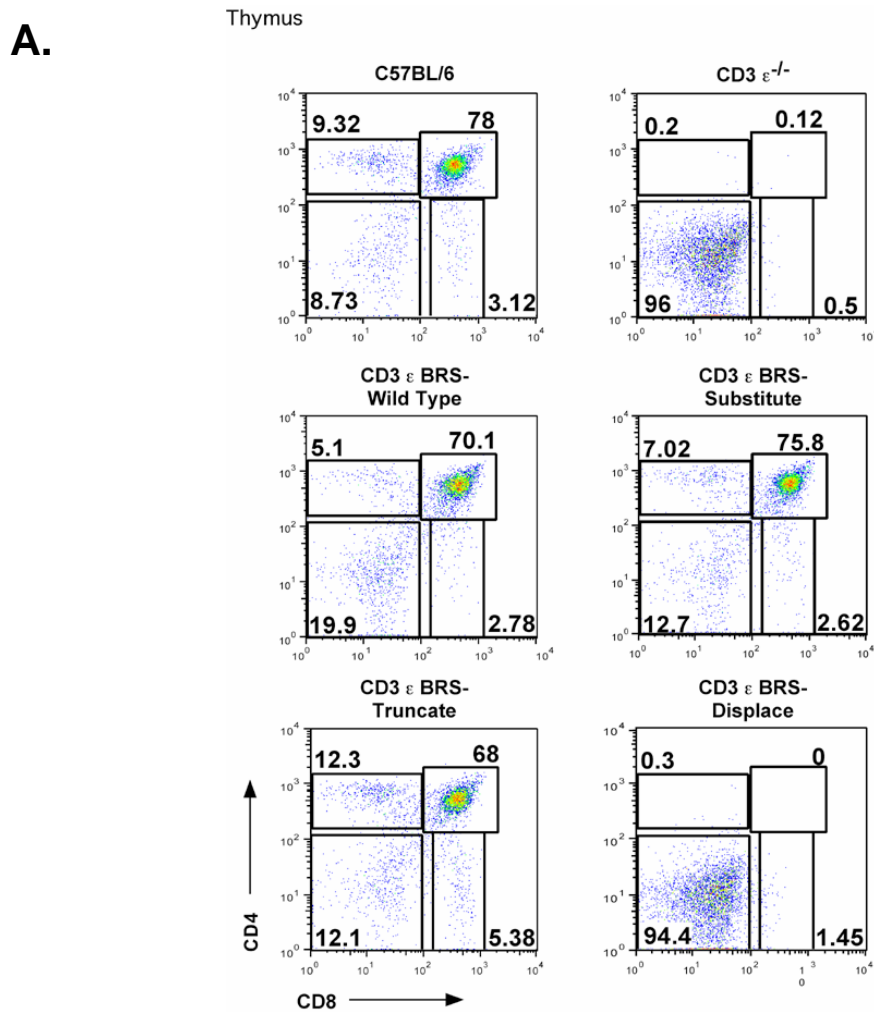


Figure 33. CD3 ϵ BRS-Substitute and -Truncate are more readily detected as phosphoproteins in transfected cells. (A) HEK293 T cells were co-transfected with the Lck and CD3 ζ or the various CD3 ϵ BRS constructs. The cells were lysed in a 1% Trion X-100 lysis buffer, and CD3 ζ (Lane 1) or CD3 ϵ (Lanes 2-6) immunoprecipitations were performed. The precipitates were resolved by SDS-PAGE and immunoblotted using anti-PO₄-Y (upper panel) or anti-CD3 ϵ (lower panel). (B) HEK293 T cells were transfected as in (A). Ten minutes prior to lysing, the cells were treated with pervanadate. Immunoprecipitations and western blotting were then performed as described in (A).



C57BL/6	$1.5 \times 10^8 \pm 0.5 \times 10^8$	BRS-Substitute	$0.5 \times 10^8 \pm 0.32 \times 10^8$
CD3 $\epsilon^{-/-}$	$1.6 \times 10^6 \pm 0.6 \times 10^6$	BRS-Truncate	$0.37 \times 10^8 \pm 0.4 \times 10^8$
BRS-Wild Type	$1.0 \times 10^8 \pm 0.5 \times 10^8$	BRS-Displace	$1.0 \times 10^6 \pm 0.8 \times 10^6$

Figure 34. Protein expression and thymic cellularity in the BRS transgenic mice. (A) Cells were isolated from the thymus (T) or lymph nodes (L) of the indicated strains of mice. WCLs were generated and subjected to anti-CD3 ϵ immunoblotting. (B) Total thymocyte numbers from the indicated strains of mice were enumerated using a hemocytometer. Cell counts from the individual mice are shown as circles. Bars represent the average number of thymocytes from each genotype. C57BL/6 (n=18); CD3 $\epsilon^{-/-}$ (n=8); CD3 ϵ BRS-Wild Type (n=16); CD3 ϵ BRS-Substitute (n=8); CD3 ϵ BRS-Truncate (n=17); CD3 ϵ BRS-Displace (n=8).

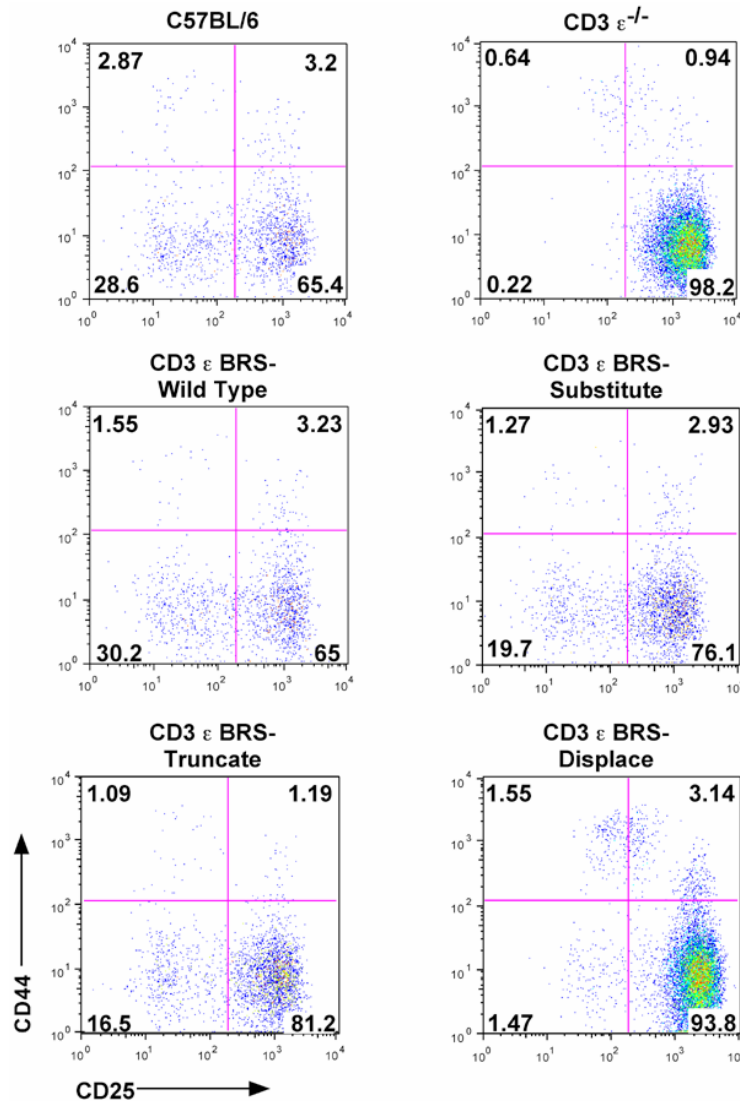


B.

	% CD4 ⁺ CD8 ⁺	% CD4 ⁺ CD8 ⁻	% CD4 ⁻ CD8 ⁺
C57BL/6	75.2±3.5	8.46±1.2	3.34±0.27
CD3 $\epsilon^{-/-}$	0.1±0.05	0.14±0.04	0.37±0.29
BRS-Wild Type	74.5±10.1	5.4±1.4	3.33±1.6
BRS-Substitute	72.5±6.14	6.88±0.7	3.2±0.8
BRS-Truncate	62.5±11.6	10.0±3.2	4.7±0.87
BRS-Displace	3.04±5.6	1.16±1.8	1.4±0.9

Figure 35. Select mutations within the BRS alter thymic development. Thymocytes were isolated from age and sex matched mice from the indicated murine strains. The cells were then stained using antibodies directed against CD4 and CD8 and analyzed by flow cytometry. (B) The average percentage of CD4⁺CD8⁺, CD4⁺CD8⁻, or CD4⁻CD8⁺ was enumerated from four independent assays.

A.



B.

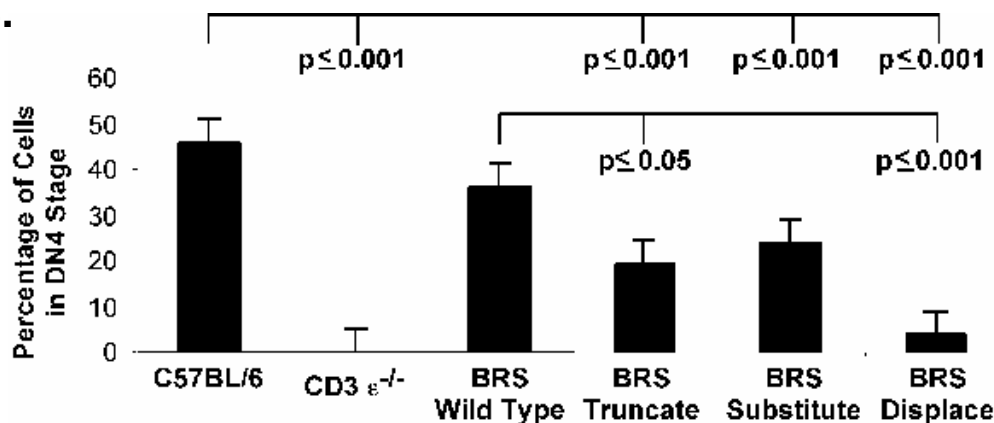


Figure 36. The BRS of CD3 ϵ contributes to the progression of thymocytes through the DN stages of development. (A) CD4⁺/CD8⁻/B220⁻/NK1.1⁻/Thy1.2⁺ thymocytes were analyzed by flow cytometric analysis for expression of CD44 and CD25. (B) The average percentage of cells progressing to the DN4 stage calculated from four independent analyses.

Lymph Node

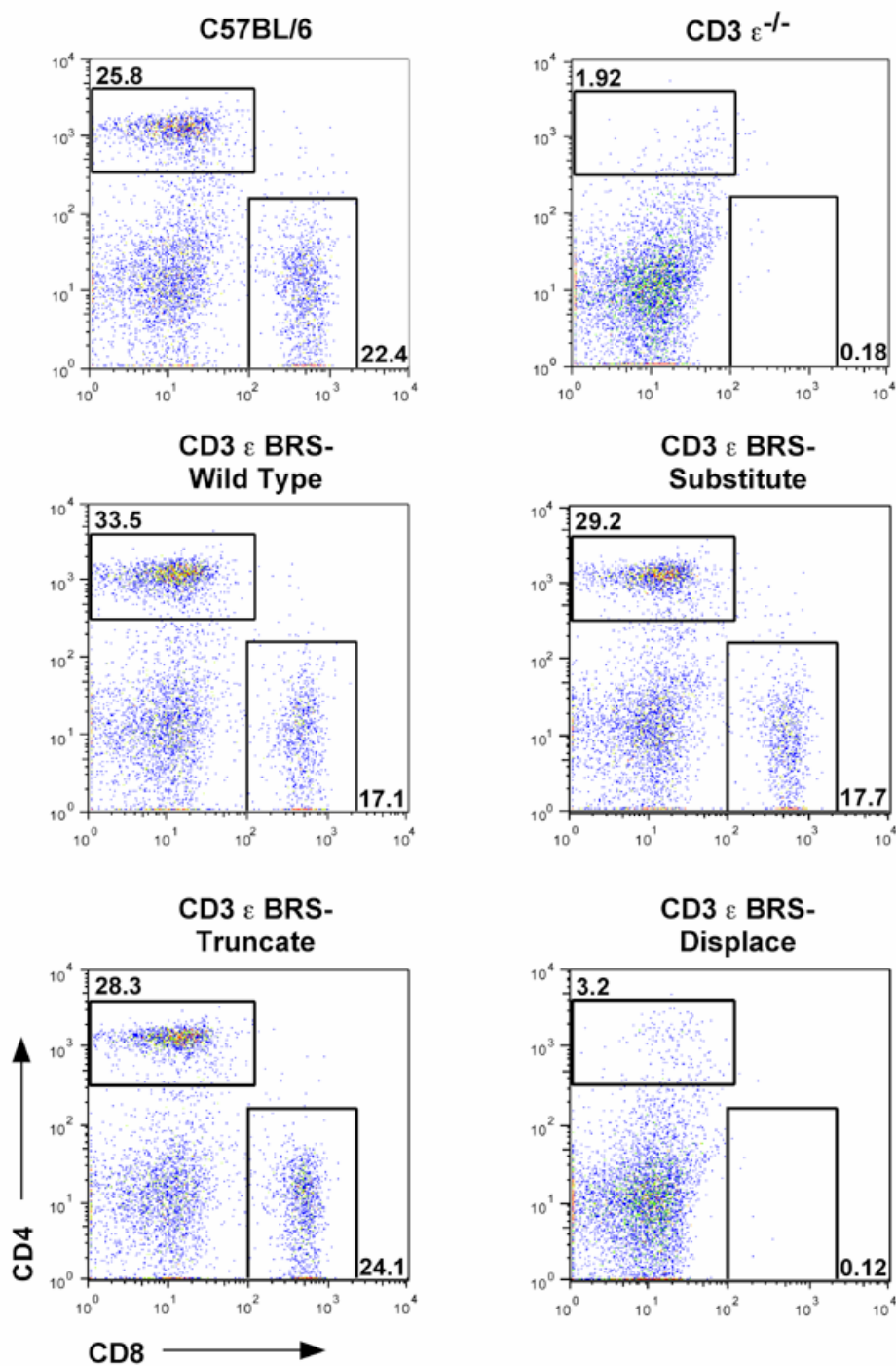


Figure 37. Select mutations within the BRS alter the production of mature T cell in the lymph node. Cells were isolated from the lymph nodes of the indicated strains of mice. Single cell suspensions were prepared and stained with mAbs against CD4 and CD8, followed by flow cytometric analysis. Results are representative of three independent assays.

Spleen

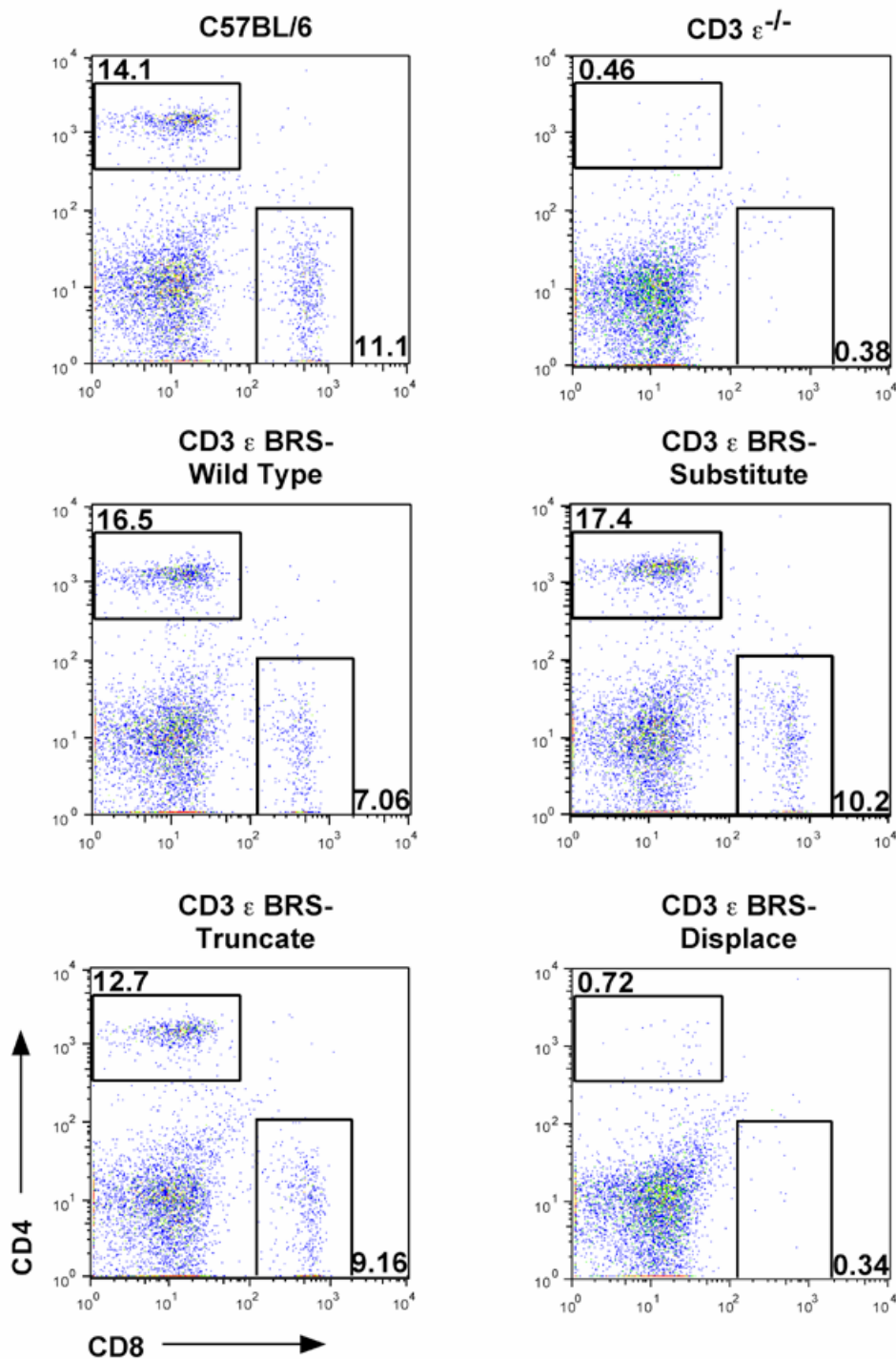
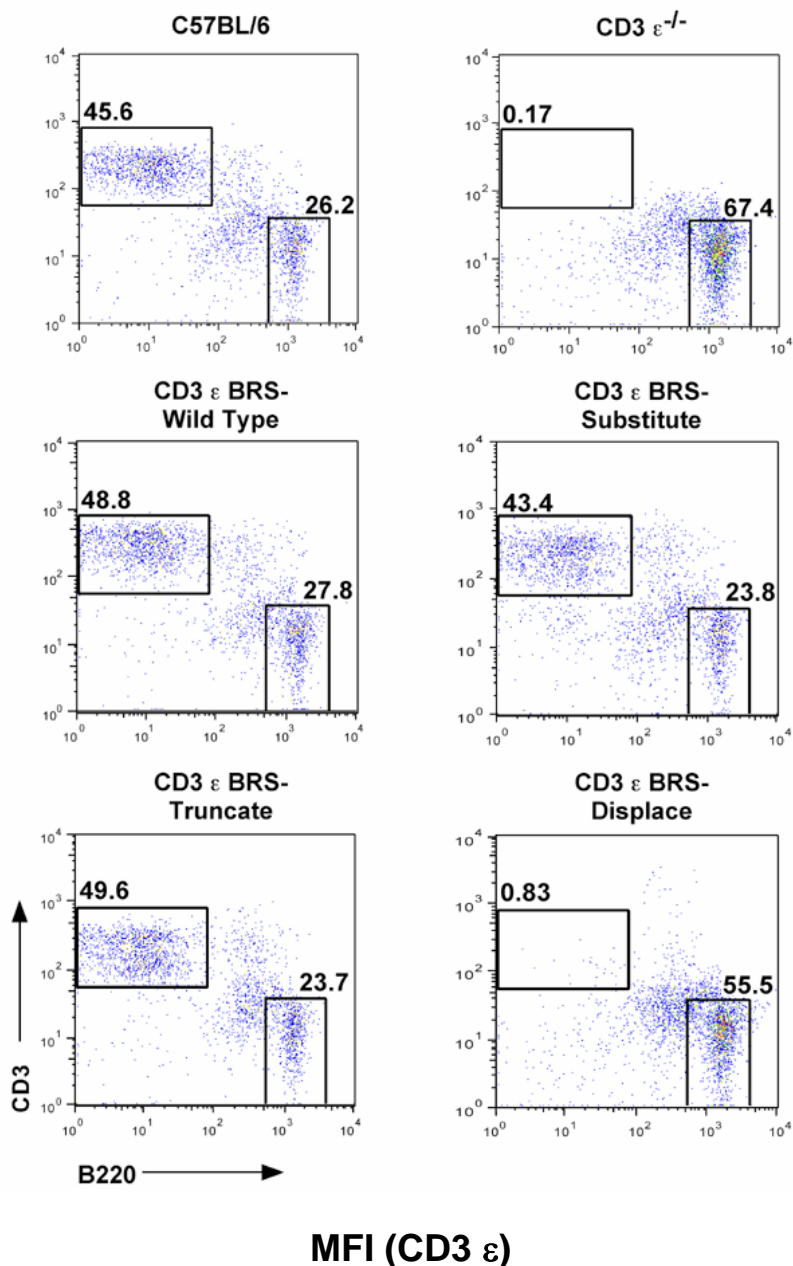


Figure 38. Certain modifications of the BRS interfere with the production of mature T cell in the spleen. Cells were isolated from the spleen of the indicated strains of mice. Single cell suspensions were prepared and stained with mAbs against CD4 and CD8, followed by flow cytometric analysis. Results are representative of three independent assays.

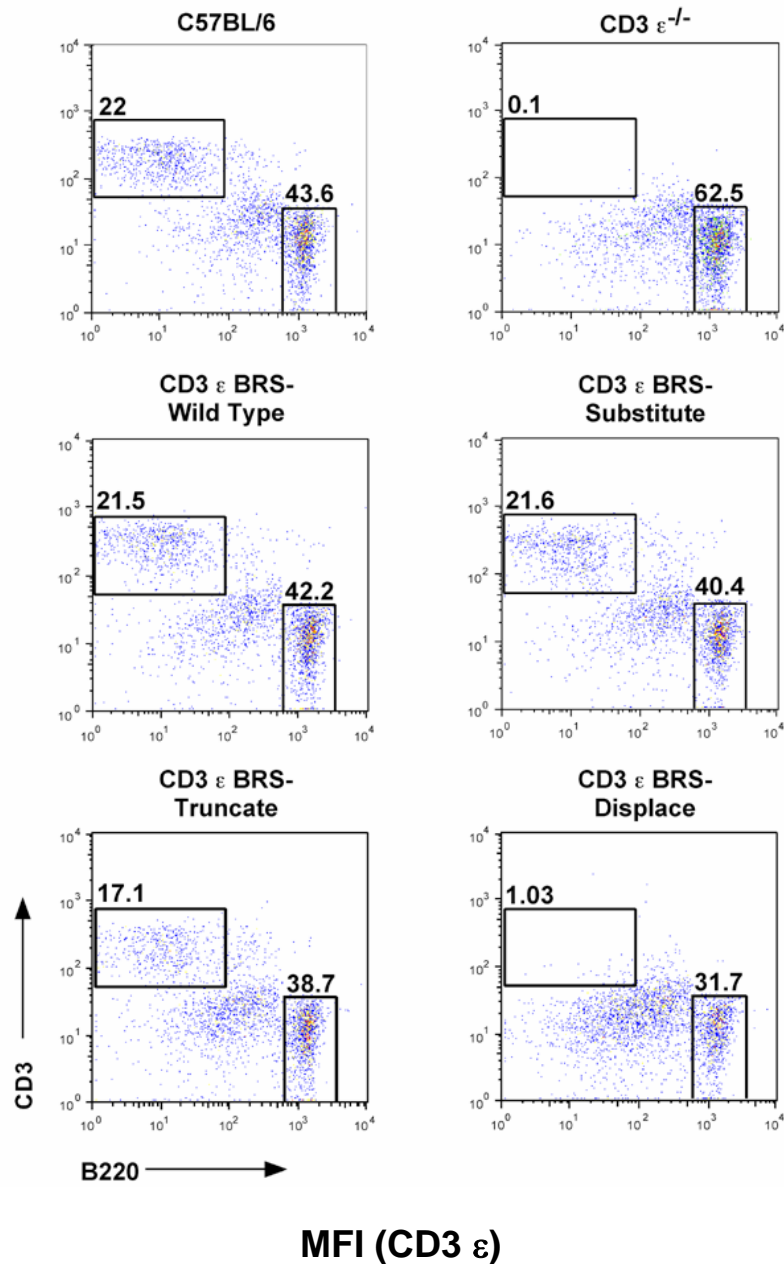
Lymph Node



C57BL/6	137	BRS-Substitute	132
BRS-Wild Type	129	BRS-Truncate	93

Figure 39. The percentage of mature T and B cells in the lymph node varies depending on the mutation made within the BRS. Lymph nodes were harvested from the indicated strains of mice. Single cell suspensions were prepared and stained with mAbs against CD3 and B220, followed by flow cytometric analysis. The mean fluorescence intensity (MFI) of surface stained CD3 ϵ is shown. Results are representative of three independent assays.

Spleen



C57BL/6	165	BRS-Substitute	131
BRS-Wild Type	150	BRS-Truncate	108

Figure 40. Select mutations of the BRS alter the percentage of mature T and B cells found in the spleen. Lymph nodes were harvested from the indicated strains of mice. Single cell suspensions were prepared and stained with mAbs against CD3 and B220, followed by flow cytometric analysis. The mean fluorescence intensity (MFI) of surface stained CD3 ϵ is shown. Results are representative of three independent assays.

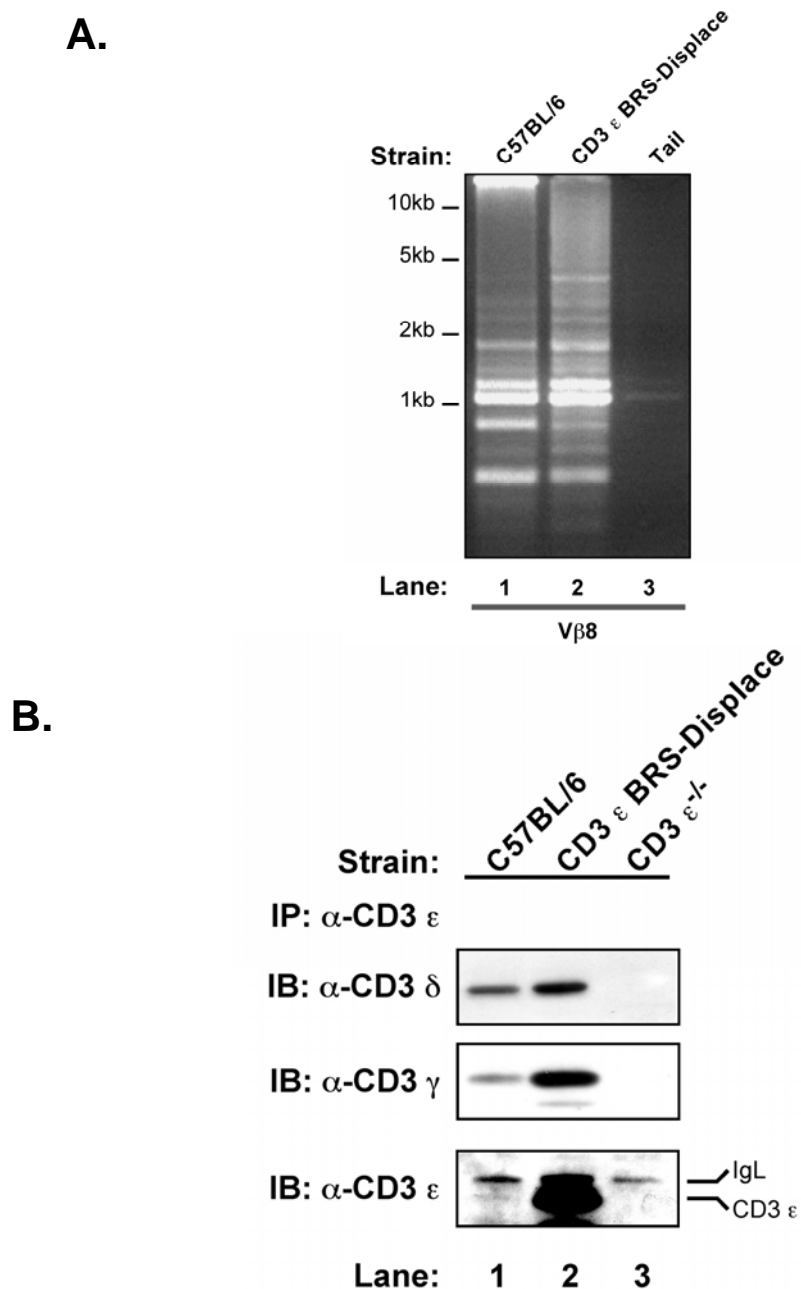


Figure 41. CD3 ϵ BRS-Displace transgenic mice exhibit normal TCR β gene rearrangements and CD3 γ/ϵ or δ/ϵ pairing. (A) Genomic DNA isolated from C57BL/6 or CD3 ϵ BRS-Displace thymocytes (Lanes 1 and 2) was used as a template in PCR reactions containing primers against the J β 8 gene segment. In Lane 3, tail DNA was used as a negative control. PCR products were resolved by electrophoresis and visualized using an Eagle Eye II system. (B) Thymocytes were isolated from the indicated strains of mice, equivalent cell numbers were lysed, and CD3 ϵ immunoprecipitations were performed. Precipitated proteins were resolved by SDS-PAGE and western blotted using anti-CD3 γ or anti-CD3 δ polyclonal antibodies. The membrane was subsequently re-probed with anti-CD3 ϵ . Similar results were obtained using three distinct lines of BRS-Displace transgenic mice.

A.

Injection	Average Cell Count
PBS	$2.6 \times 10^6 \pm 1.2 \times 10^6$
α -CD3 ϵ	$1.75 \times 10^6 \pm 0.7 \times 10^6$

B.

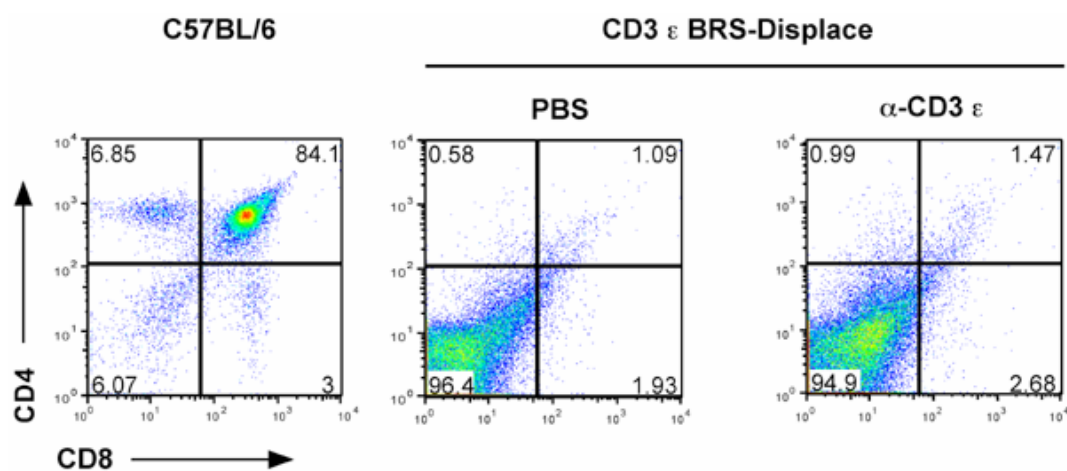


Figure 42. Anti-CD3 ϵ mAb Injections into BRS-Displace transgenic mice does not induce thymocytes proliferation or differentiation. (A)

Three BRS-Displace mice were injected with PBS or anti-CD3 ϵ . Seven days post injection their thymocyte numbers were calculated and averaged. (B) Mice bearing the CD3 ϵ BRS-Displace transgene were administered an intraperitoneal injection of PBS (middle panel) or anti-CD3 ϵ (right panel). Seven days post injection, thymocytes were analyzed by flow cytometric analysis for the expression of CD4 and CD8 (middle and right panels). C57BL/6 thymocytes from an untreated mouse were also stained with anti-CD4 and anti-CD8 antibodies as a control (left panel).

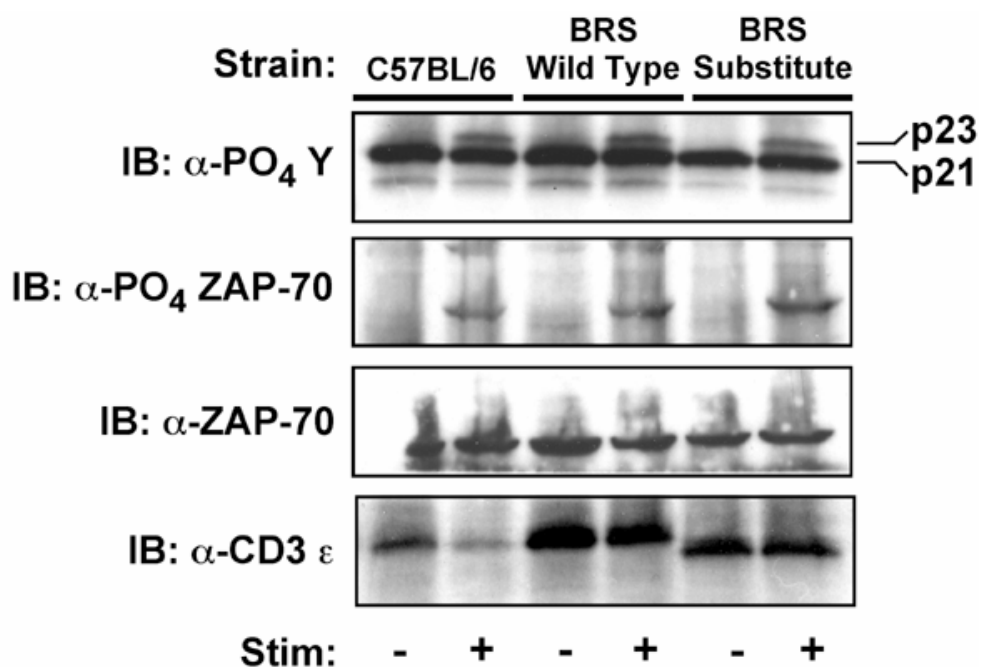


Figure 43. Early phosphoprotein induction is normal in the BRS-Truncate transgenic mice. Primary lymphocytes isolated from C57BL/6, BRS-Wild Type, or BRS-Substitute mice were stimulated for 10 minutes with mAbs against CD3 ϵ and CD28. The samples were then washed, lysed, and whole cell lysates were subjected to western blotting using antibodies specific for the phosphorylated form of ZAP-70 or for phosphotyrosine residues in general. The membranes were then stripped and re-probed with anti-ZAP-70 or anti-CD3 ϵ .

Lymph Node: CD4⁺/CD8⁻

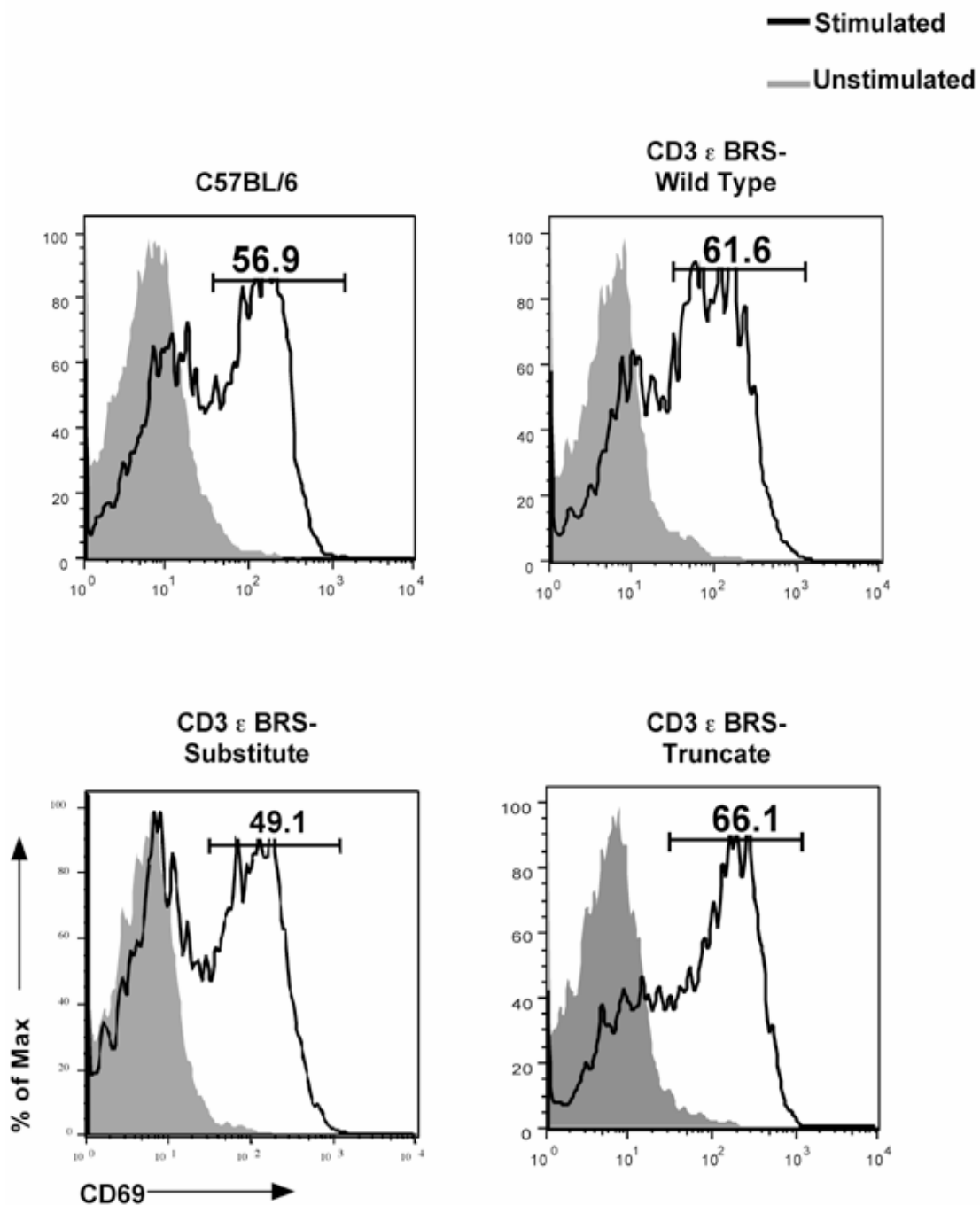


Figure 44. CD69 upregulation on CD4⁺ lymphocytes is comparable in the BRS-Wild Type, -Truncate and -Substitute transgenic mice. Cells were isolated from the lymph nodes of the indicated strains of mice and resuspended at 1.0×10^5 cells/ml in culture media. The cells were then incubated in media alone (filled gray line) or anti-CD3 ϵ plus anti-CD28 (black line) for 24 hours, washed, and analyzed by flow cytometric analysis. The graph represents the average expression of CD69 on CD4⁺ lymphocytes from samples cultured in triplicate.

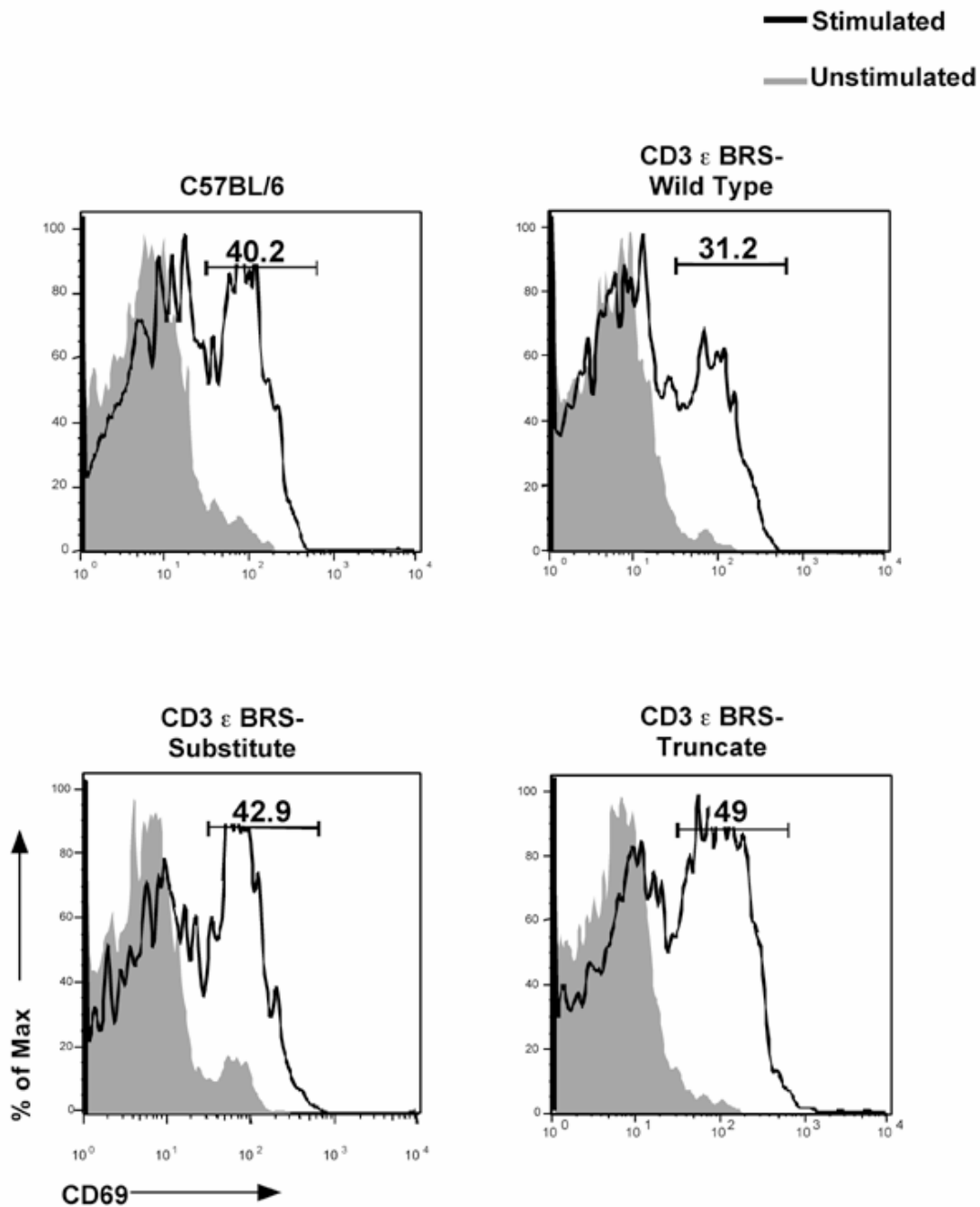
Lymph Node: CD4⁻/CD8⁺

Figure 45. CD69 upregulation on CD8⁺ lymphocytes is comparable in the BRS-Wild Type, -Truncate, and -Substitute transgenic mice. Cells were isolated from the lymph nodes of the indicated strains of mice and resuspended at 1.0×10^5 cells/ml in culture media. The cells were then incubated in media alone (filled gray line) or anti-CD3 ϵ plus anti-CD28 (black line) for 24 hours, washed, and analyzed by flow cytometric analysis. The graph represents the average expression of CD69 on CD8⁺ lymphocytes from samples cultured in triplicate.

CHAPTER V

DISCUSSION

Overview

The CD3 ϵ subunit of the TCR plays a crucial role in T cell development and effector functions (45, 56, 163, 164). Interestingly, mutations of two key signaling motifs within CD3 ϵ (the PRS and ITAM) have no effect on T cell development and/or TCR signaling (19, 50). We identified and characterized a third basic-rich signaling motif within the membrane-proximal portion of CD3 ϵ that we have termed the BRS. Our interest in the BRS was originally based on our finding that it could mediate interactions with the Ser/Thr kinase, GRK2. Subsequently, we noticed that the BRS has sequence similarity to polybasic clusters present in a number of other eukaryotic proteins. Like the polybasic clusters of these proteins, the BRS was found to associate with certain charged phospholipids.

In terms of protein interactions, we demonstrated that the BRS of CD3 ϵ constitutively associates with GRK2 within the subcellular compartments of primary T cells. The use of recombinant protein demonstrated that this interaction could occur directly, but was sensitive to changes in pH. Additionally, we determined that the ability of GRK2 to complex CD3 ϵ required several of the lysines and arginines within the BRS. These same positively charged residues were also necessary for interactions with select phospholipids. To address the role of the BRS in T cells, several BRS-transgenic mice were generated. Analysis of these animals revealed that eliminating at least five of the

positively charged residues within the BRS or relocating the BRS to the distal portion of the cytoplasmic tail significantly impacted T cell development.

Potential Role for BRS/GRK2 Interactions

The TCR and GPCRs cross regulate one another. In fact, signaling through certain GPCRs, including CXCR4, have been demonstrated to be functionally dependent on CD3 ζ and ZAP-70 (61). Because GRK2 is one of the primary regulators of GPCR signaling, its interaction with the BRS within intracellular compartments may provide a means for the TCR to communicate with GPCR, such as CXCR4. CXCR4 is expressed on T cells in both the thymus and periphery (165). In the thymus, the ligand for CXCR4 (SDF-1 α or CXCL12) is expressed by stromal cells in the cortex, the region of the thymus where progenitor T cells are under the pre-TCR developmental checkpoint. Consequently, CXCR4 expression is thought to retain T cells in the subcortical and cortical regions during the DN1 to DN4 transition (165). Engagement of the TCR is known to reduce the level of CXCR4 expressed on the surface of T cells (63, 166). However, the mechanism for this TCR-mediated reduction has not been elucidated. Our finding that GRK2 can directly bind the BRS of CD3 ϵ may provide a means whereby TCR engagement can result in the phosphorylation and internalization of CXCR4. In order to investigate this possibility, a number of different approaches might be used. First, it would be beneficial to determine if TCR engagement results in the internalization of CXCR4 via GRK2 activity. Many GPCRs, including CXCR4, are differentially phosphorylated depending on the Ser/Thr kinase acting upon them (94, 167, 168). GRK2

selectively phosphorylates Ser 338 on CXCR4 (94, 168). Consequently, Jurkat T cells could be left untreated or incubated in the presence of C305 (mAb against the TCR). CXCR4 could then be immunoprecipitated, resolved by electrophoresis, and blotted using antibodies specific for the Ser 338 phosphorylated isoforms of CXCR4 (168). If CXCR4 is more readily phosphorylated on Ser 338 following TCR engagement, this would implicate the involvement of GRK2 in the TCR-mediated regulation of this chemokine receptor.

The BRS-transgenic mice will also be useful in characterizing the role of interactions between GRK2 and CD3 ϵ . Assays using GST-fusion proteins containing mutations of the BRS suggested that the positively charged residues within this motif were necessary for GRK2 interactions and/or catalytic activity. Consequently, the mutations generated in the BRS-transgenic mice might decrease the ability of GRK2 to complex CD3 ϵ . This should first be verified by western blotting CD3 ϵ immunoprecipitates obtained from the various BRS-transgenic lines. If GRK2 binding is disrupted in the BRS-mutant lines, T cells from these mice might then be analyzed for their ability to traffic properly or to carry out chemokine receptor endocytosis after ligation of the TCR. For trafficking studies, peripheral T cells from the various mice could be subjected to transwell assays to determine if their ability to migrate toward a chemokine gradient, such as SDF-1 α , is altered when GRK2 is no longer able to bind CD3 ϵ . These same assays could be repeated using BRS-transgenic T cells that had been stimulated with anti-CD3 ϵ prior to introduction to a chemokine gradient. This would assess if defects in trafficking were specifically observed following TCR engagement.

Since TCR engagement is known to result in the endocytosis of CXCR4, the ability of TCR stimulations to induce this endocytosis in the BRS-mutant mice should also be analyzed. If mice bearing mutations within their BRS are unable to induce a TCR-mediated internalization of GPCRs, such as CXCR4, this would directly implicate the activity of GRK2 in carrying out TCR/GPCR cross talk. This possibility could be further analyzed by using mature T cell lines. In Chapter III, we demonstrated that siRNA treatment of Jurkat T cells resulted in a 40-75% decrease in the levels of GRK2 protein expressed in the cell. This experimental approach could again be exploited to determine if GRK2 is involved in the TCR-mediated internalization of CXCR4. Following siRNA treatment of Jurkat T cells, anti-CD3 ϵ stimulations could be performed. The cells could then be analyzed by flow cytometric analysis to determine their expression of CXCR4. If cells treated with GRK2 specific siRNA exhibit a defect in their ability to endocytose CXCR4 following TCR stimulations, GRK2 must contribute to these processes.

In our system, we observed that interactions between GRK2 and the BRS of CD3 ϵ occurred predominantly within subcellular compartments. It should be noted that this finding is consistent with reports demonstrating that the co-localization of the TCR and CXCR4 takes place both at the cell surface and within the cell (61). Although receptor internalization was traditionally thought to prevent signal transmission, recent studies suggest that important signaling events occur within intracellular organelles, including endosomes and the Golgi, only after receptor internalization (83, 169-171). In T cell development, the organization of TCR signaling intermediates into distinct subcellular compartments is a distinguishing factor in determining whether the cells will undergo

positive or negative selection (172, 173). In the case of CXCR4, Peter et al utilized live- and fixed-cell imaging to demonstrate that the Ser/Thr kinase, PKC α , selectively interacts with CXCR4 located in endosomal compartments (174). This kinase/receptor complex was found to enhance the rate at which the chemokine receptor was recycled back to the plasma membrane. Although the exact mechanism whereby this interaction resulted in receptor turnover was not elucidated, it supports the hypothesis that receptor interactions with distinct proteins within endosomes can deliver important regulatory signals. Internalized GPCRs also associate with certain phosphatases that are responsible for dephosphorylating their cytoplasmic tails within acidic endosomal compartments. This too allows the GPCR to be recycled back to the cell surface (Reviewed in (175)). Although GRK2 is typically classified as a cytosolic protein, it has been found to associate with a high affinity to the membranes of several intracellular compartments, indicating that it may serve a functional role within intracellular organelles (176, 177). Due to the fact that the TCR and CXCR4 physically associate within subcellular compartments, it is plausible that interactions between GRK2 and CD3 ϵ within these same subcellular organelles may allow GRK2 to remain in close enough proximity to CXCR4 so that it will not be dephosphorylated and sent back to the cell surface (Fig. 46).

Given that signals generated through both chemokine receptors and the TCR must be properly coordinated to facilitate T cell development, differentiation, migration, and cytokine production, the ability of the TCR to cross talk with GPCR through GRK2 could have important implications for human health. Since signals generated through the TCR are necessary to regulate the expression of certain GPCR, such as CXCR4, an inability of the BRS to bind GRK2 or regulate its enzymatic activity might lead to dysfunctional

regulation of chemokines receptors. Ultimately, this could impact any number of pathologies linked to dysregulation of chemokine receptors, including immunodeficiency, inflammatory diseases, and cancer (Reviewed in (178)).

Interactions Between the BRS and Phospholipids May Provide a Mechanism for Conformational Changes in CD3 ϵ

We have demonstrated that the BRS of CD3 ϵ can selectively bind to charged phospholipids. This interaction may serve several functions in T cells, ranging from TCR translocation to the plasma membrane to the initiation of TCR signaling events. To determine what role the BRS might be playing in T cells, the affinity of the BRS for different phospholipid species will need to be determined. Based on our findings using PIP strips, the BRS appeared to have the highest affinity for monophosphorylated PtdIns, including PI(4)P. If this holds true, the BRS may contribute to the translocation of the TCR through the Golgi network following receptor assembly in the ER. Alternatively, if the BRS is found to have a high affinity for PI(3)P, it may assist in the endocytosis of the TCR complex after peptide-MHC binding. If interactions between the BRS and bi-phosphorylated lipids, such as PI(4,5)P₂, occur at a physiologically relevant K_d, interactions between the BRS and the inner leaflet of the plasma membrane might facilitate the initiation of TCR signals. This hypothesis is particularly appealing, since it would provide a mechanism for how the ligand-induced conformational change occurs within CD3 ϵ 's cytoplasmic tail. This is based on the fact that the lipid environment surrounding the TCR is known to undergo modifications following peptide/MHC

interactions (Reviewed in (179)). Such modifications may influence the ability of the BRS to bind the inner leaflet of the plasma membrane, thereby regulating the conformation that is adopted by the cytoplasmic tail of the CD3 ϵ subunit. We propose two models for how this might occur (Fig. 47 and 48). In our first model, the BRS of CD3 ϵ may constitutively associate with phospholipids expressed at that plasma membrane. Following TCR engagement, the recruitment of lipid kinases to the plasma membrane might alter the species of PtdIns surrounding the TCR (180, 181). If a species for which the BRS has a lower affinity is generated, the BRS might be released, thereby inducing a conformational change within the cytoplasmic tail (Fig. 47).

It is also possible that the BRS of CD3 ϵ does not constitutively bind charged PtdIns expressed on the inner leaflet of the plasma membrane. In this model, a TCR-mediated increase in concentration of phospholipids present in the membrane environment surrounding the TCR might result in an inducible interaction between the BRS and the plasma membrane. This too might account for the conformational change that takes place in the intracellular domain of CD3 ϵ (Fig. 48).

To address whether eliminating the positively charged residues influences the conformational change within CD3 ϵ , GST-Nck pull-down assays can be performed in the BRS-transgenic mice. If the CD3 ϵ subunit isolated from BRS-Substitute and/or -Truncate mice fails to associate with GST-Nck following T cell stimulations, it is probable that interactions between the positively charged residues of the BRS and charged phospholipids at the plasma membrane influence the ability of the conformational change to take place within CD3 ϵ . Conversely, if the PRS of CD3 ϵ is constitutively available to GST-Nck binding in mice bearing mutations within the BRS, it

is likely that the BRS is necessary to hold the cytoplasmic tail of CD3 ϵ in a conformationally “closed” position.

It is tempting to speculate that the BRS may also function to provide secondary structure to the cytoplasmic tail of CD3 ϵ when associated with phospholipid. This hypothesis is based on studies demonstrating that certain peptides that lack structure in a soluble environment can adopt an α -helical conformation following phospholipid interactions (182). Some mammalian proteins are also known to take on secondary structure in the presence of PtdIns. In the case of two GTPases, RGS4 and RGS16, binding to phospholipids within intracellular membranes allowed the NH₂-terminus of these proteins to adopt an α -helical wheel. Interestingly, these helices were arranged in such a manner that charged and hydrophilic residues lined one side of the helical face, while hydrophobic residues lined the opposing side (183, 184). Based on this structure, the positively charged residues on the hydrophilic face were predicted to bind polar head groups of phospholipid express on the cytoplasmic surface of the membrane, while the hydrophobic residues could contact the tails of phospholipids inserted in the membrane bilayer. Although ¹H-NMR concluded that the membrane-proximal portion of CD3 ϵ had no secondary structure, it should be noted that these studies were performed using soluble CD3 ϵ (37). In the absence of a plasma membrane, the BRS may very well be arranged as a random coil. However, in the presence of phospholipid, it is possible that the BRS may take on a helical structure, thereby allowing for interactions with both the tails and polar head groups of membrane-associated phospholipids (Fig. 49). In order to address this, biotinylated peptides containing the BRS of CD3 ϵ could be incubated with liposomes containing charged phospholipids. These peptides could then be subjected to

circular dichroism to address whether any secondary structure is detected. As a positive control, a peptide corresponding to the ITAM of CD3 ϵ might also be used since this region of CD3 ϵ is known to adopt a helix-turn conformation (38). To address what residues within the BRS are involved in any structural formation, peptides containing a truncated form of the BRS or mutants in which positively charged residues (lysines and arginines), hydrophobic residues (alanines and prolines), or a combination of both could also be analyzed. This would determine if interactions between the positively charged residues of the BRS and anionic phospholipids alone were required for the adaptation of a secondary structure or if hydrophobic residues were also involved.

Elucidating a Role for the BRS in T cell Development

Mutating the BRS of CD3 ϵ interrupted thymic development. These results indicate that this motif serves an important role in thymopoiesis. To further analyze this possibility, the BRS-transgenic mice will be mated with HY-TCR transgenic mice. HY transgenic mice express an α/β TCR that is specific for the male HY peptide (Smcy) in the context of H2D^b. This transgenic line has a low avidity for its cognate ligand and is often used to analyze both positive and negative selection events in female and male mice, respectively (185). Previous studies have shown that both positive and negative selection in HY-TCR transgenic thymocytes is influenced by the number of ITAMs present in the TCR complex (150, 186). Consequently, if a signaling defect is present in the BRS-mutant transgenics, a HY/BRS double-transgenic might be useful in its detection. If male mice expressing the BRS-Substitute or -Truncate transgene in addition

to the HY-TCR transgene exhibit a defect in their ability to delete developing T cells, this would indicate that the positively charged residues of the BRS are necessary for negative selection (187). Conversely, if female mice bearing HY/BRS transgenes possess fewer numbers of CD4⁻CD8⁺ T cells, the BRS likely functions in positive selection.

In addition to studying developmental processes in the BRS/HY transgenics, signaling events in peripheral cells could also be evaluated. Western blotting assays indicated that there was little to no difference in early TCR-mediated signaling in the BRS-Truncate and -Substitute mice. However, it should be noted that these assays were performed using antibody induced stimulations of T cells. Such techniques not only deliver a potent signal to the T cell, but also bypass the specificity of the TCR. Consequently, differences in signaling might be discovered if a more physiologically relevant stimulus were used. To investigate the role of the BRS in signaling events, lymphocytes from the female BRS/HY mice could be cultured with peptide-loaded dendritic cells. These cells could then be analyzed for their ability to carry out normal T cell functions, including phosphoprotein induction, proliferation, cytokine production, and the upregulation of activation markers.

Overall Conclusions

Given the fact that the CD3 ϵ subunit is believed to play a critical role in T cell functions, it is surprising that the mutagenesis of two of its subdomains, the PRS and ITAM, has little consequence on T cell development and TCR signaling. What is even more surprising is the fact that, until now, potential contributions of the BRS have been

largely ignored. Herein, we provide evidence that this region of CD3 ϵ functions as a critical signaling motif. The ability of the BRS to make novel contributions to TCR signaling is due in part to its ability to uniquely associate with distinct signaling molecules, such as GRK2.

Interactions between the BRS of CD3 ϵ and phospholipid may also allow this motif to regulate TCR signaling. What is more, understanding how phospholipid interactions with BRS contribute to TCR signaling may advance our understanding of other transmembrane receptors, such as ICAM-1 & -2, CD43, and CD44 (144-146). Like CD3 ϵ , these transmembrane receptors have also been found to contain polybasic stretches within the membrane-proximal portion of their cytoplasmic tails (145, 146). It would stand to reason that the use of polybasic clusters within the juxtamembrane region of certain signaling receptors may be a common mechanism utilized by numerous receptors to control the initiation of signaling cascades. As a whole, the identification of the BRS as a critical signaling motif within the TCR signaling complex has important therapeutic implications, since it could facilitate the identification of novel drug targets capable of regulating aberrant T cell functions.

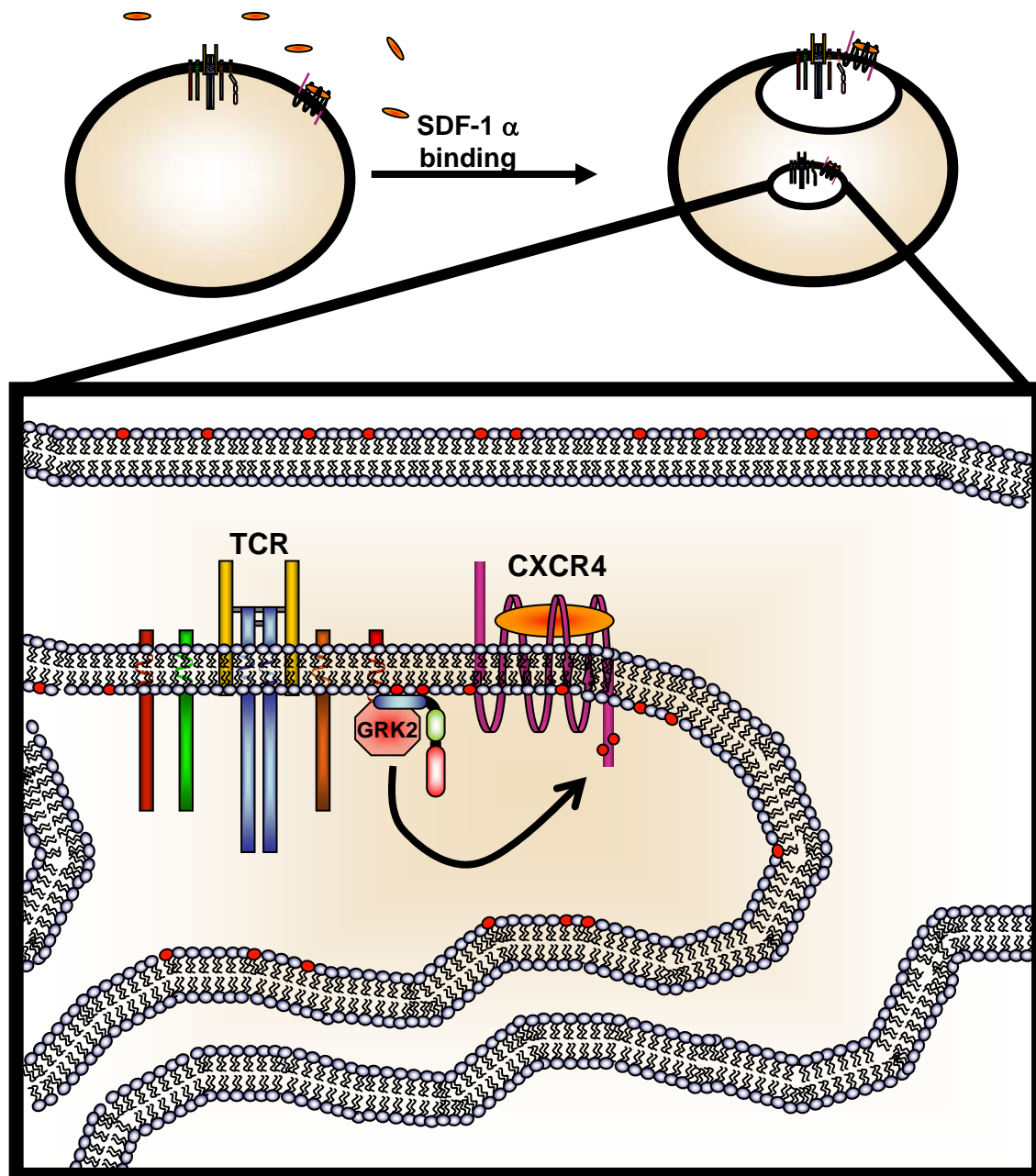


Figure 46. Functional model for BRS/GRK2 interactions within intracellular compartments. Engagement of CXCR4 allows it to physically associate with the TCR both at the cell surface and within intracellular vesicles. A drop in pH levels within the developing and intraluminal multivesicular endosomes may allow the BRS of CD3 ϵ to bind GRK2. This interaction might hold GRK2 in close proximity to CXCR4 so that if its cytoplasmic tail is dephosphorylated, GRK2 is optimally positioned to re-phosphorylate it. In this manner, GRK2 might serve to regulate the trafficking of CXCR4 to lysosomal compartments rather than back to the plasma membrane.

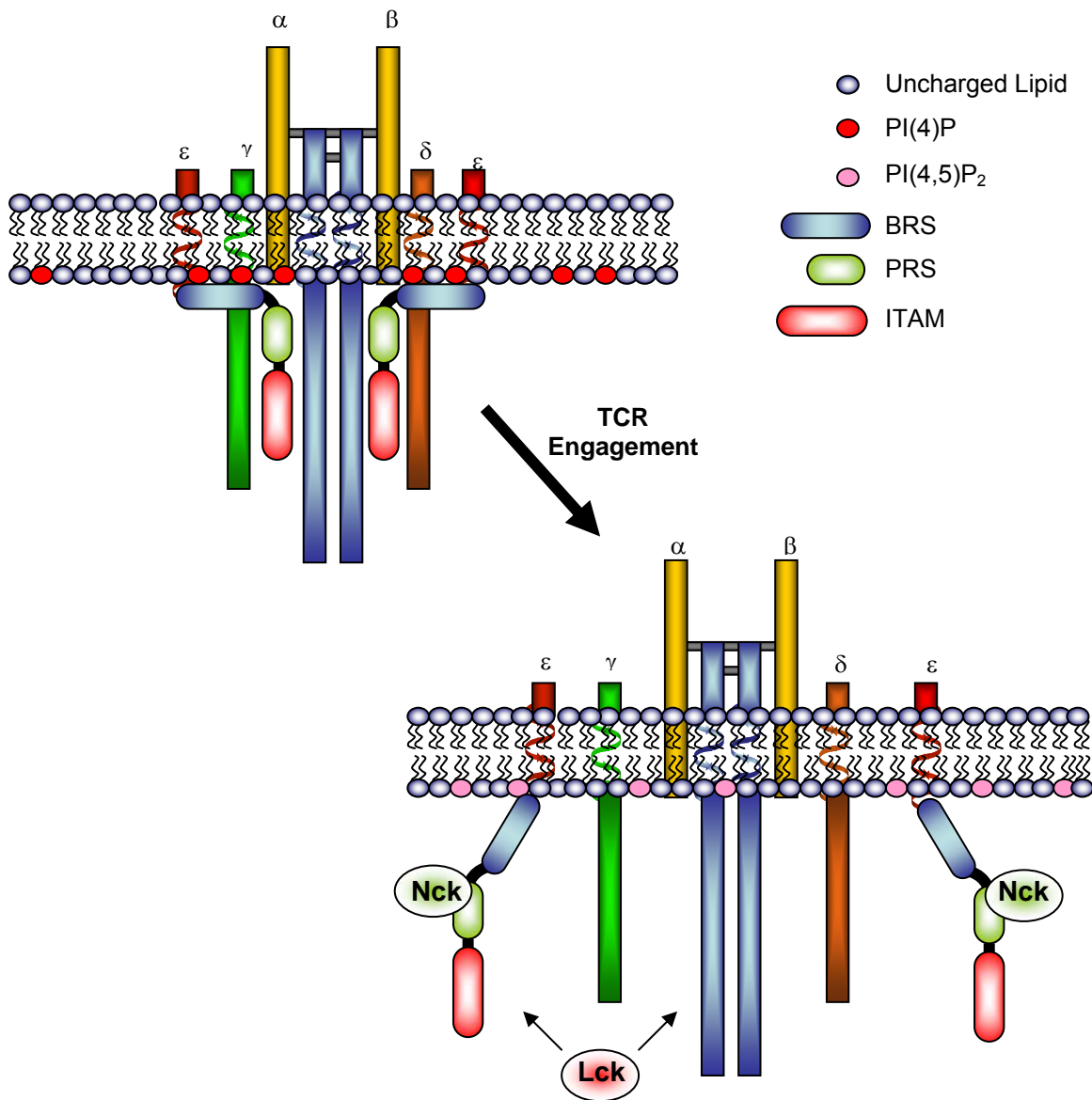


Figure 47. Model I for the regulation of TCR signaling by the BRS of CD3 ϵ . Constitutive interactions between the BRS of CD3 ϵ and phospholipids expressed on the inner leaflet of the plasma membrane may hold CD3 ϵ in a "closed" conformation. Following TCR engagement, modifications to the lipid environment surrounding the TCR might release the BRS, allowing for a conformation change to take place within the cytoplasmic tail of CD3 ϵ . This would result in the exposure of the PRS to Nck, and accesses of other signaling proteins, such as Lck, to the invariant chain ITAMs.

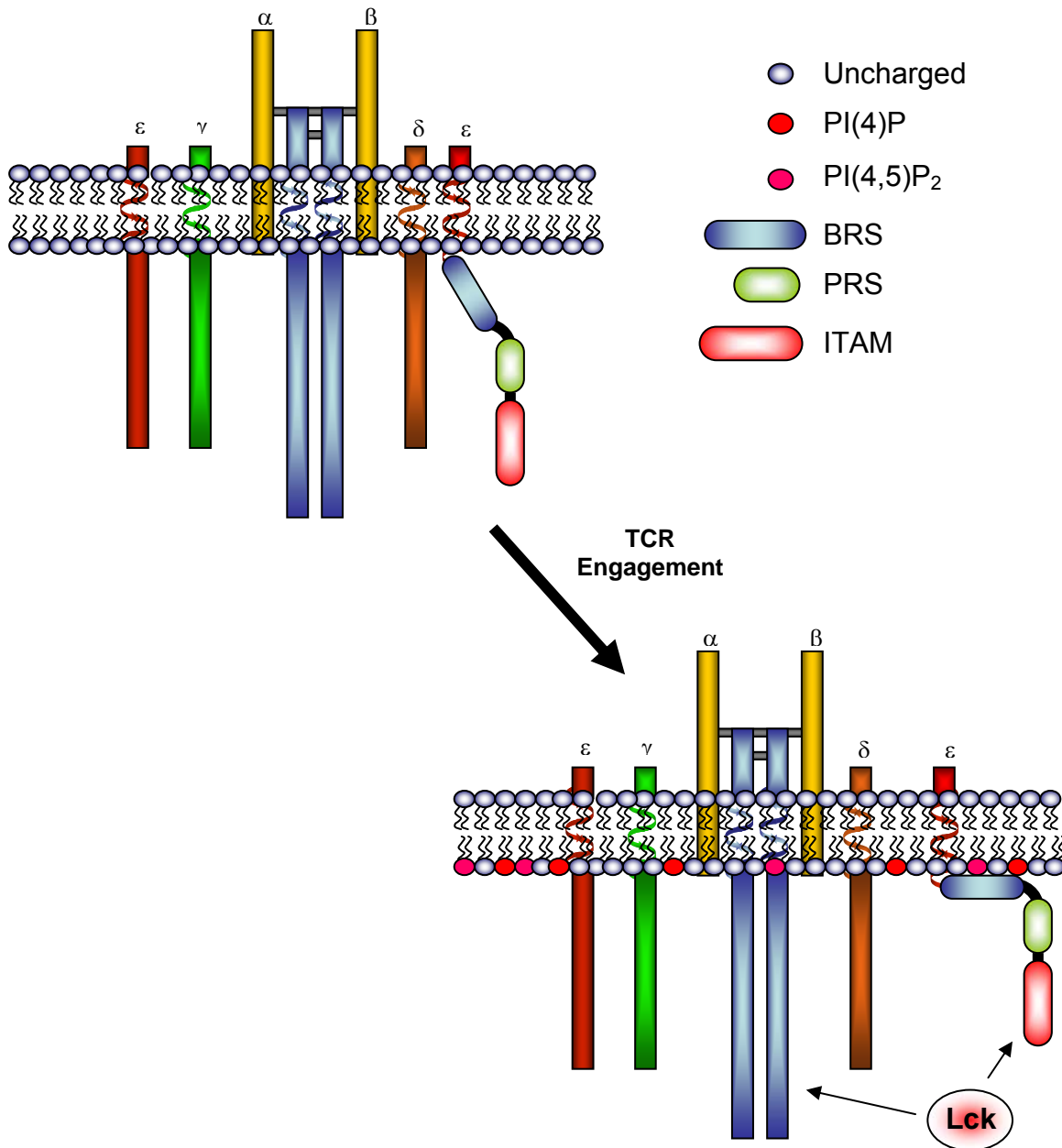
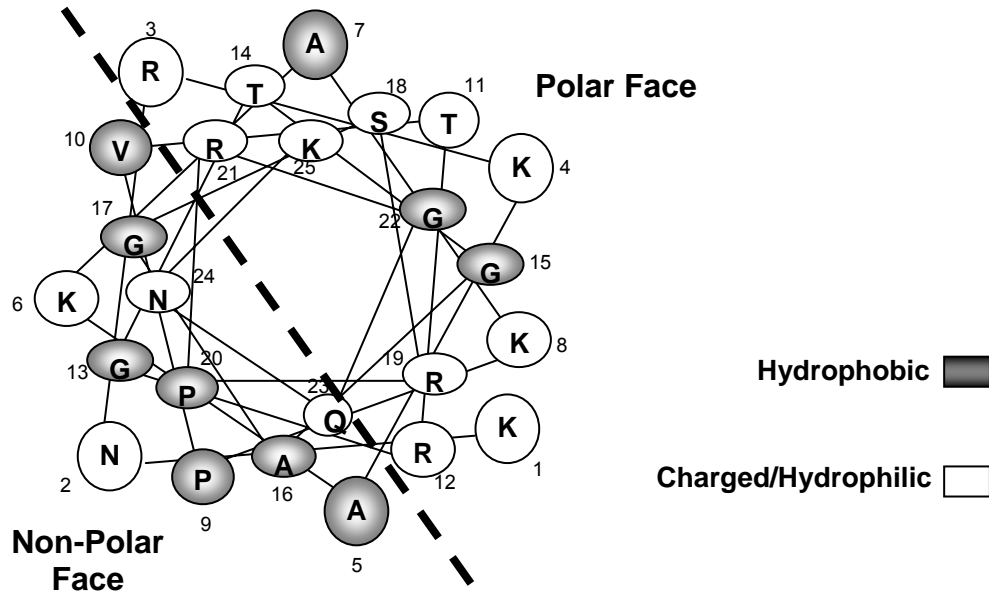


Figure 48. Model II for the regulation of TCR signaling by the BRS of CD3 ϵ . Prior to TCR engagement, the cytoplasmic tail of CD3 ϵ may hang “free” into the cytosol of the cell. Following TCR/peptide-MHC interactions, the generation of phospholipids at the plasma membrane may allow for an inducible association of the BRS. As a result, the conformational change known to take place within CD3 ϵ may be triggered, followed by the association of Src kinases, such as Lck.

A.

1 5 10 15 20 25
BRS: KNRKAKAKPVTRGTGAGSRQRGQNK



B.

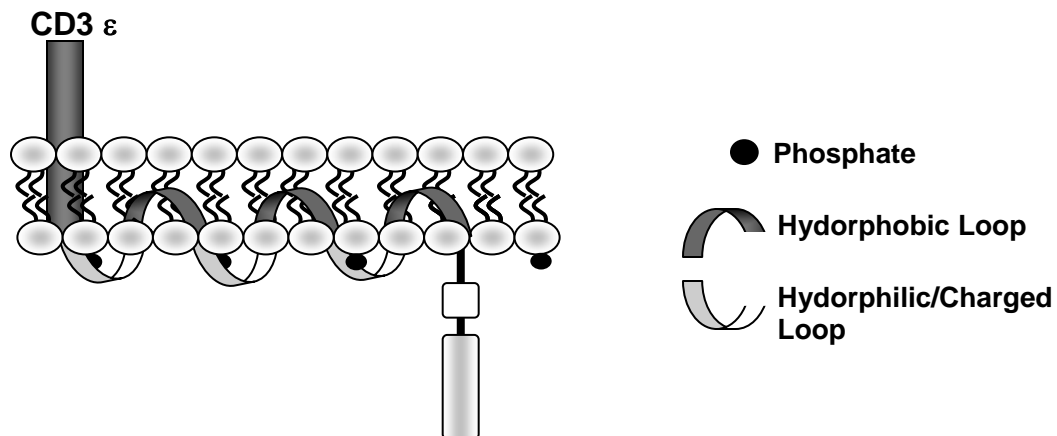


Figure 49. α -helical wheel model for the BRS of CD3 ϵ . (A and B) Interactions between the positively charged residues of the BRS (white) and the anionic head groups of phospholipids present in intracellular membranes may allow the BRS to taken on the formation of an α -helix. In this model, hydrophobic residues (gray) may also make contact with the tails of lipids within the membrane.

BIBLIOGRAPHY

1. Call ME, Wucherpfennig KW. 2005. The T cell receptor: critical role of the membrane environment in receptor assembly and function. *Annu Rev Immunol* 23: 101-25
2. Brenner MB, McLean J, Dialynas DP, Strominger JL, Smith JA, Owen FL, Seidman JG, Ip S, Rosen F, Krangel MS. 1986. Identification of a putative second T-cell receptor. *Nature* 322: 145-9
3. Samelson LE, Harford JB, Klausner RD. 1985. Identification of the components of the murine T cell antigen receptor complex. *Cell* 43: 223-31
4. Blumberg RS, Ley S, Sancho J, Lonberg N, Lacy E, McDermott F, Schad V, Greenstein JL, Terhorst C. 1990. Structure of the T-cell antigen receptor: evidence for two CD3 epsilon subunits in the T-cell receptor-CD3 complex. *Proc Natl Acad Sci U S A* 87: 7220-4
5. de la Hera A, Muller U, Olsson C, Isaaz S, Tunnacliffe A. 1991. Structure of the T cell antigen receptor (TCR): two CD3 epsilon subunits in a functional TCR/CD3 complex. *J Exp Med* 173: 7-17
6. Qian D, Weiss A. 1997. T cell antigen receptor signal transduction. *Curr Opin Cell Biol* 9: 205-12
7. Wange RL, Samelson LE. 1996. Complex complexes: signaling at the TCR. *Immunity* 5: 197-205
8. Pitcher LA, van Oers NS. 2003. T-cell receptor signal transmission: who gives an ITAM? *Trends Immunol* 24: 554-60
9. Iwashima M, Irving BA, van Oers NS, Chan AC, Weiss A. 1994. Sequential interactions of the TCR with two distinct cytoplasmic tyrosine kinases. *Science* 263: 1136-9
10. Wange RL, Malek SN, Desiderio S, Samelson LE. 1993. Tandem SH2 domains of ZAP-70 bind to T cell antigen receptor zeta and CD3 epsilon from activated Jurkat T cells. *J Biol Chem* 268: 19797-801
11. Zhang W, Sloan-Lancaster J, Kitchen J, Tribble RP, Samelson LE. 1998. LAT: the ZAP-70 tyrosine kinase substrate that links T cell receptor to cellular activation. *Cell* 92: 83-92
12. Wardenburg JB, Fu C, Jackman JK, Flotow H, Wilkinson SE, Williams DH, Johnson R, Kong G, Chan AC, Findell PR. 1996. Phosphorylation of SLP-76 by the ZAP-70 protein-tyrosine kinase is required for T-cell receptor function. *J Biol Chem* 271: 19641-4
13. Paz PE, Wang S, Clarke H, Lu X, Stokoe D, Abo A. 2001. Mapping the Zap-70 phosphorylation sites on LAT (linker for activation of T cells) required for recruitment and activation of signalling proteins in T cells. *Biochem J* 356: 461-71
14. Granja C, Lin LL, Yunis EJ, Relias V, Dasgupta JD. 1991. PLC gamma 1, a possible mediator of T cell receptor function. *J Biol Chem* 266: 16277-80
15. Imboden JB, Stobo JD. 1985. Transmembrane signalling by the T cell antigen receptor. Perturbation of the T3-antigen receptor complex generates inositol

- phosphates and releases calcium ions from intracellular stores. *J Exp Med* 161: 446-56
16. Ebinu JO, Stang SL, Teixeira C, Bottorff DA, Hooton J, Blumberg PM, Barry M, Bleakley RC, Ostergaard HL, Stone JC. 2000. RasGRP links T-cell receptor signaling to Ras. *Blood* 95: 3199-203
 17. Spitaler M, Cantrell DA. 2004. Protein kinase C and beyond. *Nat Immunol* 5: 785-90
 18. Diaz-Flores E, Siliceo M, Martinez AC, Merida I. 2003. Membrane translocation of protein kinase C θ during T lymphocyte activation requires phospholipase C-gamma-generated diacylglycerol. *J Biol Chem* 278: 29208-15
 19. Sommers CL, Dejarnette JB, Huang K, Lee J, El-Khoury D, Shores EW, Love PE. 2000. Function of CD3 epsilon-mediated signals in T cell development. *J Exp Med* 192: 913-19
 20. van Oers NS, Love PE, Shores EW, Weiss A. 1998. Regulation of TCR signal transduction in murine thymocytes by multiple TCR zeta-chain signaling motifs. *J Immunol* 160: 163-70
 21. Pitcher LA, Mathis MA, Young JA, DeFord LM, Purtic B, Wulfing C, van Oers NS. 2005. The CD3 gamma epsilon/delta epsilon signaling module provides normal T cell functions in the absence of the TCR zeta immunoreceptor tyrosine-based activation motifs. *Eur J Immunol* 35: 3643-54
 22. Minguet S, Swamy M, Alarcon B, Luescher IF, Schamel WW. 2007. Full activation of the T cell receptor requires both clustering and conformational changes at CD3. *Immunity* 26: 43-54
 23. Clevers H, Dunlap S, Saito H, Georgopoulos K, Wileman T, Terhorst C. 1988. Characterization and expression of the murine CD3-epsilon gene. *Proc Natl Acad Sci U S A* 85: 8623-7
 24. Sun ZJ, Kim KS, Wagner G, Reinherz EL. 2001. Mechanisms contributing to T cell receptor signaling and assembly revealed by the solution structure of an ectodomain fragment of the CD3 epsilon gamma heterodimer. *Cell* 105: 913-23
 25. Borroto A, Mallabiabarrena A, Albar JP, Martinez AC, Alarcon B. 1998. Characterization of the region involved in CD3 pairwise interactions within the T cell receptor complex. *J Biol Chem* 273: 12807-16
 26. Call ME, Pyrdol J, Wiedmann M, Wucherpfennig KW. 2002. The organizing principle in the formation of the T cell receptor-CD3 complex. *Cell* 111: 967-79
 27. Kjer-Nielsen L, Dunstone MA, Kostenko L, Ely LK, Beddoe T, Mifsud NA, Purcell AW, Brooks AG, McCluskey J, Rossjohn J. 2004. Crystal structure of the human T cell receptor CD3 epsilon gamma heterodimer complexed to the therapeutic mAb OKT3. *Proc Natl Acad Sci U S A* 101: 7675-80
 28. Sun ZY, Kim ST, Kim IC, Fahmy A, Reinherz EL, Wagner G. 2004. Solution structure of the CD3epsilon/delta ectodomain and comparison with CD3epsilon/gamma as a basis for modeling T cell receptor topology and signaling. *Proc Natl Acad Sci U S A* 101: 16867-72
 29. Xu C, Call ME, Wucherpfennig KW. 2006. A membrane-proximal tetracysteine motif contributes to assembly of CD3delta/epsilon and CD3gamma/epsilon dimers with the T cell receptor. *J Biol Chem* 281: 36977-84

30. Huppa JB, Ploegh HL. 1997. In vitro translation and assembly of a complete T cell receptor-CD3 complex. *J Exp Med* 186: 393-403
31. Wileman T, Carson GR, Concino M, Ahmed A, Terhorst C. 1990. The gamma and epsilon subunits of the CD3 complex inhibit pre-Golgi degradation of newly synthesized T cell antigen receptors. *J Cell Biol* 110: 973-86
32. Kim KS, Sun ZY, Wagner G, Reinherz EL. 2000. Heterodimeric CD3epsilon-gamma extracellular domain fragments: production, purification and structural analysis. *J Mol Biol* 302: 899-916
33. Ghendler Y, Smolyar A, Chang HC, Reinherz EL. 1998. One of the CD3epsilon subunits within a T cell receptor complex lies in close proximity to the Cbeta FG loop. *J Exp Med* 187: 1529-36
34. Wang J, Lim K, Smolyar A, Teng M, Liu J, Tse AG, Liu J, Hussey RE, Chishti Y, Thomson CT, Sweet RM, Nathenson SG, Chang HC, Sacchettini JC, Reinherz EL. 1998. Atomic structure of an alphabeta T cell receptor (TCR) heterodimer in complex with an anti-TCR fab fragment derived from a mitogenic antibody. *Embo J* 17: 10-26
35. Call ME, Pyrdol J, Wucherpfennig KW. 2004. Stoichiometry of the T-cell receptor-CD3 complex and key intermediates assembled in the endoplasmic reticulum. *Embo J* 23: 2348-57
36. San Jose E, Sahuquillo AG, Bragado R, Alarcon B. 1998. Assembly of the TCR/CD3 complex: CD3 epsilon/delta and CD3 epsilon/gamma dimers associate indistinctly with both TCR alpha and TCR beta chains. Evidence for a double TCR heterodimer model. *Eur J Immunol* 28: 12-21
37. Borroto A, Jimenez MA, Alarcon B, Rico M. 1997. 1H-NMR analysis of CD3-epsilon reveals the presence of turn-helix structures around the ITAM motif in an otherwise random coil cytoplasmic tail. *Biopolymers* 42: 75-88
38. Mallabiabarrena A, Jimenez MA, Rico M, Alarcon B. 1995. A tyrosine-containing motif mediates ER retention of CD3-epsilon and adopts a helix-turn structure. *Embo J* 14: 2257-68
39. Deford-Watts LM, Young JA, Pitcher LA, van Oers NS. 2007. The membrane-proximal portion of CD3 epsilon associates with the serine/threonine kinase GRK2. *J Biol Chem*
40. Yamazaki T, Hamano Y, Tashiro H, Itoh K, Nakano H, Miyatake S, Saito T. 1999. CAST, a novel CD3epsilon-binding protein transducing activation signal for interleukin-2 production in T cells. *J Biol Chem* 274: 18173-80
41. Nakano H, Yamazaki T, Miyatake S, Nozaki N, Kikuchi A, Saito T. 1996. Specific interaction of topoisomerase II beta and the CD3 epsilon chain of the T cell receptor complex. *J Biol Chem* 271: 6483-9
42. Heo WD, Inoue T, Park WS, Kim ML, Park BO, Wandless TJ, Meyer T. 2006. PI(3,4,5)P3 and PI(4,5)P2 lipids target proteins with polybasic clusters to the plasma membrane. *Science* 314: 1458-61
43. Sato TK, Overduin M, Emr SD. 2001. Location, location, location: membrane targeting directed by PX domains. *Science* 294: 1881-5
44. McLaughlin S, Smith SO, Hayman MJ, Murray D. 2005. An electrostatic engine model for autoinhibition and activation of the epidermal growth factor receptor (EGFR/ErbB) family. *J Gen Physiol* 126: 41-53

45. Gil D, Schamel WW, Montoya M, Sanchez-Madrid F, Alarcon B. 2002. Recruitment of Nck by CD3 epsilon reveals a ligand-induced conformational change essential for T cell receptor signaling and synapse formation. *Cell* 109: 901-12
46. Kesti T, Ruppelt A, Wang JH, Liss M, Wagner R, Tasken K, Saksela K. 2007. Reciprocal regulation of SH3 and SH2 domain binding via tyrosine phosphorylation of a common site in CD3epsilon. *J Immunol* 179: 878-85
47. Risueno RM, Gil D, Fernandez E, Sanchez-Madrid F, Alarcon B. 2005. Ligand-induced conformational change in the T-cell receptor associated with productive immune synapses. *Blood* 106: 601-8
48. Chen M, She H, Kim A, Woodley DT, Li W. 2000. Nckbeta adapter regulates actin polymerization in NIH 3T3 fibroblasts in response to platelet-derived growth factor bb. *Mol Cell Biol* 20: 7867-80
49. Wunderlich L, Farago A, Downward J, Buday L. 1999. Association of Nck with tyrosine-phosphorylated SLP-76 in activated T lymphocytes. *Eur J Immunol* 29: 1068-75
50. Szymczak AL, Workman CJ, Gil D, Dilioglou S, Vignali KM, Palmer E, Vignali DA. 2005. The CD3epsilon proline-rich sequence, and its interaction with Nck, is not required for T cell development and function. *J Immunol* 175: 270-5
51. Kjer-Nielsen L, Clements CS, Purcell AW, Brooks AG, Whisstock JC, Burrows SR, McCluskey J, Rossjohn J. 2003. A structural basis for the selection of dominant alphabeta T cell receptors in antiviral immunity. *Immunity* 18: 53-64
52. Levin SE, Weiss A. 2005. Twisting tails exposed: the evidence for TCR conformational change. *J Exp Med* 201: 489-92
53. Scita G, Tenca P, Areces LB, Tocchetti A, Frittoli E, Giardina G, Ponzanelli I, Sini P, Innocenti M, Di Fiore PP. 2001. An effector region in Eps8 is responsible for the activation of the Rac-specific GEF activity of Sos-1 and for the proper localization of the Rac-based actin-polymerizing machine. *J Cell Biol* 154: 1031-44
54. Reth M. 1989. Antigen receptor tail clue. *Nature* 338: 383-4
55. Isakov N, Wange RL, Burgess WH, Watts JD, Aebersold R, Samelson LE. 1995. ZAP-70 binding specificity to T cell receptor tyrosine-based activation motifs: the tandem SH2 domains of ZAP-70 bind distinct tyrosine-based activation motifs with varying affinity. *J Exp Med* 181: 375-80
56. Letourneur F, Klausner RD. 1992. Activation of T cells by a tyrosine kinase activation domain in the cytoplasmic tail of CD3 epsilon. *Science* 255: 79-82
57. Guirado M, de Aos I, Orta T, Rivas L, Terhorst C, Zubiaur M, Sancho J. 2002. Phosphorylation of the N-terminal and C-terminal CD3-epsilon-ITAM tyrosines is differentially regulated in T cells. *Biochem Biophys Res Commun* 291: 574-81
58. Osman N, Turner H, Lucas S, Reif K, Cantrell DA. 1996. The protein interactions of the immunoglobulin receptor family tyrosine-based activation motifs present in the T cell receptor zeta subunits and the CD3 gamma, delta and epsilon chains. *Eur J Immunol* 26: 1063-8
59. Mallabiabarrena A, Fresno M, Alarcon B. 1992. An endoplasmic reticulum retention signal in the CD3 epsilon chain of the T-cell receptor. *Nature* 357: 593-6

60. Bromley SK, Peterson DA, Gunn MD, Dustin ML. 2000. Cutting edge: hierarchy of chemokine receptor and TCR signals regulating T cell migration and proliferation. *J Immunol* 165: 15-9
61. Kumar A, Humphreys TD, Kremer KN, Bramati PS, Bradfield L, Edgar CE, Hedin KE. 2006. CXCR4 physically associates with the T cell receptor to signal in T cells. *Immunity* 25: 213-24
62. Patrussi L, Ulivieri C, Lucherini OM, Paccani SR, Gamberucci A, Lanfrancone L, Pelicci PG, Baldari CT. 2007. p52Shc is required for CXCR4-dependent signaling and chemotaxis in T cells. *Blood* 110: 1730-8
63. Peacock JW, Jirik FR. 1999. TCR activation inhibits chemotaxis toward stromal cell-derived factor-1: evidence for reciprocal regulation between CXCR4 and the TCR. *J Immunol* 162: 215-23
64. Dustin ML, Bromley SK, Kan Z, Peterson DA, Unanue ER. 1997. Antigen receptor engagement delivers a stop signal to migrating T lymphocytes. *Proc Natl Acad Sci U S A* 94: 3909-13
65. Gether U. 2000. Uncovering molecular mechanisms involved in activation of G protein-coupled receptors. *Endocr Rev* 21: 90-113
66. Pierce KL, Premont RT, Lefkowitz RJ. 2002. Seven-transmembrane receptors. *Nat Rev Mol Cell Biol* 3: 639-50
67. Cabrera-Vera TM, Vanhauwe J, Thomas TO, Medkova M, Preininger A, Mazzoni MR, Hamm HE. 2003. Insights into G protein structure, function, and regulation. *Endocr Rev* 24: 765-81
68. McCudden CR, Hains MD, Kimple RJ, Siderovski DP, Willard FS. 2005. G-protein signaling: back to the future. *Cell Mol Life Sci* 62: 551-77
69. Kobilka BK. 2007. G protein coupled receptor structure and activation. *Biochim Biophys Acta* 1768: 794-807
70. Hamm HE. 1998. The many faces of G protein signaling. *J Biol Chem* 273: 669-72
71. Taub DD, Conlon K, Lloyd AR, Oppenheim JJ, Kelvin DJ. 1993. Preferential migration of activated CD4+ and CD8+ T cells in response to MIP-1 alpha and MIP-1 beta. *Science* 260: 355-8
72. Bacon KB, Szabo MC, Yssel H, Bolen JB, Schall TJ. 1996. RANTES induces tyrosine kinase activity of stably complexed p125FAK and ZAP-70 in human T cells. *J Exp Med* 184: 873-82
73. Della Rocca GJ, van Biesen T, Daaka Y, Luttrell DK, Luttrell LM, Lefkowitz RJ. 1997. Ras-dependent mitogen-activated protein kinase activation by G protein-coupled receptors. Convergence of Gi- and Gq-mediated pathways on calcium/calmodulin, Pyk2, and Src kinase. *J Biol Chem* 272: 19125-32
74. Qian D, Lev S, van Oers NS, Dikic I, Schlessinger J, Weiss A. 1997. Tyrosine phosphorylation of Pyk2 is selectively regulated by Fyn during TCR signaling. *J Exp Med* 185: 1253-9
75. Stanners J, Kabouridis PS, McGuire KL, Tsoukas CD. 1995. Interaction between G proteins and tyrosine kinases upon T cell receptor.CD3-mediated signaling. *J Biol Chem* 270: 30635-42
76. Banu Y, Watanabe T. 1999. Augmentation of antigen receptor-mediated responses by histamine H1 receptor signaling. *J Exp Med* 189: 673-82

77. Kohout TA, Lefkowitz RJ. 2003. Regulation of G protein-coupled receptor kinases and arrestins during receptor desensitization. *Mol Pharmacol* 63: 9-18
78. Benovic JL, Kuhn H, Weyand I, Codina J, Caron MG, Lefkowitz RJ. 1987. Functional desensitization of the isolated beta-adrenergic receptor by the beta-adrenergic receptor kinase: potential role of an analog of the retinal protein arrestin (48-kDa protein). *Proc Natl Acad Sci U S A* 84: 8879-82
79. Kelleher DJ, Johnson GL. 1990. Characterization of rhodopsin kinase purified from bovine rod outer segments. *J Biol Chem* 265: 2632-9
80. Attramadal H, Arriza JL, Aoki C, Dawson TM, Codina J, Kwatra MM, Snyder SH, Caron MG, Lefkowitz RJ. 1992. Beta-arrestin2, a novel member of the arrestin/beta-arrestin gene family. *J Biol Chem* 267: 17882-90
81. Luttrell LM, Lefkowitz RJ. 2002. The role of beta-arrestins in the termination and transduction of G-protein-coupled receptor signals. *J Cell Sci* 115: 455-65
82. Hertel C, Muller P, Portenier M, Staehelin M. 1983. Determination of the desensitization of beta-adrenergic receptors by [3H]CGP-12177. *Biochem J* 216: 669-74
83. Daaka Y, Luttrell LM, Ahn S, Della Rocca GJ, Ferguson SS, Caron MG, Lefkowitz RJ. 1998. Essential role for G protein-coupled receptor endocytosis in the activation of mitogen-activated protein kinase. *J Biol Chem* 273: 685-8
84. Ignatova EG, Belcheva MM, Bohn LM, Neuman MC, Coscia CJ. 1999. Requirement of receptor internalization for opioid stimulation of mitogen-activated protein kinase: biochemical and immunofluorescence confocal microscopic evidence. *J Neurosci* 19: 56-63
85. Luttrell LM. 2005. Composition and function of g protein-coupled receptor signalsomes controlling mitogen-activated protein kinase activity. *J Mol Neurosci* 26: 253-64
86. Pitcher JA, Freedman NJ, Lefkowitz RJ. 1998. G protein-coupled receptor kinases. *Annu Rev Biochem* 67: 653-92
87. Pao CS, Benovic JL. 2002. Phosphorylation-independent desensitization of G protein-coupled receptors? *Sci STKE* 2002: PE42
88. Carman CV, Parent JL, Day PW, Pronin AN, Sternweis PM, Wedegaertner PB, Gilman AG, Benovic JL, Kozasa T. 1999. Selective regulation of Galpha(q/11) by an RGS domain in the G protein-coupled receptor kinase, GRK2. *J Biol Chem* 274: 34483-92
89. Day PW, Tesmer JJ, Sterne-Marr R, Freeman LC, Benovic JL, Wedegaertner PB. 2004. Characterization of the GRK2 binding site of Galphaq. *J Biol Chem* 279: 53643-52
90. Benovic JL, DeBlasi A, Stone WC, Caron MG, Lefkowitz RJ. 1989. Beta-adrenergic receptor kinase: primary structure delineates a multigene family. *Science* 246: 235-40
91. Fushman D, Najmabadi-Haske T, Cahill S, Zheng J, LeVine H, 3rd, Cowburn D. 1998. The solution structure and dynamics of the pleckstrin homology domain of G protein-coupled receptor kinase 2 (beta-adrenergic receptor kinase 1). A binding partner of Gbetagamma subunits. *J Biol Chem* 273: 2835-43

92. Koch WJ, Inglese J, Stone WC, Lefkowitz RJ. 1993. The binding site for the beta gamma subunits of heterotrimeric G proteins on the beta-adrenergic receptor kinase. *J Biol Chem* 268: 8256-60
93. Pitcher JA, Touhara K, Payne ES, Lefkowitz RJ. 1995. Pleckstrin homology domain-mediated membrane association and activation of the beta-adrenergic receptor kinase requires coordinate interaction with G beta gamma subunits and lipid. *J Biol Chem* 270: 11707-10
94. Orsini MJ, Parent JL, Mundell SJ, Benovic JL, Marchese A. 1999. Trafficking of the HIV coreceptor CXCR4. Role of arrestins and identification of residues in the c-terminal tail that mediate receptor internalization. *J Biol Chem* 274: 31076-86
95. Jaber M, Koch WJ, Rockman H, Smith B, Bond RA, Sulik KK, Ross J, Jr., Lefkowitz RJ, Caron MG, Giros B. 1996. Essential role of beta-adrenergic receptor kinase 1 in cardiac development and function. *Proc Natl Acad Sci U S A* 93: 12974-9
96. Vroon A, Kavelaars A, Limmroth V, Lombardi MS, Goebel MU, Van Dam AM, Caron MG, Schedlowski M, Heijnen CJ. 2005. G protein-coupled receptor kinase 2 in multiple sclerosis and experimental autoimmune encephalomyelitis. *J Immunol* 174: 4400-6
97. Theilade J, Haunso S, Sheikh SP. 2001. G protein-coupled receptor kinase 2--a feedback regulator of Gq pathway signalling. *Curr Drug Targets Immune Endocr Metabol Disord* 1: 139-51
98. De Blasi A, Parruti G, Sallèse M. 1995. Regulation of G protein-coupled receptor kinase subtypes in activated T lymphocytes. Selective increase of beta-adrenergic receptor kinase 1 and 2. *J Clin Invest* 95: 203-10
99. Lombardi MS, Kavelaars A, Schedlowski M, Bijlsma JW, Okihara KL, Van de Pol M, Ochsmann S, Pawlak C, Schmidt RE, Heijnen CJ. 1999. Decreased expression and activity of G-protein-coupled receptor kinases in peripheral blood mononuclear cells of patients with rheumatoid arthritis. *Faseb J* 13: 715-25
100. Borroto A, Lama J, Niedergang F, Dautry-Varsat A, Alarcon B, Alcover A. 1999. The CD3 epsilon subunit of the TCR contains endocytosis signals. *J Immunol* 163: 25-31
101. Gil D, Gutierrez D, Alarcon B. 2001. Intracellular redistribution of nucleolin upon interaction with the CD3epsilon chain of the T cell receptor complex. *J Biol Chem* 276: 11174-9
102. de Aos I, Metzger MH, Exley M, Dahl CE, Misra S, Zheng D, Varticovski L, Terhorst C, Sancho J. 1997. Tyrosine phosphorylation of the CD3-epsilon subunit of the T cell antigen receptor mediates enhanced association with phosphatidylinositol 3-kinase in Jurkat T cells. *J Biol Chem* 272: 25310-8
103. Skalhegg BS, Tasken K, Hansson V, Huitfeldt HS, Jahnsen T, Lea T. 1994. Location of cAMP-dependent protein kinase type I with the TCR-CD3 complex. *Science* 263: 84-7
104. McCarty N, Paust S, Ikizawa K, Dan I, Li X, Cantor H. 2005. Signaling by the kinase MINK is essential in the negative selection of autoreactive thymocytes. *Nat Immunol* 6: 65-72

105. Zhumabekov T, Corbella P, Tolaini M, Kioussis D. 1995. Improved version of a human CD2 minigene based vector for T cell-specific expression in transgenic mice. *J Immunol Methods* 185: 133-40
106. van Oers NS, Tohlen B, Malissen B, Moomaw CR, Afendis S, Slaughter CA. 2000. The 21- and 23-kD forms of TCR zeta are generated by specific ITAM phosphorylations. *Nat Immunol* 1: 322-8
107. van Oers NS, von Boehmer H, Weiss A. 1995. The pre-T cell receptor (TCR) complex is functionally coupled to the TCR-zeta subunit. *J Exp Med* 182: 1585-90
108. Cooper JA, Sefton BM, Hunter T. 1983. Detection and quantification of phosphotyrosine in proteins. *Methods Enzymol* 99: 387-402
109. van Oers NS, Tao W, Watts JD, Johnson P, Aebersold R, Teh HS. 1993. Constitutive tyrosine phosphorylation of the T-cell receptor (TCR) zeta subunit: regulation of TCR-associated protein tyrosine kinase activity by TCR zeta. *Mol Cell Biol* 13: 5771-80
110. Song W, Lahiri DK. 1995. Efficient transfection of DNA by mixing cells in suspension with calcium phosphate. *Nucleic Acids Res* 23: 3609-11
111. Sun L, Deng L, Ea CK, Xia ZP, Chen ZJ. 2004. The TRAF6 ubiquitin ligase and TAK1 kinase mediate IKK activation by BCL10 and MALT1 in T lymphocytes. *Mol Cell* 14: 289-301
112. Mikalsen SO, Kaalhus O. 1998. Properties of pervanadate and permolybdate. Connexin43, phosphatase inhibition, and thiol reactivity as model systems. *J Biol Chem* 273: 10036-45
113. Wange RL. 2004. TCR signaling: another Abl-bodied kinase joins the cascade. *Curr Biol* 14: R562-4
114. Manning G, Whyte DB, Martinez R, Hunter T, Sudarsanam S. 2002. The protein kinase complement of the human genome. *Science* 298: 1912-34
115. Houtman JC, Houghtling RA, Barda-Saad M, Toda Y, Samelson LE. 2005. Early phosphorylation kinetics of proteins involved in proximal TCR-mediated signaling pathways. *J Immunol* 175: 2449-58
116. Chu PC, Wu J, Liao XC, Pardo J, Zhao H, Li C, Mendenhall MK, Pali E, Shen M, Yu S, Taylor VC, Aversa G, Molineaux S, Payan DG, Masuda ES. 2004. A novel role for p21-activated protein kinase 2 in T cell activation. *J Immunol* 172: 7324-34
117. Sun Z, Arendt CW, Ellmeier W, Schaeffer EM, Sunshine MJ, Gandhi L, Annes J, Petrzilka D, Kupfer A, Schwartzberg PL, Littman DR. 2000. PKC-theta is required for TCR-induced NF-kappaB activation in mature but not immature T lymphocytes. *Nature* 404: 402-7
118. Michie AM, Trop S, Wiest DL, Zuniga-Pflucker JC. 1999. Extracellular signal-regulated kinase (ERK) activation by the pre-T cell receptor in developing thymocytes in vivo. *J Exp Med* 190: 1647-56
119. Hunter T. 2000. Signaling--2000 and beyond. *Cell* 100: 113-27
120. Grunebaum E, Sharfe N, Roifman CM. 2006. Human T cell immunodeficiency: when signal transduction goes wrong. *Immunol Res* 35: 117-26
121. Sakaguchi N, Takahashi T, Hata H, Nomura T, Tagami T, Yamazaki S, Sakihama T, Matsutani T, Negishi I, Nakatsuru S, Sakaguchi S. 2003. Altered thymic T-cell

- selection due to a mutation of the ZAP-70 gene causes autoimmune arthritis in mice. *Nature* 426: 454-60
122. Pitcher LA, Young JA, Mathis MA, Wrage PC, Bartok B, van Oers NS. 2003. The formation and functions of the 21- and 23-kDa tyrosine-phosphorylated TCR zeta subunits. *Immunol Rev* 191: 47-61
 123. Williams BL, Schreiber KL, Zhang W, Wange RL, Samelson LE, Leibson PJ, Abraham RT. 1998. Genetic evidence for differential coupling of Syk family kinases to the T-cell receptor: reconstitution studies in a ZAP-70-deficient Jurkat T-cell line. *Mol Cell Biol* 18: 1388-99
 124. Wang BH, Lu ZX, Polya GM. 1998. Inhibition of eukaryote serine/threonine-specific protein kinases by piceatannol. *Planta Med* 64: 195-9
 125. Tsuchida M, Knechtle SJ, Hamawy MM. 1999. CD28 ligation induces tyrosine phosphorylation of Pyk2 but not Fak in Jurkat T cells. *J Biol Chem* 274: 6735-40
 126. Orellana SA, McKnight GS. 1990. The S49 Kin- cell line transcribes and translates a functional mRNA coding for the catalytic subunit of cAMP-dependent protein kinase. *J Biol Chem* 265: 3048-53
 127. Carpenter B, MacKay C, Alnabulsi A, MacKay M, Telfer C, Melvin WT, Murray GI. 2006. The roles of heterogeneous nuclear ribonucleoproteins in tumour development and progression. *Biochim Biophys Acta* 1765: 85-100
 128. Cordin O, Banroques J, Tanner NK, Linder P. 2006. The DEAD-box protein family of RNA helicases. *Gene* 367: 17-37
 129. Tong A, Nguyen J, Lynch KW. 2005. Differential expression of CD45 isoforms is controlled by the combined activity of basal and inducible splicing-regulatory elements in each of the variable exons. *J Biol Chem* 280: 38297-304
 130. Mellman I, Fuchs R, Helenius A. 1986. Acidification of the endocytic and exocytic pathways. *Annu Rev Biochem* 55: 663-700
 131. van Renswoude J, Bridges KR, Harford JB, Klausner RD. 1982. Receptor-mediated endocytosis of transferrin and the uptake of Fe in K562 cells: identification of a nonlysosomal acidic compartment. *Proc Natl Acad Sci U S A* 79: 6186-90
 132. Penela P, Elorza A, Sarnago S, Mayor F, Jr. 2001. Beta-arrestin- and c-Src-dependent degradation of G-protein-coupled receptor kinase 2. *Embo J* 20: 5129-38
 133. Elorza A, Penela P, Sarnago S, Mayor F, Jr. 2003. MAPK-dependent degradation of G protein-coupled receptor kinase 2. *J Biol Chem* 278: 29164-73
 134. Pitcher JA, Tesmer JJ, Freeman JL, Capel WD, Stone WC, Lefkowitz RJ. 1999. Feedback inhibition of G protein-coupled receptor kinase 2 (GRK2) activity by extracellular signal-regulated kinases. *J Biol Chem* 274: 34531-4
 135. Loza MJ, Foster S, Peters SP, Penn RB. 2006. Beta-agonists modulate T-cell functions via direct actions on type 1 and type 2 cells. *Blood* 107: 2052-60
 136. Cong M, Perry SJ, Lin FT, Fraser ID, Hu LA, Chen W, Pitcher JA, Scott JD, Lefkowitz RJ. 2001. Regulation of membrane targeting of the G protein-coupled receptor kinase 2 by protein kinase A and its anchoring protein AKAP79. *J Biol Chem* 276: 15192-9

137. Elorza A, Sarnago S, Mayor F, Jr. 2000. Agonist-dependent modulation of G protein-coupled receptor kinase 2 by mitogen-activated protein kinases. *Mol Pharmacol* 57: 778-83
138. Ling P, Meyer CF, Redmond LP, Shui JW, Davis B, Rich RR, Hu MC, Wange RL, Tan TH. 2001. Involvement of hematopoietic progenitor kinase 1 in T cell receptor signaling. *J Biol Chem* 276: 18908-14
139. Sterne-Marr R, Tesmer JJ, Day PW, Stracquatano RP, Cilente JA, O'Connor KE, Pronin AN, Benovic JL, Wedegaertner PB. 2003. G protein-coupled receptor Kinase 2/G alpha q/11 interaction. A novel surface on a regulator of G protein signaling homology domain for binding G alpha subunits. *J Biol Chem* 278: 6050-8
140. Yi AK, Tuetken R, Redford T, Waldschmidt M, Kirsch J, Krieg AM. 1998. CpG motifs in bacterial DNA activate leukocytes through the pH-dependent generation of reactive oxygen species. *J Immunol* 160: 4755-61
141. Krasel C, Dammeier S, Winstel R, Brockmann J, Mischak H, Lohse MJ. 2001. Phosphorylation of GRK2 by protein kinase C abolishes its inhibition by calmodulin. *J Biol Chem* 276: 1911-5
142. Yin HL, Janmey PA. 2003. Phosphoinositide regulation of the actin cytoskeleton. *Annu Rev Physiol* 65: 761-89
143. Gaidarov I, Chen Q, Falck JR, Reddy KK, Keen JH. 1996. A functional phosphatidylinositol 3,4,5-trisphosphate/phosphoinositide binding domain in the clathrin adaptor AP-2 alpha subunit. Implications for the endocytic pathway. *J Biol Chem* 271: 20922-9
144. Thorne RF, Legg JW, Isacke CM. 2004. The role of the CD44 transmembrane and cytoplasmic domains in co-ordinating adhesive and signalling events. *J Cell Sci* 117: 373-80
145. Heiska L, Alfthan K, Gronholm M, Vilja P, Vaheri A, Carpen O. 1998. Association of ezrin with intercellular adhesion molecule-1 and -2 (ICAM-1 and ICAM-2). Regulation by phosphatidylinositol 4, 5-bisphosphate. *J Biol Chem* 273: 21893-900
146. Yonemura S, Hirao M, Doi Y, Takahashi N, Kondo T, Tsukita S, Tsukita S. 1998. Ezrin/radixin/moesin (ERM) proteins bind to a positively charged amino acid cluster in the juxta-membrane cytoplasmic domain of CD44, CD43, and ICAM-2. *J Cell Biol* 140: 885-95
147. Godfrey DI, Kennedy J, Suda T, Zlotnik A. 1993. A developmental pathway involving four phenotypically and functionally distinct subsets of CD3-CD4-CD8- triple-negative adult mouse thymocytes defined by CD44 and CD25 expression. *J Immunol* 150: 4244-52
148. Mombaerts P, Clarke AR, Rudnicki MA, Iacomini J, Itohara S, Lafaille JJ, Wang L, Ichikawa Y, Jaenisch R, Hooper ML, et al. 1992. Mutations in T-cell antigen receptor genes alpha and beta block thymocyte development at different stages. *Nature* 360: 225-31
149. Starr TK, Jameson SC, Hogquist KA. 2003. Positive and negative selection of T cells. *Annu Rev Immunol* 21: 139-76

150. Shores EW, Tran T, Grinberg A, Sommers CL, Shen H, Love PE. 1997. Role of the multiple T cell receptor (TCR)-zeta chain signaling motifs in selection of the T cell repertoire. *J Exp Med* 185: 893-900
151. Hogquist KA. 2001. Signal strength in thymic selection and lineage commitment. *Curr Opin Immunol* 13: 225-31
152. Wang B, Wang N, Whitehurst CE, She J, Chen J, Terhorst C. 1999. T lymphocyte development in the absence of CD3 epsilon or CD3 gamma delta epsilon zeta. *J Immunol* 162: 88-94
153. Malissen M, Gillet A, Ardouin L, Bouvier G, Trucy J, Ferrier P, Vivier E, Malissen B. 1995. Altered T cell development in mice with a targeted mutation of the CD3-epsilon gene. *Embo J* 14: 4641-53
154. Sussman JJ, Bonifacino JS, Lippincott-Schwartz J, Weissman AM, Saito T, Klausner RD, Ashwell JD. 1988. Failure to synthesize the T cell CD3-zeta chain: structure and function of a partial T cell receptor complex. *Cell* 52: 85-95
155. Saint-Ruf C, Ungewiss K, Groettrup M, Bruno L, Fehling HJ, von Boehmer H. 1994. Analysis and expression of a cloned pre-T cell receptor gene. *Science* 266: 1208-12
156. Wang B, Biron C, She J, Higgins K, Sunshine MJ, Lacy E, Lonberg N, Terhorst C. 1994. A block in both early T lymphocyte and natural killer cell development in transgenic mice with high-copy numbers of the human CD3E gene. *Proc Natl Acad Sci U S A* 91: 9402-6
157. Levelt CN, Wang B, Ehrfeld A, Terhorst C, Eichmann K. 1995. Regulation of T cell receptor (TCR)-beta locus allelic exclusion and initiation of TCR-alpha locus rearrangement in immature thymocytes by signaling through the CD3 complex. *Eur J Immunol* 25: 1257-61
158. Levelt CN, Mombaerts P, Iglesias A, Tonegawa S, Eichmann K. 1993. Restoration of early thymocyte differentiation in T-cell receptor beta-chain-deficient mutant mice by transmembrane signaling through CD3 epsilon. *Proc Natl Acad Sci U S A* 90: 11401-5
159. Falk I, Potocnik AJ, Barthlott T, Levelt CN, Eichmann K. 1996. Immature T cells in peripheral lymphoid organs of recombinase-activating gene-1/-2-deficient mice. Thymus dependence and responsiveness to anti-CD3 epsilon antibody. *J Immunol* 156: 1362-8
160. Ley SC, Tan KN, Kubo R, Sy MS, Terhorst C. 1989. Surface expression of CD3 in the absence of T cell receptor (TcR): evidence for sorting of partial TcR/CD3 complexes in a post-endoplasmic reticulum compartment. *Eur J Immunol* 19: 2309-17
161. Kanaho Y, Miyazaki H, Yamazaki M. 2003. Activation of PI(4)P 5-kinase by small G proteins. *Adv Enzyme Regul* 43: 107-19
162. Roth MG. 2004. Phosphoinositides in constitutive membrane traffic. *Physiol Rev* 84: 699-730
163. DeJarnette JB, Sommers CL, Huang K, Woodside KJ, Emmons R, Katz K, Shores EW, Love PE. 1998. Specific requirement for CD3epsilon in T cell development. *Proc Natl Acad Sci U S A* 95: 14909-14

164. Shinkai Y, Ma A, Cheng HL, Alt FW. 1995. CD3 epsilon and CD3 zeta cytoplasmic domains can independently generate signals for T cell development and function. *Immunity* 2: 401-11
165. Berkowitz RD, Beckerman KP, Schall TJ, McCune JM. 1998. CXCR4 and CCR5 expression delineates targets for HIV-1 disruption of T cell differentiation. *J Immunol* 161: 3702-10
166. Suzuki G, Nakata Y, Dan Y, Uzawa A, Nakagawa K, Saito T, Mita K, Shirasawa T. 1998. Loss of SDF-1 receptor expression during positive selection in the thymus. *Int Immunol* 10: 1049-56
167. Iyer V, Tran TM, Foster E, Dai W, Clark RB, Knoll BJ. 2006. Differential phosphorylation and dephosphorylation of beta2-adrenoceptor sites Ser262 and Ser355,356. *Br J Pharmacol* 147: 249-59
168. Woerner BM, Warrington NM, Kung AL, Perry A, Rubin JB. 2005. Widespread CXCR4 activation in astrocytomas revealed by phospho-CXCR4-specific antibodies. *Cancer Res* 65: 11392-9
169. Vieira AV, Lamaze C, Schmid SL. 1996. Control of EGF receptor signaling by clathrin-mediated endocytosis. *Science* 274: 2086-9
170. Chiu VK, Bivona T, Hach A, Sajous JB, Silletti J, Wiener H, Johnson RL, 2nd, Cox AD, Philips MR. 2002. Ras signalling on the endoplasmic reticulum and the Golgi. *Nat Cell Biol* 4: 343-50
171. Mor A, Philips MR. 2006. Compartmentalized Ras/MAPK signaling. *Annu Rev Immunol* 24: 771-800
172. Daniels MA, Teixeira E, Gill J, Hausmann B, Roubaty D, Holmberg K, Werlen G, Hollander GA, Gascoigne NR, Palmer E. 2006. Thymic selection threshold defined by compartmentalization of Ras/MAPK signalling. *Nature* 444: 724-9
173. Mariathasan S, Bachmann MF, Bouchard D, Ohteki T, Ohashi PS. 1998. Degree of TCR internalization and Ca²⁺ flux correlates with thymocyte selection. *J Immunol* 161: 6030-7
174. Peter M, Ameer-Beg SM, Hughes MK, Keppler MD, Prag S, Marsh M, Vojnovic B, Ng T. 2005. Multiphoton-FLIM quantification of the EGFP-mRFP1 FRET pair for localization of membrane receptor-kinase interactions. *Biophys J* 88: 1224-37
175. Lefkowitz RJ. 2004. Historical review: a brief history and personal retrospective of seven-transmembrane receptors. *Trends Pharmacol Sci* 25: 413-22
176. Murga C, Ruiz-Gomez A, Garcia-Higuera I, Kim CM, Benovic JL, Mayor F, Jr. 1996. High affinity binding of beta-adrenergic receptor kinase to microsomal membranes. Modulation of the activity of bound kinase by heterotrimeric G protein activation. *J Biol Chem* 271: 985-94
177. Garcia-Higuera I, Penela P, Murga C, Egea G, Bonay P, Benovic JL, Mayor F, Jr. 1994. Association of the regulatory beta-adrenergic receptor kinase with rat liver microsomal membranes. *J Biol Chem* 269: 1348-55
178. Rossi D, Zlotnik A. 2000. The biology of chemokines and their receptors. *Annu Rev Immunol* 18: 217-42
179. Zeyda M, Stulnig TM. 2006. Lipid Rafts & Co.: an integrated model of membrane organization in T cell activation. *Prog Lipid Res* 45: 187-202

180. Srivastava R, Sinha RK, Subrahmanyam G. 2006. Type II phosphatidylinositol 4-kinase beta associates with TCR-CD3 zeta chain in Jurkat cells. *Mol Immunol* 43: 454-63
181. Inokuchi S, Imboden JB. 1990. Antigen receptor-mediated regulation of sustained polyphosphoinositide turnover in a human T cell line. Evidence for a receptor-regulated pathway for production of phosphatidylinositol 4,5-bisphosphate. *J Biol Chem* 265: 5983-9
182. Tang J, Signarvic RS, Degrado WF, Gai F. 2007. Role of helix nucleation in the kinetics of binding of mastoparan x to phospholipid bilayers. *Biochemistry* 46: 13856-63
183. Bernstein LS, Grillo AA, Loranger SS, Linder ME. 2000. RGS4 binds to membranes through an amphipathic alpha -helix. *J Biol Chem* 275: 18520-6
184. Chen C, Seow KT, Guo K, Yaw LP, Lin SC. 1999. The membrane association domain of RGS16 contains unique amphipathic features that are conserved in RGS4 and RGS5. *J Biol Chem* 274: 19799-806
185. Pitcher LA, Mathis MA, Subramanian S, Young JA, Wakeland EK, Love PE, van Oers NS. 2005. Selective expression of the 21-kilodalton tyrosine-phosphorylated form of TCR zeta promotes the emergence of T cells with autoreactive potential. *J Immunol* 174: 6071-9
186. Love PE, Lee J, Shores EW. 2000. Critical relationship between TCR signaling potential and TCR affinity during thymocyte selection. *J Immunol* 165: 3080-7
187. Kisielow P, Bluthmann H, Staerz UD, Steinmetz M, von Boehmer H. 1988. Tolerance in T-cell-receptor transgenic mice involves deletion of nonmature CD4+8+ thymocytes. *Nature* 333: 742-6

VITAE

Laura Michelle DeFord-Watts was born in Temple, Texas, on June 2, 1979. She is the daughter of William and Lisa DeFord and Carl and Martha Baugh. After completing her high school education at Glen Rose High School, Laura attended the University of Mary Hardin-Baylor located in Belton, Texas. There Laura majored in Business Administration, served as a resident assistant on campus, and participated as a member of the University's women's basketball team. After graduating cum laude, Laura obtained a Research Assistant I position at Scott & White Hospital where she worked for a year. In August, 2002 she entered into the Graduate School of Biomedical Sciences at the University of Texas Southwestern (UTSW) Medical Center at Dallas. During her graduate career, Laura met Jonathan Michael Watts, a medical student at UTSW. In March of 2006, they were married. Laura completed her graduate career in March, 2008 and was awarded the degree of Doctor of Philosophy with an emphasis in Immunology.

Permanent Address: 217 Oak Bluff

Murphy, Texas 75094